

DEVELOPMENT OF AN EQUIVALENT MODEL OF ALUMINUM
HONEYCOMB SANDWICH STRUCTURES SUBJECTED TO TRANSVERSE
LOADS

A THESIS SUBMITTED TO
THE GRADUATE SCHOOL OF NATURAL AND APPLIED SCIENCES
OF
MIDDLE EAST TECHNICAL UNIVERSITY

BY

OZAN YARDIMCI

IN PARTIAL FULFILLMENT OF THE REQUIREMENTS
FOR
THE DEGREE OF MASTER OF SCIENCE
IN
AEROSPACE ENGINEERING

AUGUST 2019

Approval of the thesis:

**DEVELOPMENT OF AN EQUIVALENT MODEL OF ALUMINUM
HONEYCOMB SANDWICH STRUCTURES SUBJECTED TO
TRANSVERSE LOADS**

submitted by **OZAN YARDIMCI** in partial fulfillment of the requirements for the degree of **Master of Science in Aerospace Engineering Department, Middle East Technical University** by,

Prof. Dr. Halil Kalıpçılar
Dean, Graduate School of **Natural and Applied Sciences**

Prof. Dr. İsmail Hakkı Tuncer
Head of Department, **Aerospace Engineering**

Assoc. Prof. Dr. Ercan Gürses
Supervisor, **Aerospace Engineering, METU**

Examining Committee Members:

Prof. Dr. Altan Kayran
Aerospace Engineering, METU

Assoc. Prof. Dr. Ercan Gürses
Aerospace Engineering, METU

Assoc. Prof. Dr. Melin Şahin
Aerospace Engineering, METU

Prof. Dr. Afşin Sarıtaş
Civil Engineering, METU

Assist. Prof. Dr. Ali Javili
Mechanical Engineering, Bilkent University

Date: 01.08.2019

I hereby declare that all information in this document has been obtained and presented in accordance with academic rules and ethical conduct. I also declare that, as required by these rules and conduct, I have fully cited and referenced all material and results that are not original to this work.

Name, Surname: Ozan Yardımcı

Signature:

ABSTRACT

DEVELOPMENT OF AN EQUIVALENT MODEL OF ALUMINUM HONEYCOMB SANDWICH STRUCTURES SUBJECTED TO TRANSVERSE LOADS

Yardımcı, Ozan

Master of Science, Aerospace Engineering

Supervisor: Assoc. Prof. Dr. Ercan Gürses

August 2019, 111 pages

Sandwich structures are commonly employed in aviation because of the weight and strength advantages they provided. This common application has turned the accurate finite element analyses of them into a critical issue. In this thesis, a genetic algorithm-based optimization method is employed for creating accurate two-dimensional layered shell models of the sandwich panels with honeycomb cores. Firstly, the sandwich panels subjected to transverse loads with hexagonal honeycomb cores having different face sheet thicknesses are modeled in their original shapes. Secondly, the layered shell models of the sandwich panels under consideration are created using the equivalent properties. Then, the reaction forces obtained from both models are compared for different face sheet thicknesses. In order to lessen the difference between the reaction forces obtained from different finite element modeling approaches, an optimization tool is employed. The tool optimizes the equivalent core properties used in the layered shell models by eliminating the difference between the reaction forces. Finally, finite element models of the sandwich panels with different geometrical properties, loads and boundary conditions are created to verify the results of the optimization. The results show that the optimization which also considers the effect of the stiffness of

the face sheets improves the accuracy of the equivalent models of the sandwich panels under transverse loads.

Keywords: Sandwich Structures, Finite Element Method, Honeycomb, Genetic Algorithm, Optimization, Equivalent Properties, Transverse Load, Layered Shell Modeling

ÖZ

ENİNE YÜKLEME ALTINDAKİ ALÜMİNYUM BAL PETEĞİ SANDVİÇ YAPILARIN EŞDEĞER MODELİNİN GELİŞTİRİLMESİ

Yardımcı, Ozan
Yüksek Lisans, Havacılık ve Uzay Mühendisliği
Tez Danışmanı: Doç. Dr. Ercan Gürses

Ağustos 2019, 111 sayfa

Sandviç yapılar sağladıkları ağırlık ve dayanım nedeniyle havacılık alanında sıkça kullanılmaktadır. Sandviç yapıların havacılıkta sıklıkla kullanılmaya başlanması, bu yapıların sonlu eleman analizlerinin hatasız bir şekilde yapılmasını önemli bir konu haline getirmiştir. Bu tezde, bal peteği dolgu malzemesine sahip sandviç yapıların iki-boyutlu katmanlı kabuk sonlu eleman modelinin doğru bir şekilde oluşturabilmesi için genetik algoritma temelli bir optimizasyon aracı kullanılmıştır. İlk olarak, enine yükleme altındaki altıgen bal peteği dolgu malzemesine ve farklı yüzey levhası kalınlıklarına sahip bir sandviç panelin orijinal boyutlardaki sonlu eleman modeli oluşturulmuştur. İkinci adımda, bu sandviç panellerin literatürdeki formüller kullanılarak elde edilen iki-boyutlu eşdeğer malzeme özelliklerine sahip katmanlı kabuk sonlu eleman modelleri oluşturulmuştur. Bu iki farklı modelden her bir yüzey levhası kalınlığı için tepki kuvvetleri elde edilmiştir. Elde edilen tepki kuvvetleri karşılaştırıldığında arada fark olduğu tespit edilmiştir. Aynı sandviç yapı için farklı sonlu eleman modelleme yöntemleri kullanılması nedeniyle ortaya çıkan bu farkın ortadan kaldırabilmesi için bir optimizasyon aracı kullanılmıştır. Bu optimizasyon aracı dolgu malzemesinin eşdeğer malzeme özelliklerini optimize ederek iki model arasında oluşan farkı kapatmaktadır. Son olarak, optimizasyon sonucu elde edilen malzeme özellikleri farklı geometrik özelliklere, yük ve sınır koşullarına sahip sandviç

yapıların sonlu elemanlar modelleri üzerinde doğrulanmıştır. Sonuç olarak, yüzey levhalarının kalınlıklarından gelen katılık etkisini de dikkate alan bir optimizasyon sürecinin enine yükleme altındaki sandviç panellerin eşdeğer sonlu eleman modellerinin doğruluğu üzerinde iyileştirme sağladığı tespit edilmiştir.

Anahtar Kelimeler: Sandviç Yapılar, Sonlu Elemanlar Yöntemi, Bal Peteği Dolgu, Genetik Algoritma, Optimizasyon, Eşdeğer Malzeme Özellikleri, Enine Yükleme, Katmanlı Kabuk Modeli

To abandoned and stray dogs

ACKNOWLEDGMENTS

First and foremost, I would like to express my gratitude to my supervisor Assoc. Prof. Dr. Ercan Gürses for his constant support, guidance and patience throughout the preparation of this study

I would like to give my special thanks to Prof. Dr. Altan Kayran and Assoc. Prof. Dr. Demirkan Çöker for their devoted assistance and guidance. They have always been there for me whenever I needed help. Their suggestions and comments made a great contribution to this thesis.

I would like to thank to the members of my thesis committee Prof. Dr. Altan Kayran and Assoc. Prof. Dr. Melin Şahin, Prof Dr. Afşin Sarıtaş and Assist. Prof. Dr. Ali Javili for their valuable and effective comments.

Lastly, I also would like to thank my parents and my sister for their caring and love throughout my whole life. Their encouragement and support brought me to these days.

TABLE OF CONTENTS

ABSTRACT	v
ÖZ	vii
ACKNOWLEDGMENTS.....	x
TABLE OF CONTENTS.....	xi
LIST OF TABLES	xiv
LIST OF FIGURES.....	xvi
LIST OF ABBREVIATIONS	xxiii
LIST OF SYMBOLS	xxiv
CHAPTERS	
1. INTRODUCTION	1
1.1. Definition of Sandwich Structures	1
1.2. Brief History of Sandwich Structures in Aviation	3
1.3. Scope of Thesis.....	5
1.4. Outline of the Thesis	5
2. LITERATURE SURVEY.....	9
2.1. Finite Element Analysis and Equivalent Properties	9
2.2. Optimization of Sandwich Structures and the Genetic Algorithm.....	12
3. SANDWICH PANELS AND ANALYSIS	19
3.1. Basic Information about Sandwich Panels	19
3.2. Sandwich Panel Analysis	27
3.3. Determination of Equivalent Core Properties	28
3.4. Finite Element Models	32

3.4.1. Detailed Models	33
3.4.2. Mesh Convergence Study.....	39
3.4.3. Layered Shell Models.....	41
4. OPTIMIZATION USING GENETIC ALGORITHM	47
4.1. Genetic Algorithm Terms and Parameters	47
4.1.1. Fitness Scaling.....	49
4.1.2. Selection	53
4.1.3. Reproduction	54
4.1.4. Mutation	55
4.1.5. Crossover.....	56
4.1.6. Hybrid Function	58
4.1.7. Stopping Criteria	58
4.2. Problem Setup and Flowchart	59
4.2.1. Definition of the Problem.....	60
4.2.2. Selection of Variables	61
4.2.3. Fitness Function	64
4.2.4. Selection of Parameters	69
4.2.4.1. Population Size	69
4.2.4.2. Operational Options.....	73
4.2.5. Algorithm of the Optimization Process.....	77
5. RESULTS.....	81
5.1. Results of the Optimization.....	81
5.2. Results of the Verification Models	88
5.2.1. Results of Verification of the Model Group 2.....	88

5.2.2. Results of Verification of the Model Group 3	91
5.2.3. Results of Verification of the Model Group 4	93
6. DISCUSSION AND FUTURE WORK	97
REFERENCES.....	103
APPENDICES.....	107

LIST OF TABLES

TABLES

Table 2.1. Sandwich structures finite element modeling approaches [10]	10
Table 3.1. Sandwich structure characteristics [9]	21
Table 3.2. Unit Cell Parameters	29
Table 3.3. Formulas of the equivalent properties derived by Masters and Evans [11]	30
Table 3.4. Formulas of the equivalent properties derived by Gibson and Ashby [37] and Grediac [21]	31
Table 3.5. Formulas of the equivalent properties derived by Nast [17]	32
Table 3.6. Mesh convergence data table. The difference between the data expected to be due to the numeric error accumulations occurring during the analysis and post- processing.	40
Table 4.1. Effect of G_{12} on the reaction force	62
Table 4.2. Impact of G_{13} on the reaction force while the other parameters were kept constant	63
Table 4.3. Impact of G_{23} on the reaction force while the other parameters were kept constant	63
Table 4.4. Material Properties of AL5052 H38 Sheet [41]	63
Table 4.5. Honeycomb Core Material Specifications [38]	64
Table 4.6. Definition of fitness function variables	65
Table 4.7. Comparison of the results obtained with different population size	73
Table 4.8. Genetic Algorithm Options	73
Table 4.9. Reference GA options	74
Table 4.10. Reference Optimized Results	74
Table 4.11. Effect of fitness scaling options	74
Table 4.12. Effect of selection options	75

Table 4.13. Effect of crossover options	75
Table 4.14. Stall generations test	76
Table 5.1. Detailed and analytical reaction forces of model group 1. Initial error is the percentage difference between the total detailed and analytical reaction forces	83
Table 5.2. The detailed and optimum reaction forces. Error after optimization is the percentage difference between the total detailed and optimum reaction forces. The error reduces almost to zero percent after optimization.	84
Table 5.3. Analytical and optimized shear modulus values with respect to face sheet thicknesses. The analytical values are independent of the face sheet thickness.	86
Table 5.4. The rate of initial and optimum errors for model group 2. Initial error is the percentage difference between the detailed reaction forces and the analytical reaction forces. Optimum error is the percentage difference between the detailed reaction forces and the reaction force obtained by using optimized material parameters of the model group 1.	90
Table 5.5. The rate of initial and optimum errors for model group 3. Initial error is the percentage difference between the detailed reaction forces and the analytical reaction forces. Optimum error is the percentage difference between the detailed reaction forces and the reaction force obtained by using optimized material parameters of the model group 1.	93
Table 5.6. The rate of initial and optimum errors for model group 4. Initial error is the percentage difference between the detailed reaction forces and the analytical reaction forces. Optimum error is the percentage difference between the detailed reaction forces and the reaction force obtained by using optimized material parameters of the model group 1.	95
Table A.1. Individuals In the last iteration.....	107

LIST OF FIGURES

FIGURES

Figure 1.1. Honeycomb sandwich panel. It has upper and lower face sheets, adhesive layers and a core in between [1].	1
Figure 1.2. (a) Aerodynamic profile of a wind turbine blade. (b) Design details of a wind turbine blade. Sandwich panels are employed in the leading edge [2].....	2
Figure 1.3. Steel-concrete-steel sandwich structure with J-hook connectors [3].	3
Figure 1.4. Airbus A380 has sandwich structures used in vertical and horizontal stabilizers, fuselage belly fairings, pylons, spoilers and ailerons, wing edges, nose landing gear doors and cabin interiors [6].	4
Figure 1.5. Sandwich panel with monolithic edge, ramp and plain sandwich regions [9].....	8
Figure 3.1. Design similarity between an I-beam and a sandwich panel. Flanges become face sheets and the web becomes core [10].....	20
Figure 3.2. Expansion Manufacturing Process. Adhesive lines are printed on the sheets and stacked. Then HOBE (honeycomb before expansion) block is obtained. Then, HOBE is cut in to slices per required thickness and expanded in width direction by causing plastic deformation on the vertical walls [1].	22
Figure 3.3. Adhesive Line (Print Line) Orientation. The print lines define the ribbon direction of the core. In line adhesive printing limits the ribbon length into the web width [1].....	23
Figure 3.4. Corrugation Process. This process is labor intensive and used for the production of high-density cores. First, the sheets are corrugated. Then, they are attached to each other at their nodes and cured in an oven [1].....	24
Figure 3.5. Cell Configurations. The most common cell shape is the hexagon. The core cell shape is selected according to design purpose. An over-expanded can form into a cylinder or a flex core can easily cover curved surfaces [10].....	25

Figure 3.6. Unit Honeycomb Core Cell [1].....	28
Figure 3.7. The Detailed Finite Element Model of the Model Group 1.....	34
Figure 3.8. Enforced displacement of 0.1 mm applied downward (in z-direction) on the upper face sheet of model group1	34
Figure 3.9. Boundary conditions applied on the lower face sheet of model group 1.....	35
Figure 3.10. The Detailed Model of the Model Group 2 with the Core Ribbon Aligned with x Axis and the Boundary Conditions	36
Figure 3.11 The Detailed Model of the Model Group 2 with the Core Ribbon Aligned with y Axis and the Boundary Conditions	36
Figure 3.12. The Detailed Model of the Model Group 3 with the Core Ribbon Aligned with x Axis and the Boundary Conditions	37
Figure 3.13. The Detailed Model of the Model Group 3 with the Core Ribbon Aligned with y Axis and the Boundary Conditions	37
Figure 3.14. The Detailed Model of the Model Group 4 with Loading Along x Axis	38
Figure 3.15. The Detailed Model of the Model Group 4 with Loading Along y Axis	38
Figure 3.16. Mesh Convergence	40
Figure 3.17. Layered Shell Model of the Model Group 1	42
Figure 3.18. Layered Shell Model of the Model Group 2.....	43
Figure 3.19. Material Orientation, Mat-1 axis is aligned with the global x-axis and the stacking direction is the global z-axis	43
Figure 3.20. The Layered Shell Model of the Model Group 3 Simulating the 3-Point Bending	44
Figure 3.21. The layered shell model of the model group 4 with loading in z-direction parallel to y-axis.....	44
Figure 3.22. The layered shell model of the model group 4 with loading in z-direction parallel to y-axis.....	45
Figure 4.1. Problem with 2 Variables Mapped on the Chromosome Using 10 Bits for x_1 and 15 Bits.....	49

Figure 4.2. Raw scores of a population of 20 individuals. The scores are ranked in increasing order. Score of an individual determines its probability to form an offspring for the next generation. Raw scores are usually not preferred for selecting the parents, instead they are used as inputs to scaling functions [39].	50
Figure 4.3. Scaled raw values using Rank scaling function. Fitness scaling removes the effects of the spread of the raw scores. Since the GA minimizes the fitness function, lower raw scores have higher scaled values. The higher the scaled value of an individual, the better its chance to form an offspring [38].	51
Figure 4.4. Comparison of rank and top scaling options. Top scaling function assigns high scaled values to the best individuals while lower scores are given to the others. The generations formed by top scaling function is less diverse compared to the ones formed by rank scaling. Top scaled populations are likely to converge faster; however, top scaling is likely to prevent the GA to search for other points in the space [39].	52
Figure 4.5. Distance between individuals (shows diversity in a population) is less when the generations are formed by top scaling. Rank scaling enables user to search for a broader space [38].	52
Figure 4.6. Stochastic uniform selection assigns individual to lines whose lengths are proportional to their expectation values. Then the GA moves along that line in step sizes of equal lengths and selects the parent. Step size is determined by dividing the total of expectation values into the number of desired children.	53
Figure 4.7. Individuals are given proportions according to their expectations. The GA determines a random number to choose a parent. The larger the area of an individual, the higher chance it has to form an offspring.	53
Figure 4.8. Three ways of forming a child in GA. Elite children are the ones formed from the best performing parents. Crossover children are mixture of two different parents. Elite and crossover children direct the population towards the best solution. However, the responsibilities of mutation children are different. Main responsibility of mutation. They is are toto ensure the diversity of the population. In other words, mutation enlarges the search space of the algorithm by making random changes in the selected parents.	55

Figure 4.9. Scattered crossover. Genes are selected from the parents according to a random crossover vector [22].....	56
Figure 4.10. Single point crossover. Until a column number less than number of variables, the genes are selected from a parent and the remaining are taken from the other parent.....	57
Figure 4.11. Two-point crossover	57
Figure 4.12. Binary Genetic Algorithm Flowchart [40]	60
Figure 4.13. Reference reaction forces are obtained from detailed model. Reaction forces obtained from the constrained nodes along x and y direction are evaluated separately.....	66
Figure 4.14. The reaction force obtained from the nodes along x-direction of the layered shell model is RF_{xnodes} and the reaction force obtained from the nodes along y-direction is the RF_{ynodes} . The reaction forces obtained from the layered shell model tried to be adjusted to reference reaction forces obtained from the detailed model. This is done by changing equivalent G_{13} and G_{23} modulus values of the layered shell model using genetic algorithm optimization method.	66
Figure 4.15. Fitness Function Flowchart.....	68
Figure 4.16. Best and mean fitness values of population of 50 individuals at each generation. The lower the fitness value, the better the performance of a generation. As the mean fitness value goes to zero, the solution becomes convergent.	70
Figure 4.17. Fitness of each individual at the last iteration for population size of 50 while the mean fitness value is close to zero.	70
Figure 4.18. Best and mean fitness values of population of 100 individuals at each generation. The lower the fitness value, the better the performance of a generation. As the mean fitness value goes to zero, the solution becomes convergent.	71
Figure 4.19. Fitness of each individual at the last iteration for population size of 100 while the mean fitness value is close to zero.	71
Figure 4.20. Best and mean fitness values of population of 200 individuals at each generation. The lower the fitness value, the better the performance of a generation. As the mean fitness value goes to zero, the solution becomes convergent.	72

Figure 4.21. Fitness of each individual at the last iteration for population size of 200 while the mean fitness value is close to zero. Although the mean fitness value is close to zero there are 5 individuals whose fitness values are obviously higher than the others.....	72
Figure 4.22. Optimization Process Flowchart	78
Figure 4.23. Verification process flowchart. Optimized G_{13} and G_{23} values are tested on sandwich panels with different geometries and loads and boundary conditions..	79
Figure 5.1. Total of the reaction forces in z-direction obtained from the detailed model (RF-detailed) compared with the reaction force obtained from the layered shell whose shear modulus obtained from analytical formulas in the literature (RF-analytical). The analytical core equivalent formulas are empirically driven and gives high error rates with respect to reference reaction forces. The aim of the optimization is to deal with this error gap by optimizing equivalent G_{13} and G_{23} shear modulus values.	82
Figure 5.2. The rate of initial error. It is the percentage difference between the total reaction forces of the detailed and analytical layered shell models. The error is as high as 95 percent in the beginning and reduces to 86 percent as the face sheet thickness increases. The error after optimization is not presented since it reduces to zero percent.	83
Figure 5.3. Detailed reaction forces vs. optimized reaction forces obtained from the constrained nodes along x-axis (RF13) and along y-axis (RF23). The optimum reaction forces and the reference reaction forces are coincident. Thus, the GA is able to perfectly match the reaction forces in each of the planes.....	84
Figure 5.4. Analytical shear modulus vs. Optimum shear modulus. The dashed lines are analytical values and they are independent of the face sheet thicknesses. The solid lines are optimized shear modulus. The convergence of optimum G_{23} to analytical G_{23} is considered as a coincidence.	85
Figure 5.5. Best and mean fitness values of the optimization for face sheet thickness of 0.36 mm. The algorithm converges to zero fitness value in 10 generations.	87
Figure 5.6. Fitness value of each individual at the last generation. Fitness values of the most individuals were reduced to zero.	87

Figure 5.7 Detailed, analytical and optimum reaction force comparison of the model group 2. Ribbon direction is in the x-axis direction. The optimum reaction force is obtained by plugging in the optimum shear modulus of the optimized model (model group 1) into model group 2. This model group has a central loading and ramp region. RF-optimum results are better than RF-analytical results.....	89
Figure 5.8. Detailed, analytical and optimum reaction force comparison of the model group 2. Ribbon direction is in the y-axis direction. RF-optimum results are better than RF-analytical.	89
Figure 5.9. Comparison of rate of errors stemming from the differences of the reaction forces of the detailed models and analytical models (initial error) with the optimum models. The error rates of the optimum models are lower than the rate of analytical models for all the face sheet thicknesses.....	90
Figure 5.10. Detailed, analytical and optimum reaction force comparison of the model group 3. Ribbon direction is in the x-axis direction. The optimum reaction force was obtained by plugging in the optimum shear modulus of the optimized model (model group 1) into model group 3. This model group is under three-point bending. RF-optimum results are significantly better than RF-analytical results.....	91
Figure 5.11. Detailed, analytical and optimum reaction force comparison of the model group 3. Ribbon direction shifted to the y-axis direction. RF-optimum results are better than RF-analytical.	92
Figure 5.12. Comparison of rate of errors of the analytical models (initial error) with the optimum errors. Optimum errors are less for all face sheet thicknesses.....	92
Figure 5.13. Detailed, analytical and optimum reaction force comparison of the model group 4. Ribbon direction is in the x-axis direction. This model represents a cantilever structure. RF-optimum results are very close to the reference values while RF-analytical results can both over- and under-predict the reference values.	94
Figure 5.14. Detailed, analytical and optimum reaction force comparison of the model group 4. Load and boundary conditions were replaced in the y-direction. RF-optimum results are significantly better than RF-analytical.....	94

Figure 5.15. Comparison of rate of errors of the analytical models (initial error) with the optimum errors. Optimum errors are less for all face sheet thicknesses.	95
Figure A.1. Average distance between the individuals.	109
Figure B.2. Von Mises stress results of the detailed FE model of the model group 1 with face sheet thickness equal to 0.36 mm.	111

LIST OF ABBREVIATIONS

ABBREVIATIONS

<i>Diff.</i>	Difference
<i>FE</i>	Finite Element
<i>GA</i>	Genetic Algorithm
<i>HOBE</i>	Honeycomb Before Expansion
<i>Ind.</i>	Individuals
<i>Nomex</i>	Aramid paper material impregnated in phenolic resin
<i>No.</i>	Number
<i>opt</i>	Optimum
<i>RF</i>	Reaction Force
<i>Rib</i>	Ribbon
<i>RibX</i>	Core ribbon direction in global x-axis
<i>RibY</i>	Core ribbon direction in global y-axis

LIST OF SYMBOLS

SYMBOLS

a	Inclined cell wall length
b	Horizontal cell wall length
d	Distance between two horizontal cell walls
E	Young's Modulus
E^*	Young's modulus of the core material
G^*	Transverse shear modulus of the core material
h	Core height
L	Core ribbon direction
t	Thickness of an inclined cell wall
t'	Thickness of a horizontal cell wall
W	Core width direction
φ	Cell angle
ρ	Core density
ν	Poisson's ratio
G_{13}	Transverse shear modulus in 13-direction
G_{23}	Transverse shear modulus in 23-direction

CHAPTER 1

INTRODUCTION

1.1. Definition of Sandwich Structures

A sandwich structure is type of composite structure consisting of different layers of materials brought together to form a new structural element which can efficiently react against a large spectrum of loads. A typical honeycomb core sandwich panel is shown in Figure 1.1; it has upper and lower faces, a core material and adhesive layers which bond faces to the core. The faces are thin, core is lightweight and weak in strength. However, when they are bonded together a sandwich structure with a high overall bending stiffness and low density is formed.

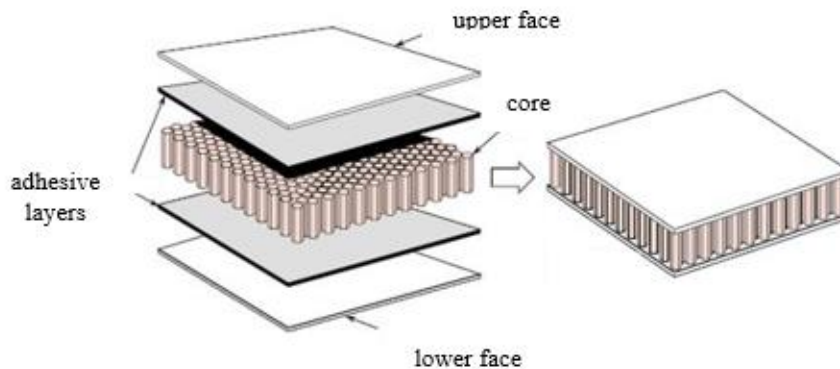


Figure 1.1. Honeycomb sandwich panel. It has upper and lower face sheets, adhesive layers and a core in between [1].

Sandwich structures have different application areas ranging from energy to aerospace. For instance, sandwich structures are used in the wind turbine blades. A typical design of a wind turbine blade is shown in Figure 1.2. There are sandwich panels employed in the leading edges of a wind turbine blade to increase the buckling resistance against edgewise loading. Further application of sandwich panels to the wind turbines are under investigation as the spans of blades become larger. The

maximum rotor diameter of a wind turbine was 16 meters in 1978 while it has increased to 125 meters in 2004 and the energy production capacity has increased from 50 kW to 5MW. This inevitably means that a wind turbine blade is subject to higher edgewise and flatwise bending moments and new structural solutions such as sandwich panels are likely to be employed [2].

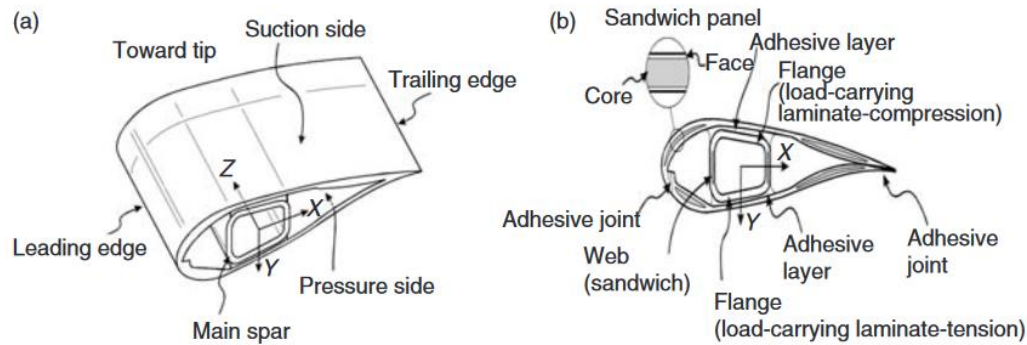


Figure 1.2. (a) Aerodynamic profile of a wind turbine blade. (b) Design details of a wind turbine blade. Sandwich panels are employed in the leading edge [2].

Another application area of the sandwich structures is the civil engineering. Steel-concrete-steel (SCS) sandwich structures are formed to benefit from the advantages of both steel and reinforced concrete. SCS sandwich structures were designed as an alternative to roadway decking for long and medium span bridges in 1970s. However, the strength of interface bonding between steel and concrete was found to be weak. In 1989, the weak bonding problem was solved using shear connectors shown in Figure 1.3 and SCS structures were used in the submerged tunnels. Then, the application area was enlarged to oil production facilities, storage vessels, ship hull and caissons [3].

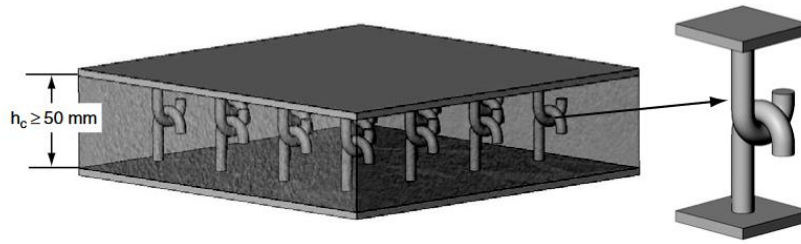


Figure 1.3. Steel-concrete-steel sandwich structure with J-hook connectors [3].

1.2. Brief History of Sandwich Structures in Aviation

The concept of sandwich construction is as old as the nature itself. Sandwich applications are the structural optimization of the nature, indeed. The trunk of a tree is an example for a sandwich structure with a foam core. The animal skeleton is another instance of it. The bones in skeleton are optimized in a foam core sandwich structure to handle diverse and combined loads they are subject to for years. On the other hand, bones of birds are filled with air sacs and porous core to minimize the weight. Like their broad appearance in the nature, the sandwich technology carves out a niche in the industries created by human such as aerospace.

The first usage of sandwich structures in aviation dates back to first flight of Wright Brothers in 1903. They used balsa wood sandwich construction in the wings of their flying machine [4]. In 1924, a glider plane whose fuselage was a sandwich structure was patented by T. von Karman and P. Stock. However, the usage of sandwich structures for weight saving and optimum design purposes started with World War II. The plywood sandwich construction was employed in the wing and fuselage parts of Mosquito night bombers built by the UK. In 1943, Vultee BT-15 fuselage was built by using fiberglass reinforced polyester as the face material and glass fabric as the core material. The first research paper about sandwich panels was written in 1944 by Marguerre in Germany. The first paper concerning the structural optimization of sandwich panels was published by Flugge in 1949. However, the industrial application of the sandwich panels was driven by Hexcel Corporation founded by two World War II veterans in 1940s. The company, today, produces more than half of the cores used

in the world [5]. However, the invention of commercially available honeycombs was made by a circus proprietor George May and exhibited in Farnborough Airshow in 1940s. Later, his idea was improved by impregnating the honeycomb paper with the phenolic resin, which resulted in today's semi-finished product [6].

With development of the new materials and need for lighter aircraft, composites and sandwich structures have started to appear more often in the aviation. In 1983, Airbus started using composites for large structures and the rudder of A310 aircraft was equipped with honeycomb sandwich panels [6]. The usage of sandwich in commercial aviation is also increasing very fast. For instance, it was only 8% of the wetted surface of Boeing 707 made of sandwich but it is 46% for Boeing 757. The fuselage of Boeing 747 is primarily Nomex sandwich [1]. Airbus A380 which is one of the largest aircraft, has also many sandwich parts such as radome, fairings, rudder, aileron, spoiler and interior parts shown in Figure 1.4.

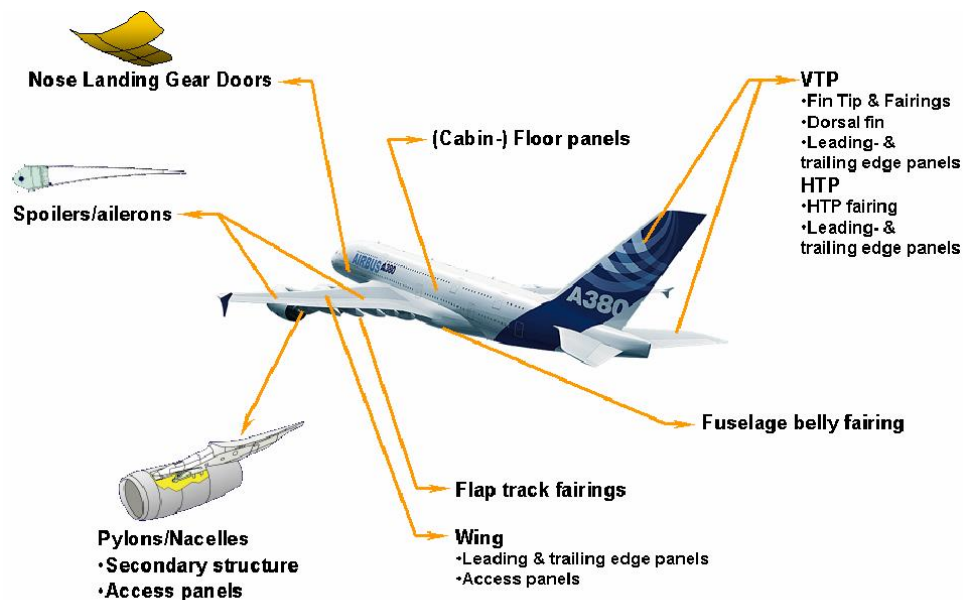


Figure 1.4. Airbus A380 has sandwich structures used in vertical and horizontal stabilizers, fuselage belly fairings, pylons, spoilers and ailerons, wing edges, nose landing gear doors and cabin interiors [6].

1.3. Scope of Thesis

Chapter 1 includes a brief historical development, definition and general usage areas of the sandwich structures. Then, sandwich applications specific to aviation are explained. Chapter 2 involves a literature survey about finite element modeling and analysis of sandwich structures, determination of equivalent core properties. Then, a brief history of the genetic algorithms is explained and studies about optimization of sandwich structures are presented. Chapter 3 delivers basic information about sandwich panels such as their mechanical behavior, advantages over traditional structures and manufacturing methods. Then, the equivalent core formulas are given. Finally, the finite element modeling methods are explained. The mesh convergence study is shown and the details of the finite element models are explained. Chapter 4 focuses on the genetic algorithms and defines their important parameters. In this chapter, the algorithm parameters are tested and the interface which connects ABAQUS, ABAQUS2MATLAB tool to the genetic algorithm is explained. In Chapter 5 the results and verification of the optimized parameters are given. The improvement obtained by optimization is shown. In the last chapter, Chapter 6, discussion related to the results are presented and the further development possibilities of the work are issued.

1.4. Outline of the Thesis

Sandwich structures consist of two or more individual components with different properties to form a light weight and high strength, ultra-performing new structure. A typical sandwich panel has two face sheets, a core between the sheets and adhesive layers which bond the core to them. The face sheets are responsible for carrying the in-plane loads while the core carries the transverse loads. The core of a sandwich panel is usually a continuous, porous and low weight material. There are cores commercially available to the use of aviation industry, today. In this study, the core of the sandwich panel is selected from one of those and it is made of aluminum and in hexagonal honeycomb shape.

The usage of the sandwich structures in the aviation industry has been rapidly increasing especially for weight saving purposes, lately. This high demand has turned the accurate finite element analyses of them into a critical issue. There are several finite element modeling approaches developed. The first one is the detailed modeling approach. It involves modeling the core in its original three-dimensional shape. The second one is solid core modeling approach in which the core is replaced with a solid. The third one is the layered shell approach. It is a two-dimensional model and the core is replaced by a layer of a composite shell. The second and third approaches involve representing a porous and heterogeneous core as a continuous solid or shell. This transformation is called creating an equivalent core. There are analytically developed equivalent core formulas in the literature. Determination of the equivalent core properties is the most critical step in creating an accurate finite element model since detailed modelling is a difficult and costly approach. Out of three approaches, the most preferred and practical one is the layered shell approach. It is the computationally least expensive one. In this thesis, a genetic algorithm-based optimization method is employed for creating accurate two-dimensional layered shell models of the sandwich panels with honeycomb cores.

The optimization method is based on the comparison of the reaction forces obtained from the detailed and layered shell models which are under transverse loads. There are four model groups created. All model groups involve a detailed and two layered shell models. One of the layered shell models use elastic properties from the literature that are analytically derived. The other layered shell model is the optimum model in which optimized core properties are employed. It is only the first model group whose core properties are optimized; the remaining three groups are created to test the performance of the optimization. They differ from the first group in terms of geometrical properties, loading or boundary conditions. A uniform transverse displacement was applied to the upper faces of the sandwich panels in all groups. Therefore, the sandwich panels are mainly subjected to bending and transverse shear which activate the transverse shear moduli of the core. These values are selected as

the key equivalent material properties to be optimized. The reaction forces obtained from the detailed models are considered as the reference ones and the optimization objective is to match the reaction forces obtained from the layered shell models with the reference ones. Then, the verification models are used to check whether the reaction forces obtained from the optimum layered shell models are in good agreement with the reference ones. If this is true, the optimization is considered to be successful. For this purpose, the genetic algorithm tool available in MATLAB is used. The analyses are done using ABAQUS [7]. Another tool called ABAQUS2MATLAB [8] is used to reorganize the analysis output data into MATLAB matrix format. An interface code is developed integrate the finite element solver, the post processing, the converter tool and the genetic algorithm together. The optimization is run for a certain type of core with six different face sheet thicknesses to investigate the effect of the stiffness of the face sheets on the equivalent core properties and the reaction forces.

There are studies in the literature which optimize the transverse core properties using different approaches whose overview is given in Chapter 2. Among the other studies, this study combines three different focus points together. Firstly, in this study, the optimization process is based on the reaction forces because one of the main design criteria from static analysis point of view is to check the reaction forces occurring in a certain location of a structure. In other words, for an efficient sizing of a design solution, accurate reaction forces must be obtained. This involves creating accurate finite element models with verifiable degree of simplification. For instance, two-dimensional layered shell modeling approach is the most common method for the analysis of the sandwich structures; however, the transformation of core properties from a three-dimensional porous medium to a layer of a composite shell comes with an error. The erroneous results may misdirect the design process and cause unexpected failures of heavy components. Secondly, the verification models in this study include sandwich designs with monolithic, ramp and full sandwich regions shown in Figure 1.5. In the real aviation applications, the sandwich structures are installed to airframe from their monolithic edge regions. These are the beginning or end regions where two

face sheets are attached to each other without a core in-between. The sandwiches are fastened from these regions. Thus, reaction forces occurring on them are important sizing inputs. In addition, a typical industrial sandwich panel has ramp regions where the height of a core is escalated to its full length gradually. Ramp regions are designed to avoid abrupt thickness changes and stress concentrations. However, material level testing of the sandwich structures are done on the plain sandwich panels. In this study, a similar method is followed. The optimization is done on a plain sandwich panel; then, the performance of the optimized results are tested on sandwich structures with monolithic edge and ramp regions. Thirdly, the effect of the stiffness of the face sheets on the equivalent core properties are investigated by changing and re-optimizing. Six different face sheet thicknesses which are commonly used values for aluminum are selected and for each of them optimum transverse core shear moduli are extracted. In this way, the effect of the face sheet thicknesses are also included.

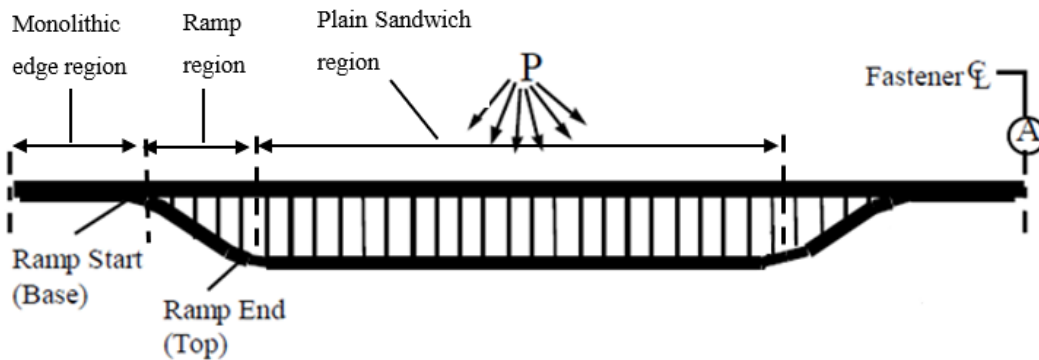


Figure 1.5. Sandwich panel with monolithic edge, ramp and plain sandwich regions [9].

CHAPTER 2

LITERATURE SURVEY

2.1. Finite Element Analysis and Equivalent Properties

There has been an increased interest in sandwich panels in the aviation. This has turned the structural analysis of them into an important issue. The finite element method is the most prevalent method used in the structural analysis problems for the last few decades. Depending on the required output and degree of accuracy different finite element modeling approaches can be used. There are three types of sandwich finite element modeling approaches used in the industry today [10]. These are detailed modeling, layered shell modeling and continuum modeling approaches. A summary of the modelling approaches is presented in Table 2.1. The detailed modeling approach involves modeling the core in its original shape. This is a computationally expensive method and usually not preferred. However, detailed modeling approach is useful when certain behavior of sandwich panels needed to be investigated. The other methods are more practical. In these approaches, the core is replaced by an equivalent model whose mechanical behavior is assumed to present the detailed core. This transformation process is done by employing equivalent properties for the core and the related material properties are the equivalent properties.

Table 2.1. *Sandwich structures finite element modeling approaches* [10]

Detailed Modeling Approach	<ul style="list-style-type: none"> • Detailed geometry of a core presented with shell elements • Computationally expensive
Layered Shell Modeling Approach	<ul style="list-style-type: none"> • Face sheets and core are modelled as different layers of a composite beam using shell elements • First order shear deformation theory is used as element formulation • Computationally less expensive • Requires equivalent core properties
Continuum Modeling Approach	<ul style="list-style-type: none"> • Core is modeled with continuum elements • Higher order shear deformations theories can be used • Computationally expensive • Requires equivalent core properties

The determination of the equivalent properties of the core is the most critical process for the finite element analysis of the sandwich panels. There has been a great academic effort to create the mathematical models of the cores.

Masters and Evans [11] worked on honeycomb properties by taking deformation caused by flexure, stretching and hinging type of loadings into the account. They developed mathematical models for each of the material constants in terms of the cell geometry and the cell wall material. They developed 2D analytical models for in-plane elastic constants E_1 , E_2 , G_{12} and ν_{12} .

Grediac [12] worked on unit cell using finite element method to calculate the transverse shear moduli of honeycomb core including the effect of the core thickness. In the study, finite element study was conducted on a representative unit cell and through the thickness stress fields were obtained. However, prior to Grediac, Kelsey et al. [13] employed minimization of potential energy method and did experimental studies on the core and proposed upper and lower limits for transverse shear moduli. Shi et al. [14] also worked on the study of Kelsey by two scale method of equivalent

property determination for periodic media and obtained first order equivalent transverse shear moduli. Then, they evaluated the equivalent transverse shear stiffness by finite element method and proposed that the equivalent transverse shear stiffness of a honeycomb core is dependent on the geometry of sandwich panel.

Gibson and Ashby [15] also worked on the material properties of the honeycomb. They assumed uniformly distributed shear stress through the cell walls and employed the energy approach to derive transverse shear moduli of honeycomb. Then, they conducted experiments on the honeycombs and found a good agreement between the analysis and the experimental data. They provided formula for E_3 , G_{13} , G_{23} and ν_{13} . Zhang and Ashby [16] also performed test on honeycombs to validate the numerical modeling of Nomex honeycombs. They focused on the out-of-plane properties of honeycombs and checked the related failure modes such as buckling and core shear failure. They also found agreement between the model and the data. Nast [17] also followed an experimental approach and derived equations for the elastic constants.

Burton et al. [18] modeled the sandwich core and the face sheets with three-dimensional solid element and two-dimensional shell elements to predict free-vibration responses of sandwich panels. They employed different approaches and compared the vibration frequencies obtained from continuum model with the two-dimensional model and found that their results are close to upper bound energy approach [19].

Aydincak and Kayran [20] evaluated performance of the existing equivalent material models in a comparative study. In their study, detailed models of sandwich panels and related continuum models with different equivalent elastic constants were created. The performance of an equivalent elastic constant was evaluated by comparing the total reaction force obtained from continuum model with the detailed model. It was found that in-plane constants of Master and Evans [11] and out-of-plane constants of Grediac [21] give the best results.

Cinar et al. [22] studied with the equivalent core properties to simulate the modal behavior of sandwich panels. In their study, detailed and layered shell modeling approaches were used and equivalent core properties were taken from the literature. The modal analysis results between different modeling approaches were compared. The differences between the results were found to be stemming from the equivalent core properties.

The academic papers involving determination of equivalent properties and finite element analysis of sandwich structures are countless. The common point of those studies is that equivalent core properties are one of the most important issues for an accurate analysis of the sandwich structures but they come with an error. There is a significant amount of work done to overcome this adverse impact. Analytical and experimental improvements on the equivalent properties are still an attractive issue for the researches. In addition to this, computer simulation-based numerical methods are popular. Optimization is one of these methods.

2.2. Optimization of Sandwich Structures and the Genetic Algorithm

Optimization is a methodology which makes a design, system or decision as functional and effective as possible. Optimization methodology can be applied to different areas ranging from banking to engineering. Structural design and analysis are one of the areas where the optimization methodology is employed. There are certain types of algorithms which are employed for the structural optimization and the genetic algorithms are one of those.

Genetic algorithms are optimization algorithms which can maximize or minimize certain problems and find optimum solution(s). The genetic algorithms belong to the evolutionary computation field and imitate the biological evolution process such as natural selection, mutation and survival of the fittest [23]. That is the reason why they are called genetic algorithms. The genetic algorithms are powerful tools because they are independent of gradients and their search processes are random like that of the biological evaluation [24]. In fact, this is a unique point of the genetic algorithms and

it enables genetic algorithms to deal with broader selection of problems without requiring any extra information about them.

The genetic algorithms have been attracting great attention of the scientists who have studied artificial intelligence since mid-twentieth century. Many of them tried to create a program which can simulate the evolution theory. In 1954, Nils Barricelli published "*Esempi Numerici di processi di evoluzione*", a study in what would now be called artificial life [9, 11] which is one of the first studies about evolutionary computation and made him pioneer of the field. After Barricelli, the genetic algorithms had been extensively studied by the biologists to observe evaluation via a computer simulation since the real evaluation process takes millions of years. On the other hand, in 1950s Alan Turing had already started working on simulating the chemistry of biological growth what is now considered as the earliest works on the artificial intelligence [26].

The algorithms developed until 1960s had focused on the simulation of the mutation. It was John Holland who was inspired by the systems adopting themselves to the surroundings and invented the genetic algorithm as in the context used today [13, 14]. Holland was able to carry the evolutionary programming to a new level by adding crossover, recombination, reversion and *theory of survival of the fittest* to the genetic algorithms. Later, in 1975 he published the book *Adaption in Natural and Artificial Systems* in which the mathematics beyond the evaluation are explained [28]. However, it was not Holland but his doctoral student Kenneth De Jong who presented a subtle work for employing the genetic algorithms to solve the optimization problems [29].

In 1970s and 1980s, the idea of employing the optimization methods to solve the problems started to be coupled with the fast improvements in the information technologies. This resulted in, increased attention on the optimization methods and genetic algorithms in particular. The researches had faced the limitations of the traditional optimization methods when the complexity of the world problems increased. There are several traditional methods which have been used and still appear as the best solution to the problems with certain level of complexity. The first

traditional method is the calculus-based method which includes finding maximum and minimum values of a function using basic technics such as first and second derivative tests or Lagrange multipliers. The calculus methods must deal with point-by-point solution and gradients. Although they are easy to apply and likely to converge fast, they might be stuck around a local optimum point. The second method is the exhaustive search method. This method was found to overcome the local optimum problem of the calculus methods since it discretizes a finite space and tests all the points. However, the drawback with this method is that if the finite solution space is expected to be large, reaching a solution becomes exhaustive as its name suggests [24]. As a response to points where traditional methods have paralyzed, the genetic algorithms came with salient solutions to the researchers. Firstly, they solved the local optimum problem of calculus-based methods by starting the processes with a population of possible solutions instead of a single point. In addition, the genetic algorithms do not need derivatives to pass to another solution point; instead, the guidance of the genetic algorithms is the numerical fitness value it assigns a solution point. Secondly, the genetic algorithms do not need to evaluate all the points in a space like exhaustive search methods do. They work on a set of a randomly selected points which is called a population and can alter the population by evolutionary operations such as mutation and crossover. Therefore, they can converge faster to a global optimum point without exhaustively evaluating every single solution candidate [24].

The advantages of the genetic algorithms over traditional algorithms also raised commercial and industrial interests. In 1980, General Electric Company made the first industrial genetic algorithm code available for the optimization of the production lines. In 1989 the first commercial genetic algorithm code, Evolver, released. Evolver is still commercially used tool by various businesses [30]. In addition to controversial commencement of the genetic algorithms to simulate the evaluation for biological purposes, they have become the basis of the machine learning and artificial intelligence today, as Alan Turing suggested in 1950s [26]. Today, the algorithm is employed in smart phones, self-driving cars, windmills, logistics, finance or any other

products such as a refrigerator in an ordinary kitchen where an optimum solution is needed. Therefore, the genetic algorithms have become one of the most commonly used optimization tools in different research areas.

The genetic algorithms are employed in the structural optimization, as well. Abouhamze [31] used genetic algorithms for the buckling optimization of the sandwich panels. In the study, foam and honeycomb cores were used. Foam core was modeled as an isotropic material while the honeycomb core was orthotropic material. A finite element solver was created using MATLAB and the differential equations of the buckling problem were solved using the MATLAB genetic algorithm tool. The sandwich structure was optimized for the buckling strength for different boundary conditions.

Wang et al. [32] optimized sandwich panels to benefit from their sound insulation purposes at minimum weight. A balance between acoustical and mechanical properties of a sandwich panel was set and the genetic algorithm was employed to minimize the area mass density of the sandwich panel. Eight different face sheet thicknesses and 16 different cores are evaluated. The material properties, thickness of face sheets and the core were optimized. Finally, mechanically efficient, light weight sound insulating sandwich panel configuration is offered.

Boudjemai et al. [33] worked with sandwich structures in terms of modal analysis. The study includes testing and the finite element analysis of the sandwich structures with clamped-free boundary conditions. A finite element model of the honeycomb core in its original hexagonal shape and an equivalent solid core model were created. The equivalent properties of the sandwich panel were reduced to an equivalent isotropic plate by determining its membrane and bending stiffness. The modal frequency results obtained from the equivalent model and the experimental data were compared. The difference was found to be less than 4% for the first two modes and 10% for the third mode. Thus, the equivalent modeling was found to have a good accuracy. In addition, it was found that the geometry and the material modeling of the

sandwich structures are effective on their modal responses. In another study conducted by, Boudjemai et al. [34] the sandwich panels used in the small sandwich structures are analyzed. The optimal width of the sandwich panel used in the iso-grid structures was determined using genetic algorithm. Iso-grid structures are arrays of equilateral triangle cuts and mostly used in space applications. Similar to previous study, an equivalent finite element solid model of the iso-grid structure consisting of sandwich panels was created. Then, the model was structurally optimized to achieve good strength and minimum weight. It was concluded that the application of the genetic algorithms to sandwich optimization results in a global solution; however, the solid modeling of the sandwich panels is expensive in terms of computing time and the memory.

Çınar et al. [22] employed MATLAB Genetic Algorithm tool to obtain accurate equivalent layered shell model. In the study, the detailed and 2-dimensional layered shell models were created. The modal frequencies are obtained from the detailed model and used as reference values for the genetic algorithm optimization. The equivalent properties of the honeycomb core were determined by analytical method into a 2-dimensional layer. The maximum difference between the natural frequencies obtained from the reference and layered shell models with aluminum core was around 4% and it was reduced to 1% percent after optimization. For the sandwich panel with Nomex core the maximum error was reduced from 13% to 1.20%. Similar improvements were also provided for displacement and the stress results. The optimization process was done for the sandwich with different face sheet and core materials. It was concluded that the stiffness of the sheets have impact on the optimized core material properties.

The optimization of the sandwich structures is not limited to genetic algorithm method although it is one the most common one used today. Qiao et al. [35] also worked on the optimization of the transverse shear moduli of the honeycomb cores. In their study, the honeycomb core is considered as a spatial repetitive material and determination of the equivalent core properties was based on a representative volume element

approach. The determination of equivalent properties was combined with a multi-objective optimization where transverse and overall shear stiffness values of the core are maximized by changing the geometric parameters such as cell wall thickness, cell angle of composite honeycomb cores. The results were verified using finite element method and the combination of the processes of the determination of equivalent properties and optimization was found to improve the transverse shear properties of the honeycomb cores.

Optimization based improvements are applied to the sandwich structures from material level to manufacturing processes. Particularly, the determination of the equivalent core properties, complexity of core and the effect of the stiffness of the face sheets make the sandwich structures open to improvements. Furthermore, the increased interest of the aviation industry to use of sandwich panels for lighter air vehicles motivates the research done on these structures.

CHAPTER 3

SANDWICH PANELS AND ANALYSIS

3.1. Basic Information about Sandwich Panels

The aircraft design has been evolving since the first flight of Wright brothers in 1903. The development in the materials and manufacturing industries provides new structural improvements to the aircraft. These improvements also lead the way to the unconventional designs such as composite structures and more complex shapes. Today, most of the aircraft benefit from both conventional and unconventional designs. Conventional design principles employ the conventional structures such as metallic materials or I-beams while unconventional designs include use of advanced materials and structures such as composite materials or sandwich beams. Although, the unconventional designs are considered to be under the development phase most aircraft companies try to increase the usage of them in their products. At this point, the sandwich beams appear more often than ever on the aircraft. There are similarities and differences between sandwich and I-beams.

There is a strong analogy between a sandwich beam and a conventional I-beam in terms of their design principles. According to Figure 3.1, in terms of design, the flow of the load thru an I-beam is similar to load flow of a sandwich beam. In an I-beam, the flanges are mainly responsible for carrying the in-plane loads and in the sandwich beam face sheets are responsible for the in-plane loads. The web of a flange carries mostly the shear loads and in a sandwich beam the core is designed to handle the shear loads. In spite of the similarities in their load flow paths, the sandwich beams have several advantages over traditional structures.

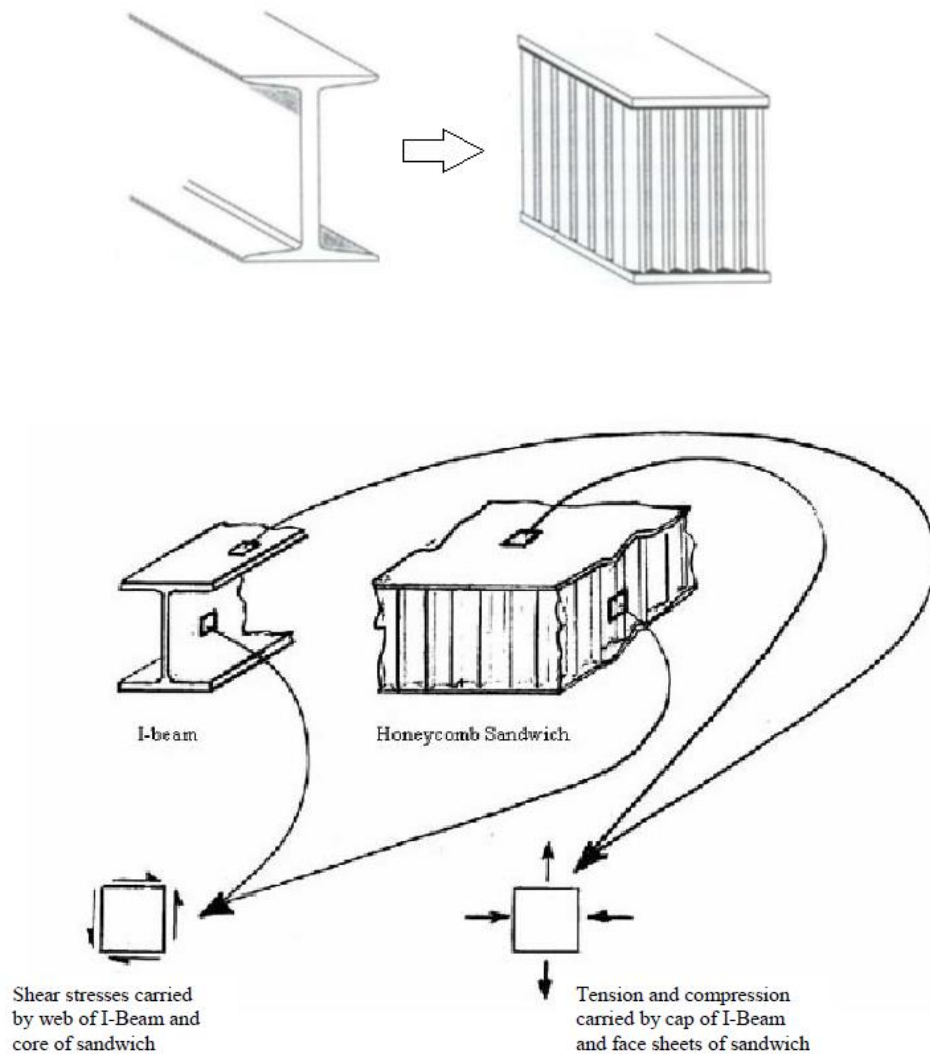


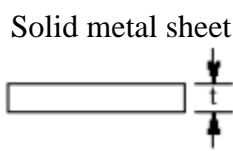
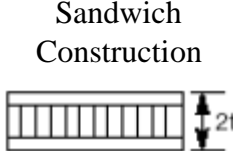
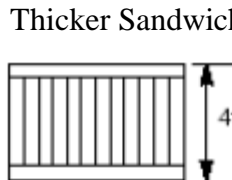
Figure 3.1. Design similarity between an I-beam and a sandwich panel. Flanges become face sheets and the web becomes core [10].

Firstly, a typical sandwich beam is stronger in bending stiffness than traditional structures. It is an efficient composition of different materials and can effectively react against both in-plane and out-of-plane loads. Thus, a sandwich beam can provide a better bending stiffness compared to a typical I-beam.

Secondly, the sandwich structures can provide great weight saving advantages compared to conventional structures. A comparison between a sandwich beam and a solid sheet is provided in Table 3.1 where the stiffness and weight values of a solid sheet of thickness t is normalized to 100. It is shown in the table that only 6% increase in weight leads to 925 times higher value of bending strength compared to those of the traditional solid metal sheet.

Thus, the sandwich panels and I-beams have similar load flow path but they differ in composition of materials and structural performance. A sandwich beam can provide satisfying stiffness and strength characteristics while not compromising on weight. These advantages made the sandwich structures high in demand of the aviation industry and resulted in a fast development in the design, analysis and manufacturing methods.

Table 3.1. *Sandwich structure characteristics* [9]

	 <p>Solid metal sheet</p>	 <p>Sandwich Construction</p>	 <p>Thicker Sandwich</p>
bending stiffness	100	700	3700
bending strength	100	350	925
weight	100	103	106

Since the Second World War, sandwich structures have been used as the primary aircraft components and the core materials have been manufactured with different methods and in various shapes [1]. There are mainly 5 methods to manufacture honeycomb cores. They are classified based on the technique attaching the cell walls to each other. These are thermal fusion, diffusion bonding, brazing, resistance welding and adhesive bonding. Thermal fusion, diffusion bonding, resistance welding and

brazing are not the most applicable methods to manufacture cores although they must be used if the core will be subjected to severe environmental conditions such as very high temperatures. The adhesive bonding method is the most common one. A great deal of the commercially available cores is manufactured with adhesive bonding method. It is less expensive compared to other methods. The adhesives used in this process are usually nylon epoxy and nitrile phenolic with maximum service temperatures about 204°C (400° F) or polyimide adhesives with 400°C (750°F) [1].

The adhesive bonding method involves 2 main processes to build honeycombs out of sheet materials. They are the expansion and corrugation processes. The first adhesive core manufacturing process is the expansion process. The expansion process appears to be more practical than corrugation process which is more labor intensive. The expansion process shown in Figure 3.2 involves cutting and stacking the sheets of the honeycomb material with adhesive lines printed on them. This results in a block of honeycomb material which is called HOBE (honeycomb before expansion). Then, the HOBE is cut into the slices per required thicknesses and expanded by causing plastic deformation in the adhesive-free sheets. At the end, a honeycomb core in its original shape is obtained.

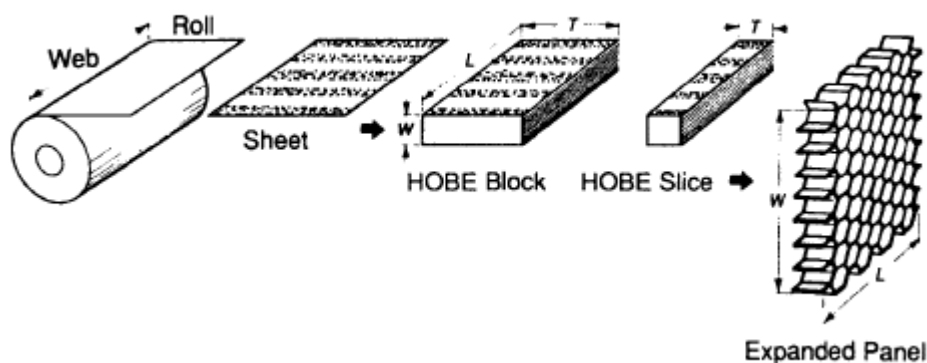


Figure 3.2. Expansion Manufacturing Process. Adhesive lines are printed on the sheets and stacked. Then HOBE (honeycomb before expansion) block is obtained. Then, HOBE is cut in to slices per required thickness and expanded in width direction by causing plastic deformation on the vertical walls [1].

There are nuances between the expansion process for the metallic and non-metallic cores. Unlike non-metallic cores, a corrosive resistance coating is applied on the metallic sheets before printing the adhesive lines on them. The honeycomb cores usually show difficulty in retaining their shapes after expansion. At this point, the metallic cores are better at retaining their shapes after expansion while the non-metallic cores have difficulty and must be held in a rack. Another difference stems from density requirements. To fulfil the required honeycomb core densities for non-metallic cores, the HOBE block is dipped in liquid resin of phenolic or polyimide and cured in an oven. This dipping and curing cycle is repeated not only for 2-3 times but sometimes for up to 30 times until the density requirements are satisfied [1]. Therefore, there are differences in the manufacturing processes of metallic and non-metallic cores.

The print lines on the sheets are also important for honeycomb manufacturing. The adhesive lines define the ribbon direction of the honeycomb cores and also limits the length of the core in ribbon direction. The lines can be printed as cross-line or in-line as shown in Figure 3.3. While the cross-line adhesive printing does not limit the length of the ribbon direction, the in-line adhesive printing limits it to the width of the HOBE block. The adhesive printing orientation can be important if long ribbon direction is needed or the sheet material is not isotropic.

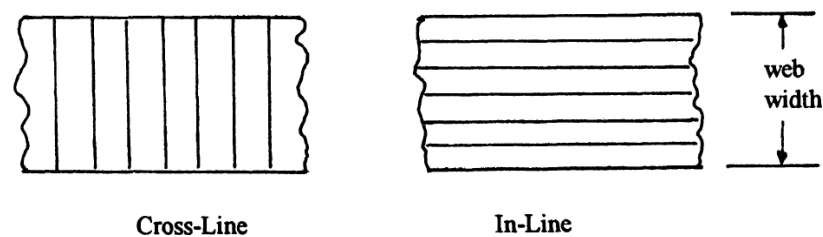


Figure 3.3. Adhesive Line (Print Line) Orientation. The print lines define the ribbon direction of the core. In line adhesive printing limits the ribbon length into the web width [1].

The second adhesive manufacturing process is the corrugation process. It is employed for specific types of honeycombs. Although it is a labor-intensive method, it is needed for the manufacturing of high-density cores. This method involves corrugating the

core as the first step and applying the adhesive afterwards. The process is shown in Figure 3.4. The corrugated sheets are attached to each other at their nodes and the corrugated block is cured in an oven. Since it is not possible to apply high pressure onto the corrugated block during curing, the adhesive is thicker compared to that of expansion process. For instance, when the cure temperature is set high, the press on a HOBE block can be elevated to 2.1 MPa (300 Psi), nevertheless; the maximum pressure which can be applied on a corrugated core remains far less [1]. This results in the differences of the percentage of adhesive a core contains. For instance, the adhesive can account for 10% of the total weight of a corrugated core while it is 1% for an expanded one. In addition, the non-metallic corrugated core blocks need resin dipping to achieve their target densities.

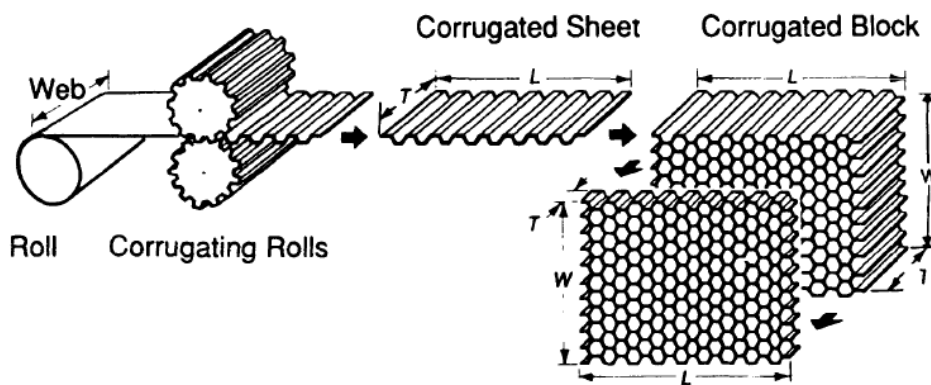


Figure 3.4. Corrugation Process. This process is labor intensive and used for the production of high-density cores. First, the sheets are corrugated. Then, they are attached to each other at their nodes and cured in an oven [1].

There is a large variety for the core sheet materials but the most common and commercially available ones are aluminum, Nomex, Kraft paper and fiberglass for the expanded cores and steel for the corrugated cores. However, it is possible to produce core from any sheet material including balsa wood. Particularly for the aviation industry, balsa wood honeycomb cores were used in the aircraft built by Wright Brothers for their first flight [36]. Today, the most preferred materials are aluminum and Nomex.

As a rule of thumb, it is suggested to prefer expanded products over corrugated ones [1]. Nevertheless, if the required core density for a certain design solution is higher than 192 kg/m^3 (12 pcf) then corrugated manufacturing process must be employed. On the other hand, the higher the density of a core the lower its geometric and manufacturing precision due to the resin dipping process. The common application in the aviation industry, today, is to use core with different densities and avoid high density corrugated cores wherever possible. In other words, such cores are used only in the regions where high stresses are observed.

There is another criterion to be considered when selecting the type of core for a certain design. The majority of the aviation components are curved and it is sometimes physically not possible to place a core appropriately. Different cell shapes shown in Figure 3.5 are developed to overcome this problem.

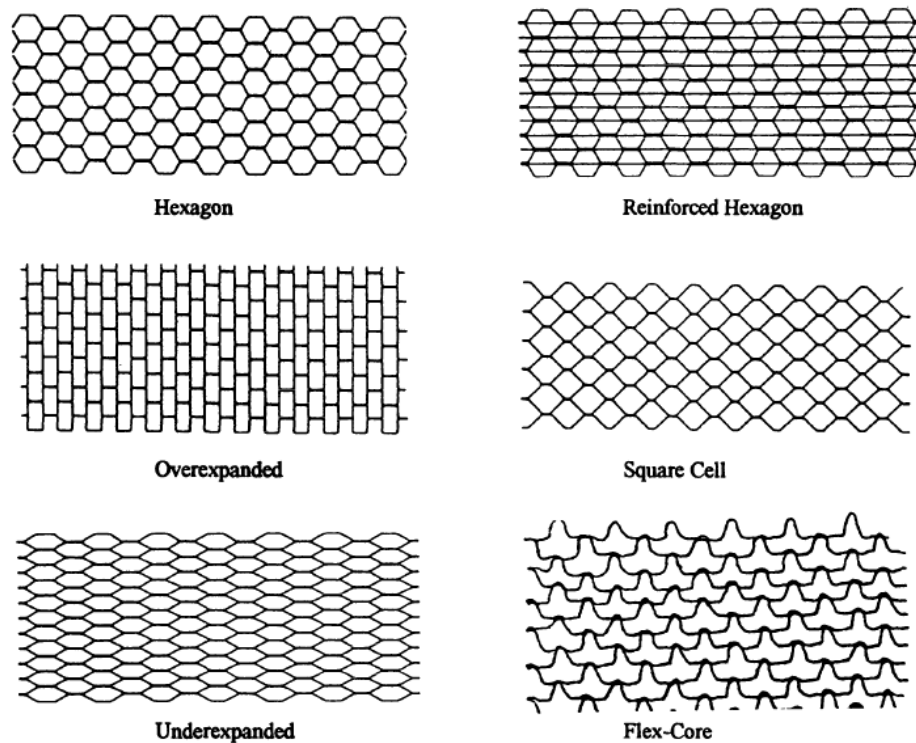


Figure 3.5. Cell Configurations. The most common cell shape is the hexagon. The core cell shape is selected according to design purpose. An over-expanded can form into a cylinder or a flex core can easily cover curved surfaces [10].

The hexagonal core the most common configuration. The over-expanded core is the over expanded rectangular form of hexagonal cells. Although the hexagonal configuration is suitable for most of the curved surfaces, the over-expanded cores are used for tubular surfaces since they can easily be formed into a cylinder around the width direction. The square cells have narrow nodes and they are produced using resistance welding or brazing manufacturing methods. The reinforced hexagonal core has extra sheets in the ribbon direction. They are particularly required if it is known that a component is loaded more in a certain direction. The flex core is the easiest to shape. For instance, it can be wrapped around a spherical structure. Therefore, the curvature of a surface is a critical parameter on the type of core to be used for a certain design solution.

To sum up, there are thermal fusion, diffusion bonding, brazing, resistance welding and adhesive bonding methods for honeycomb manufacturing. The first four methods are used if the design solution is required to operate under severe environmental conditions, else, the adhesive bonding method is preferred. The adhesive bonding method has two different manufacturing processes. They are the expansion and corrugation manufacturing processes. The honeycombs produced using expansion process should be preferred over corrugated cores because of their manufacturing precision on bonded walls, lower costs and successes in meeting the required core densities. However, if a very dense core is needed then the corrugated cores must be used. In addition, one should also pay attention to the shape of a core cell. Although the most common cell shape is hexagon, other cell shapes may perform better for highly curved surfaces. Therefore, the manufacturing method, required core density and the curvature of the application region are critical in the design of sandwich structures.

3.2. Sandwich Panel Analysis

The finite element method is the most common structural analysis method in the aviation industry. The wide spread of the method has been driven by the advances in the information technologies such as high-performance computers and user-friendly finite element software. Its typical application areas are structural analysis, aerodynamics and heat transfer. The unique point of the finite element method is that it creates system of algebraic equations and moves from one solution grid to another with the help of the pace a computer instead of human mind. This property of the finite element method has enabled engineers to deal with comprehensive boundary value problems. Thus, it has become easier to analyze advanced designs such as sandwich panels. There are special technics developed for the accurate finite element analysis of the sandwich panels. These are detailed modeling, layered shell modeling and solid modeling. The detailed modeling technics involve modeling the sandwich core in its original shape. However, this is difficult and computationally expensive. In response to detailed modeling an easier and more practical method has been developed which is called layered shell modeling. In this technic, the face sheets and the core are considered as different layers and the sandwich panel is modeled by stacking those layers. The model created becomes 2 dimensional. Hence, the modeling and computation time is considerably reduced. However, in this technic 3D core needs to be represented in 2D. The last finite element technic is the solid modeling. Compared to the shell representation of the core in the layered shell approach, solid modeling technic models the core with solid elements. Depending on the output required the face sheets might be modeled with solid elements or shell elements. This technic is preferred when there are direct transverse loads such as a point load on the sandwich panel and needs to be checked against the core crush failure. The details of the finite element modeling approaches are discussed in the following chapters

3.3. Determination of Equivalent Core Properties

Layered shell approach is one of the most common sandwich finite element modeling approach used today. In this approach 3-dimensional sandwich core is represented as a 2-dimensional layer. This requires transformation of 3D core material into 2D properties. This is done by employing the equivalent core properties.

The formulas derived for the determination of the equivalent material properties depend on the properties of the material the core is produced from and the geometric characteristics of a single cell. A sample geometry of a hexagonal honeycomb unit cell is shown in Figure 3.6. In the figure, a is the length of the inclined cell wall and b is the length of the horizontal cell wall. The wall thickness of the inclined wall is t while t' is the cell wall thickness. The parameter d is the cell size and it is the distance between two vertical cell walls of a unit cell. Another parameter is the cell angle, ϕ . The sandwich cores show anisotropic behavior. Thus, a material axis definition is needed. The axis named as L is aligned with the direction of the horizontal cell walls and it is called the ribbon direction. W direction is the core width direction and it is perpendicular to ribbon direction. An ideal hexagonal core has equal lengths for a and b and the cell angle is 30° . In addition, due to the expansion manufacturing method the cell wall thickness t' is 2 times of the inclined cell wall thickness t .

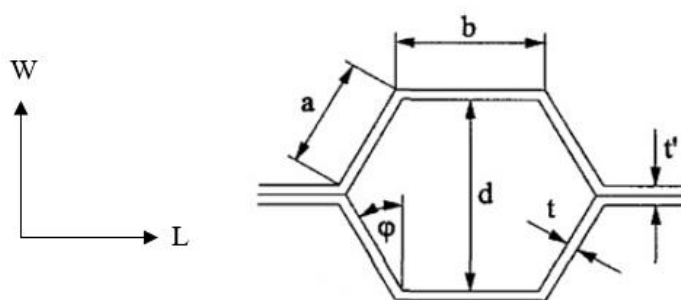


Figure 3.6. Unit Honeycomb Core Cell [1]

A summary of the unit cell parameters is shown in Table 3.2.

Table 3.2. *Unit Cell Parameters*

Parameter	Explanation
a	Inclined cell wall length
b	Horizontal cell wall length
φ	Cell angle
d	Distance between 2 horizontal cell walls
t	Thickness of an inclined cell wall
t'	Thickness of a horizontal cell wall
L	Core ribbon direction
W	Core width direction

In this study, the selection of the analytical material constants is based on the study conducted by Aydıncak and Kayran [20] in which an optimum combination of the constants developed by Masters and Evans [11] shown in Table 3.3, Gibson and Ashby [37] shown in Table 3.4, Nast [17] shown in Table 3.5 and Grediac [21] are used. The formulas developed by Grediac for the transverse core modulus are also used by Gibson and Ashby; they are shown in Table 3.4. In their study, Aydıncak and Kayran [20] found that the best combination of the equivalent properties involves using the formulas developed by Masters and Evans for E_1 , ν_{12} and G_{12} , Nast for E_2 , Gibson and Ashby or Grediac for G_{13} and G_{23} .

Table 3.3. *Formulas of the equivalent properties derived by Masters and Evans [11]*

Formulas by Masters and Evans [11]	
$E_1 =$	$\frac{1}{\frac{h \cdot \cos \varphi}{(a/b + \sin \varphi)} \cdot \left[\frac{\cos^2 \varphi}{K_f} + \frac{\cos^2 \varphi}{K_h} + \frac{2a/b + \sin^2 \varphi}{K_s} \right]}$
$E_2 =$	$\frac{1}{h \cdot \left(\frac{a}{b} + \sin \varphi \right) \left[\frac{\sin^2 \varphi}{K_f \cdot \cos \varphi} + \frac{\sin^2 \varphi}{K_h \cdot \cos \varphi} + \frac{\cos \varphi}{K_s} \right]}$
$v_{12} =$	$-\sin \varphi \cdot \left(\frac{a}{b} + \sin \varphi \right) \cdot \left[\frac{-\frac{1}{K_f} - \frac{1}{K_h} + \frac{1}{K_s}}{\frac{\cos^2 \varphi}{K_f} + \frac{\cos^2 \varphi}{K_h} + \frac{2a/b + \sin^2 \varphi}{K_s}} \right]$
$G_{12} =$	$\frac{1}{\left\{ A + \frac{1}{K_h} \cdot \left[\frac{b^2 + 2a^2}{a \cdot (b + a \cdot \sin \varphi)} \right] \cdot h \cdot \cos \varphi + B \cdot \left[\frac{\cos \varphi}{(b + a \cdot \sin \varphi)} + \frac{\sin \varphi}{\cos \varphi} \right] \right\}}$
$A =$	$\frac{h \cdot b^2 \cdot (a + 2b) \cdot \cos \varphi}{K_f \cdot a^2 \cdot (b + a \cdot \sin \varphi)}$
$B =$	$\frac{h \cdot (a \cdot \cos^2 \varphi + (b + a \cdot \sin \varphi) \cdot \sin \varphi)}{K_s}$
$K_f =$	$\frac{Ebt^3}{a^3}, K_s = \frac{Ebt}{a}, K_h = \frac{Gbt}{a}$

Table 3.4. *Formulas of the equivalent properties derived by Gibson and Ashby [37] and Grediac [21]*

Formulas by Gibson and Ashby [37] and Grediac [21]
$E_1 = \left(\frac{t}{a}\right)^3 \cdot \frac{\cos \varphi}{\left(\frac{b}{a} + \sin \varphi\right) \cdot \sin^2 \varphi} \cdot E^*$
$E_2 = \left(\frac{t}{a}\right)^3 \cdot \frac{(b/a + \sin \varphi)}{\cos^3 \varphi} \cdot E^*$
$E_3 = \left(\frac{t}{a}\right)^3 \frac{(1 + b/a)}{(\sin \varphi + b/a) \cdot \cos \varphi} \cdot E^*$
$\nu_{12} = \frac{\cos^2 \varphi}{(\sin \varphi + b/a) \cdot \sin \varphi}$
$\nu_{13} = \nu_{23} \approx 0$
$G_{12} = \left(\frac{t}{a}\right)^3 \frac{(\sin \varphi + b/a)}{(b/a)^2 \cdot \cos \varphi \cdot (1 + 16 b/a)} \cdot E^*$
$G_{13} = \left(\frac{t}{a}\right) \frac{\cos \varphi}{(\sin \varphi + b/a)} \cdot G^*$
$G_{23_{lower}} = \left(\frac{t}{a}\right) \frac{(\sin \varphi + b/a)}{(1 + b/a) \cdot \cos \varphi} \cdot G^*$
$G_{23_{upper}} = \left(\frac{t}{a}\right) \frac{(\sin^2 \varphi + b/a)}{(\sin \varphi + b/a) \cdot \cos \varphi} \cdot G^*$
$G_{23} \cong G_{23_{lower}} + \frac{0.787}{(h/a)} \cdot (G_{23_{upper}} - G_{23_{lower}})$

Table 3.5. *Formulas of the equivalent properties derived by Nast [17]*

Formulas by Nast [17]	
$E_1 =$	$\frac{t^3 \cdot (1 + \sin \varphi)}{12a^3 \cos^2 \varphi \left[\frac{\cos \varphi}{3} - \frac{1 + \cos \varphi}{8} \right]} \cdot \frac{E}{1 - \nu^2}$
$E_2 =$	$\frac{t^3 \cdot \cos \varphi}{(1 + \sin \varphi)a^3 \sin^2 \varphi} \cdot \frac{E}{1 - \nu^2}$
$E_3 =$	$\frac{2E^3 \cos \varphi}{(1 + \sin \varphi) \cos^2 \varphi} \cdot \frac{t}{a}$
$\nu_{12} =$	$\frac{(1 + \sin \varphi)^2 \cdot \sin^2 \varphi}{12a^3 \cos^2 \varphi \cdot \left(\frac{\cos \varphi}{3} - \frac{1 + \cos \varphi}{8} \right)}$
$\nu_{13} =$	$\frac{(1 + \sin \varphi)^2 \cdot t^2}{24a^2 \cos \varphi \cdot \left(\frac{\cos \varphi}{3} - \frac{1 + \cos \varphi}{8} \right)} \cdot \frac{\nu}{(1 - \nu^2)}$
$\nu_{23} =$	$\frac{t^2 \cos^2 \varphi}{2a^2 \sin^2 \varphi \cdot (1 - \nu^2)} \cdot \nu$
$G_{12} =$	$\frac{t^3 \cdot (1 + \sin \varphi)}{a^3 \cdot (1 - \nu^2) \cdot \cos \varphi \cdot (6.25 - 6 \sin \varphi)}$
$G_{13} =$	$\frac{2t}{a \cdot \cos \varphi \cdot (1 + \sin \varphi)} \cdot G$
$G_{23} =$	$\frac{10t}{9a \cdot \cos^3 \varphi \cdot (1 + \sin \varphi)} \cdot G$

In this study, the honeycomb was selected from the industrial catalog provided by Hexcel [38] which is one of the largest honeycomb producers in the world. The cell size is 9.53 mm (3/8 inch) and the cell wall thickness is 0.1016 mm (0.004 inch). The details of the calculation are explained in Chapter 4.2.

3.4. Finite Element Models

In this study several finite element models were created based on detailed and layered shell modeling approaches. The detailed models are used as reference models while the layered shell models are used for optimization and verification. There are 5 different finite element model groups in this study. Each group has both the detailed

and related layered shell models. The difference between the model groups is about their geometries or load types. Only one of the model groups were used for the optimization. The remaining 4 model groups are used to evaluate the performance of the optimization results with different shapes and under different loads. All the model groups were investigated with 6 face sheet thickness values. In the following chapters finite element models are explained in detail.

3.4.1. Detailed Models

The detailed model is the model where the cell walls are modelled with shell elements in their original hexagonal geometry. The detailed models are used to obtain reference reaction forces from a certain sandwich panel configuration.

The detailed model of the model group 1 is the reference model group and used for the optimization. The geometric properties of the detailed model are based on the number of cells. The model has 10 cells in the ribbon and width directions and considered to be square in terms of number of cells. The load applied to model group 1 is the downward enforced displacement of 0.1 mm. It is uniformly distributed to a square area of 2 cells length and width located in the middle of the upper face sheet. The boundary conditions are applied to the edges of the lower face sheet and to the point which is exactly in the middle of it. The edges are constrained in the global z direction and the middle point is constrained in the global x and y directions to avoid rigid body modes. The related visualization can be seen in Figure 3.7, Figure 3.8 and Figure 3.9.

There are 2 reference reaction forces obtained from the detailed model of model group 1. These are the reaction forces in the ribbon and width directions. Studying with the separate reaction forces was preferred to increase the accuracy of the optimization since the stiffness in the ribbon direction of the core is higher compared to width direction due to the double cell walls.

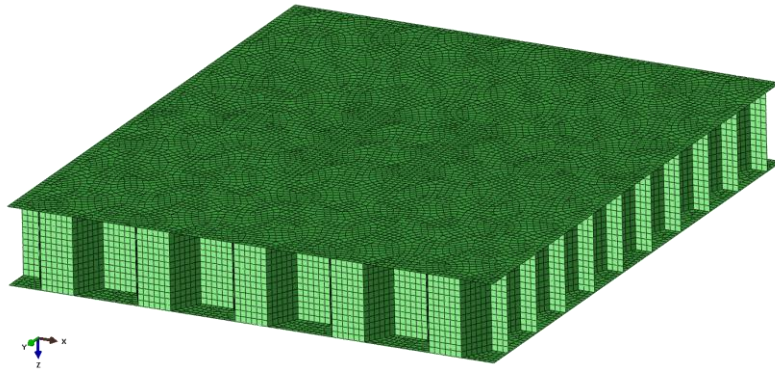


Figure 3.7. The Detailed Finite Element Model of the Model Group 1

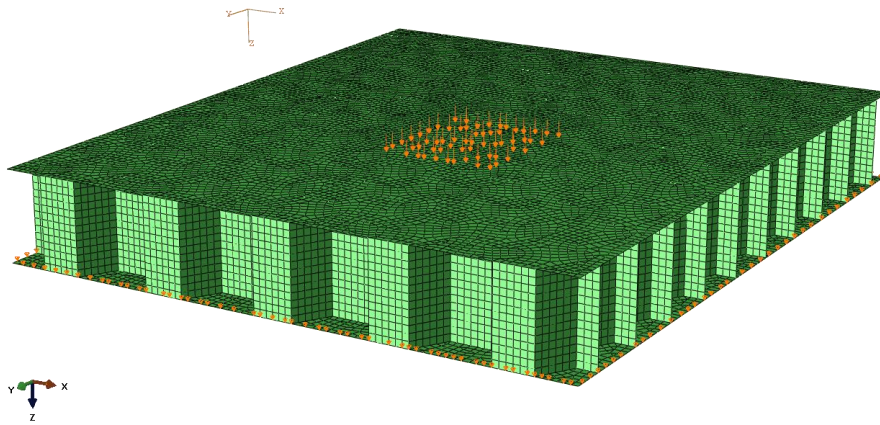


Figure 3.8. Enforced displacement of 0.1 mm applied downward (in z-direction) on the upper face sheet of model group1

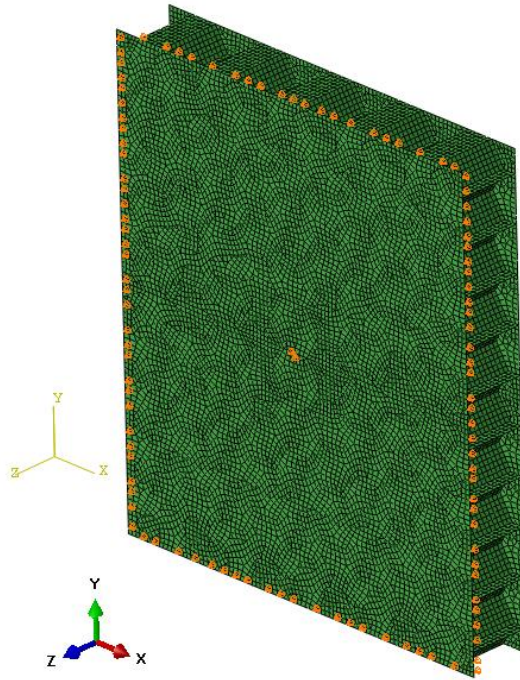


Figure 3.9. Boundary conditions applied on the lower face sheet of model group 1

The detailed model of the model group 2 is a verification model. It is quarter-model of a sandwich panel with a ramp region. There are 2 detailed models created for this model group. The difference between the detailed models is the orientation of the ribbon direction which is in global x and y directions to study its effect on the reaction forces. In both detailed models the load and boundary conditions were kept the same. Enforced uniform displacement of 0.1 mm is applied to the right lower corner of the upper face. The panel is constrained in z direction from the monolithic edge region and x and y symmetrical boundary conditions were applied to the ends. The models are shown in Figure 3.10 and Figure 3.11. The total reaction forces were collected from the detailed models with different core ribbon orientations as reference values.

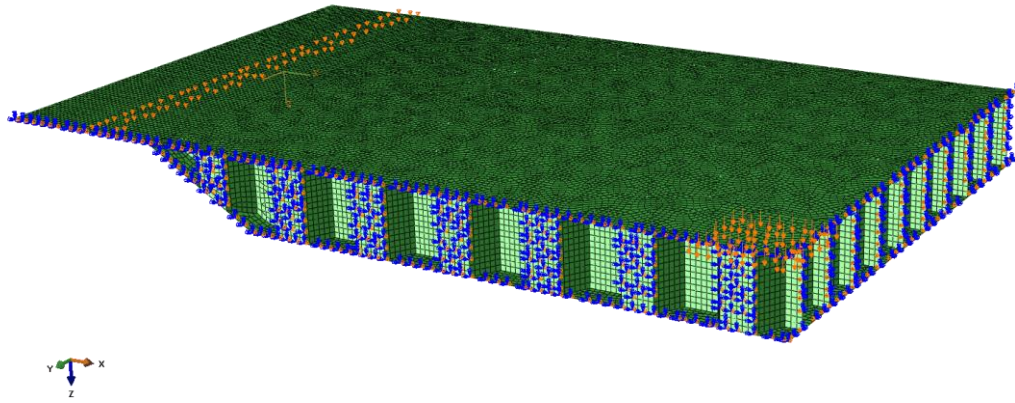


Figure 3.10. The Detailed Model of the Model Group 2 with the Core Ribbon Aligned with x Axis and the Boundary Conditions

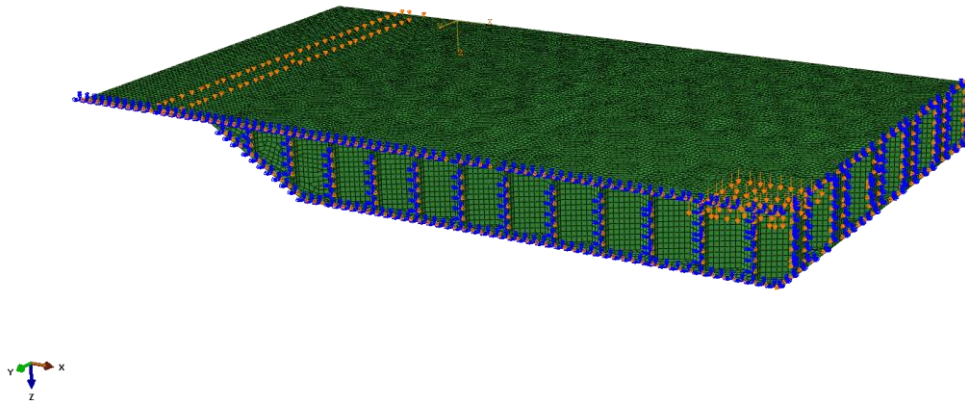


Figure 3.11 The Detailed Model of the Model Group 2 with the Core Ribbon Aligned with y Axis and the Boundary Conditions

The detailed model of the model group 3 is also a verification model and it is similar to the detailed model of model group 2. However, this time 3-point bending was simulated. The ribbon direction is also in x and y directions and total reaction forces were obtained from the models. Figure 3.12 and Figure 3.13 show the finite elements models of the model group 3 in both ribbon directions.

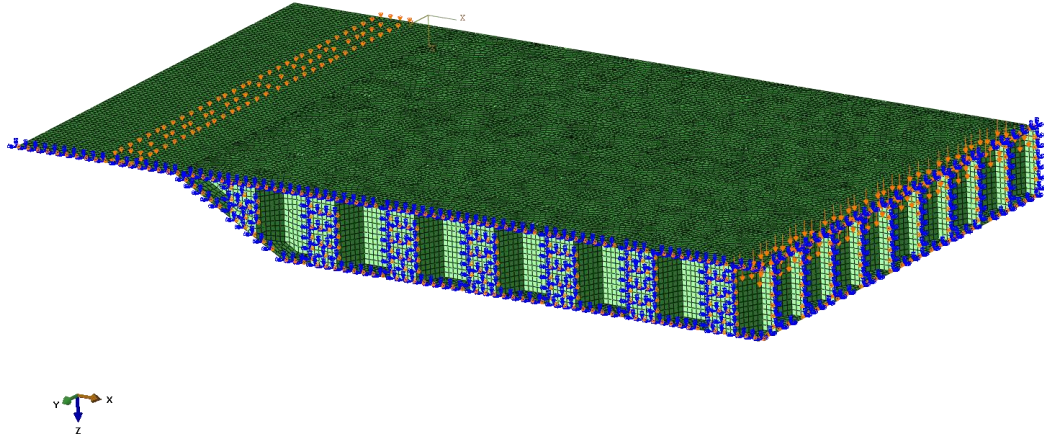


Figure 3.12. The Detailed Model of the Model Group 3 with the Core Ribbon Aligned with x Axis and the Boundary Conditions

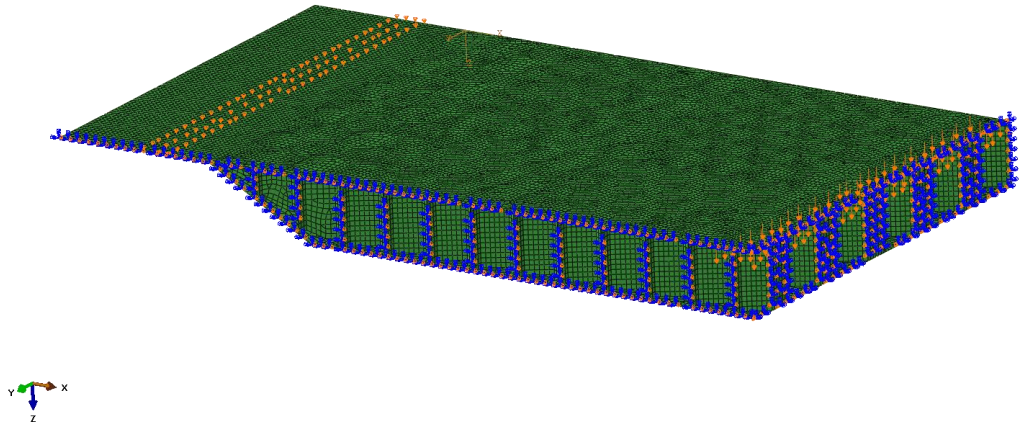


Figure 3.13. The Detailed Model of the Model Group 3 with the Core Ribbon Aligned with y Axis and the Boundary Conditions

The detailed model of the model group 4 is the last verification model has the same geometric properties with the model group 1. The difference is the regions where loads and boundary conditions were applied. Unlike the central and even loading of the first model, the fourth model simulates a sandwich beam under cantilever conditions. The displacement of 0.1 mm was applied to right and lower edges of upper faces and the beam was constrained in x, y, z directions in the left and lower edges of the lower face,

separately. Since this model has 10 cells in both directions, the region where the displacement and boundary conditions were applied shifted from x axis to the y axis instead of shifting the ribbon directions. Models are show in Figure 3.14 and Figure 3.15.

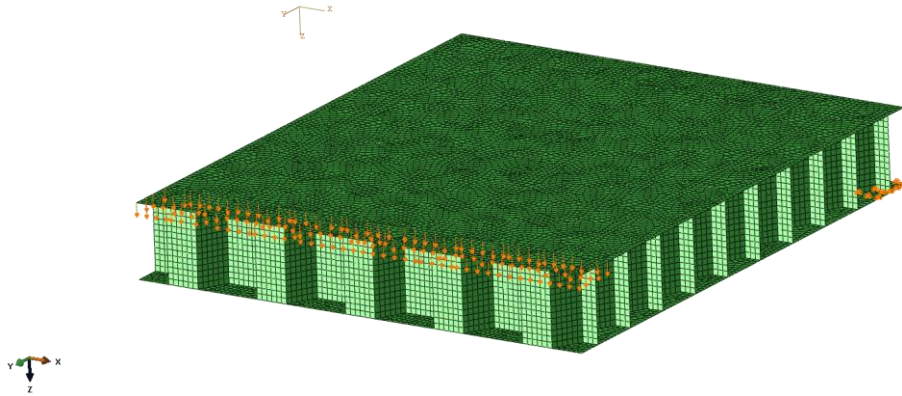


Figure 3.14. The Detailed Model of the Model Group 4 with Loading Along x Axis

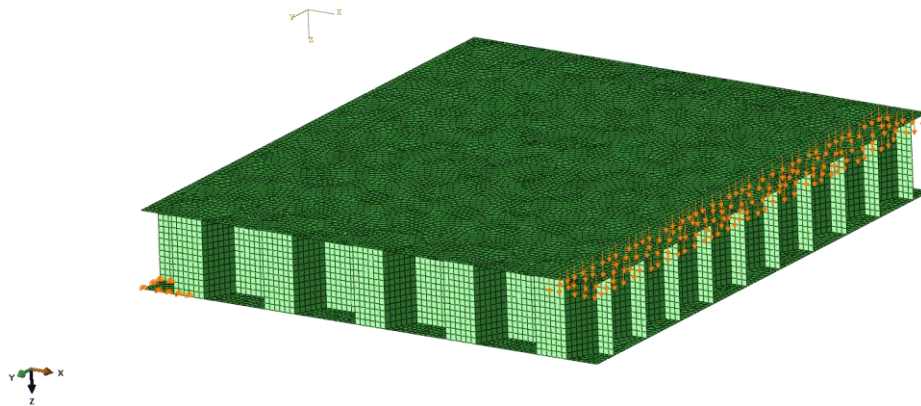


Figure 3.15. The Detailed Model of the Model Group 4 with Loading Along y Axis

3.4.2. Mesh Convergence Study

The mesh convergence study is done on the detailed model of the model group 1 shown in Figure 3.7, Figure 3.8 and Figure 3.9 Figure 3.7 by setting the element edge length to 0.5, 1 and 2 mm.

According to the mesh convergence criterion is satisfied. The details of the mesh convergence data are provided in . The reaction forces occurred due to the transverse loading obtained for 3 different element edge lengths (EEL) are almost coincidence. The maximum percentage difference between the reaction forces is around 1% which due to numerical error accumulations occurring during the analysis and processing. Therefore, the element edge length of 1 mm was selected.

The geometric orders of the elements are also tested by comparing the reaction forces in z-direction for the face sheet thickness of 0.36 mm. The reaction force is 725.45 N when linear elements (S4R and S3) are used while it is 727.83 N when quadratic elements (S8R and STRI65). Although the difference in the reaction forces is negligible, the solution time for higher order elements are significantly longer. Therefore, first order elements whose element edge lengths are 1 mm are preferred.

The finite element model whose element edge length is 1mm consists of 37712 nodes and 4118 elements of which 39191 are linear quadrilateral elements of type S4R and 1990 linear triangular elements of type S3. In Abaqus elements are named according to their formulations and properties. S4R elements are conventional stress-displacement shell (S) elements with 4 nodes and reduced integration (R). Similarly, S3 elements are triangular shell elements with 3 nodes.

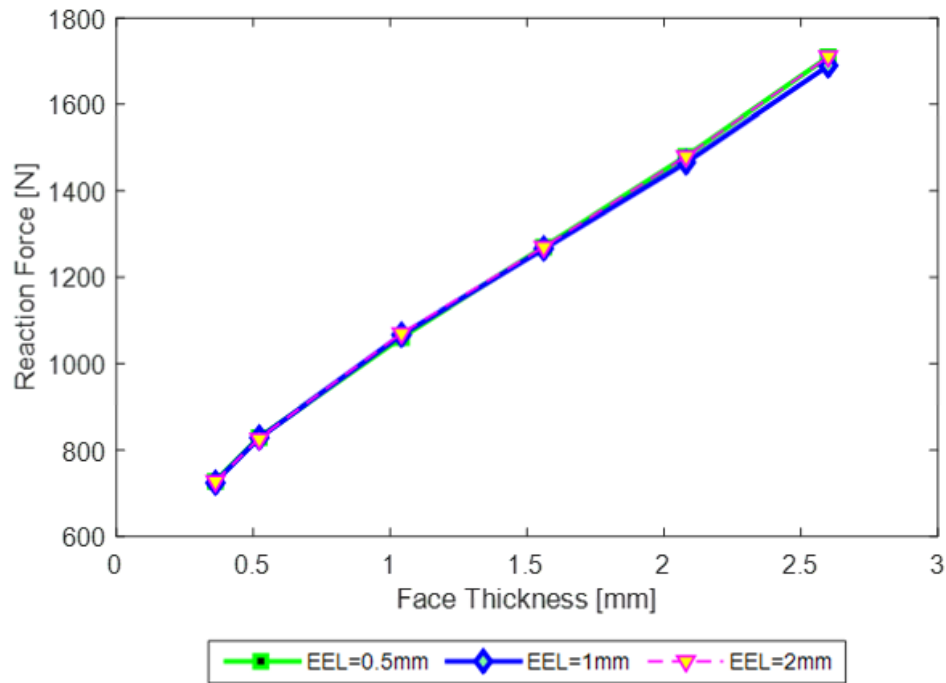


Figure 3.16. Mesh Convergence

Table 3.6. Mesh convergence data table. The difference between the data expected to be due to the numeric error accumulations occurring during the analysis and post-processing.

Face Sheet Thickness [mm]	RF for EEL=0.5 mm [N]	RF for EEL=1.0 mm [N]	RF for EEL=1.5 mm [N]
0.36	727.95	725.45	726.39
0.52	829.38	827.45	826.64
1.04	1066.37	1066.39	1068.41
1.56	1272.88	1265.33	1271.91
2.08	1478.19	1471.16	1477.62
2.60	1710.09	1707.89	1710.03

3.4.3. Layered Shell Models

The layered shell model is the 2D representation of the detailed models. In the layered shell models, the upper and lower face sheets and core are modeled as different layers of a composite beam. There are 2 different layered shell models for each of the detailed models.

The first one is the analytical layered shell model. It is called analytic because the 2D orthotropic material properties of the core are obtained from the formulas of the equivalent core properties explained in Chapter 3.3.

The second one is the optimum layered shell model. The optimum layered shell model has the optimized core shear moduli material inputs. The model group 1 is the only optimized model. The optimum layered shell models of the other model groups have the optimum material inputs obtained from the model group 1 and they are used for the verification purposes.

Each analytical and optimum layered shell model corresponds to its detailed model in terms of geometrical properties and boundary conditions. All the groups were investigated for 6 different face sheet thickness values.

The first layered model shown in Figure 3.17 is the 2D representation of the detailed model of model group 1 shown in Figure 3.7. This is the layered shell model which was provided to genetic algorithm as the finite element model input. There is an enforced displacement of 0.1 mm applied to the center and the edges are fixed in z direction. The node in the symmetry point was constrained in x and y direction to avoid singularity. These conditions are the same with the detailed model of group 1. The reaction force data is collected from the edges. Like in the detailed model, separate reaction force data were extracted from the nodes along x and y axis. The optimization process was run to match the reaction forces to the ones obtained from the detailed model. At the end of the optimum G sets (shear moduli) were obtained for each face thicknesses and the performance of the optimum G values were evaluated by plugging them into the layered shells models of the verification models shown from

Figure 3.10 to Figure 3.15. The details of the optimization process are explained in the following chapters.

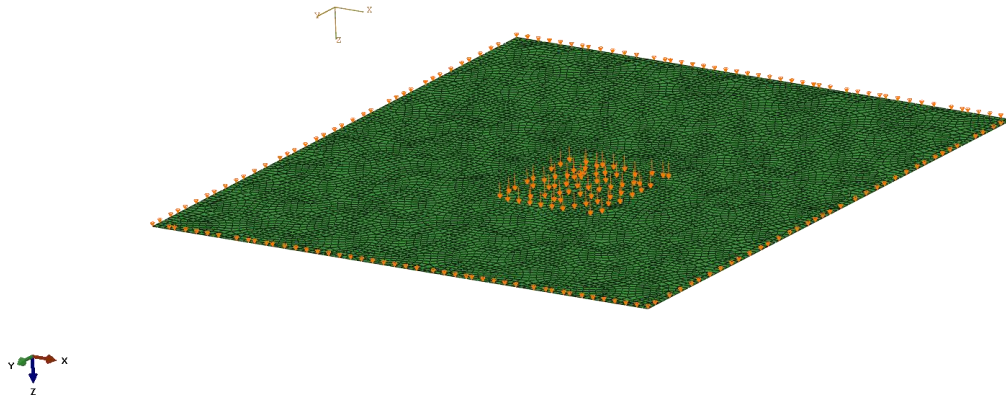


Figure 3.17. Layered Shell Model of the Model Group 1

The second layered shell model shown in Figure 3.18 is the layered shell model of the detailed model of group 2 shown in Figure 3.10 and Figure 3.11. The boundary conditions and the geometrical properties are the same. There are 4 layered shell models in this group. These are the analytical model whose core ribbon direction was aligned with the x axis and the optimum layered shell model whose out-of-plane core shear moduli were obtained from the optimization of the model 1. The remaining 2 layered shell models were created with the same logic; however, the core ribbon direction was shifted from x axis to y axis. This ribbon shift was done by changing the orientation of the layer representing the core from 0 degree to 90 degree with respect to material axis 1 shown in Figure 3.19.

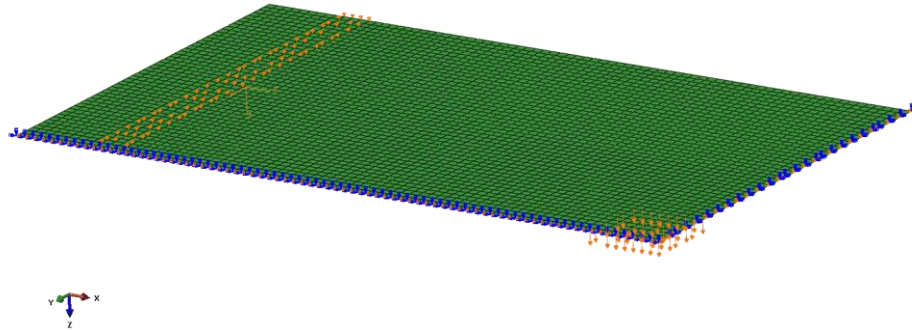


Figure 3.18. Layered Shell Model of the Model Group 2

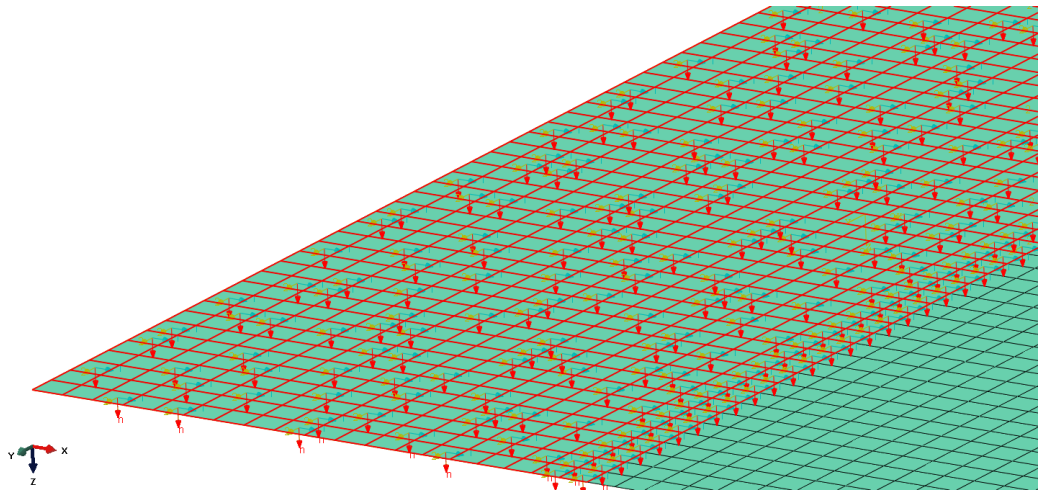


Figure 3.19. Material Orientation, Mat-1 axis is aligned with the global x-axis and the stacking direction is the global z-axis

The third layered shell model is the 2D model of the detailed model shown in Figure 3.12 and Figure 3.13. They were created as it was done for the layered shell models of the model group 2. The difference is that the third model group simulates the three-point bending. The model is shown Figure 3.20.

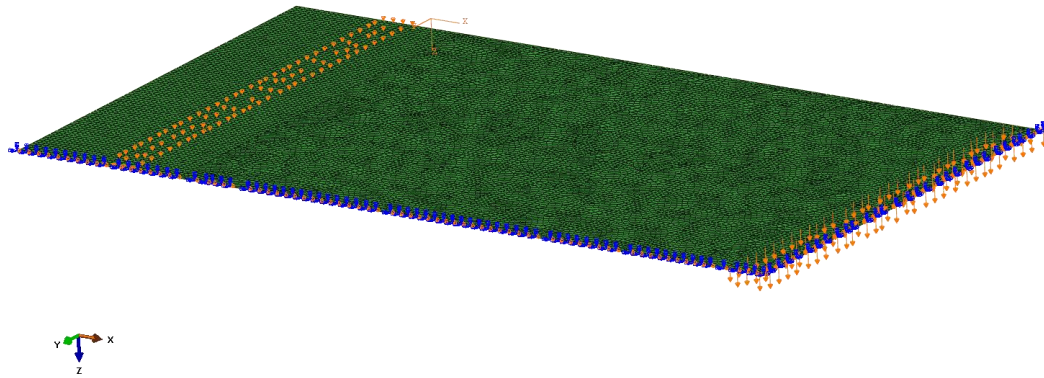


Figure 3.20. The Layered Shell Model of the Model Group 3 Simulating the 3-Point Bending

The fourth and the last layered shell model shown in Figure 3.21 and Figure 3.22 are the related 2D models shown in Figure 3.14 and Figure 3.15 of group 4.

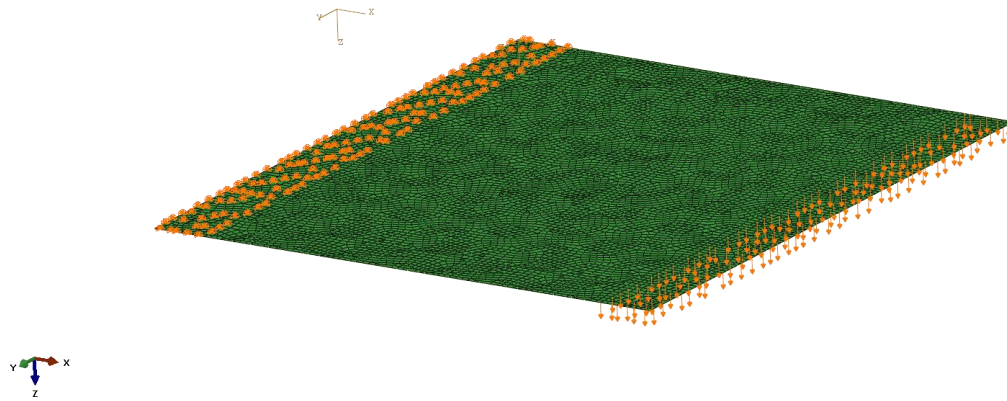


Figure 3.21. The layered shell model of the model group 4 with loading in z-direction parallel to y-axis.

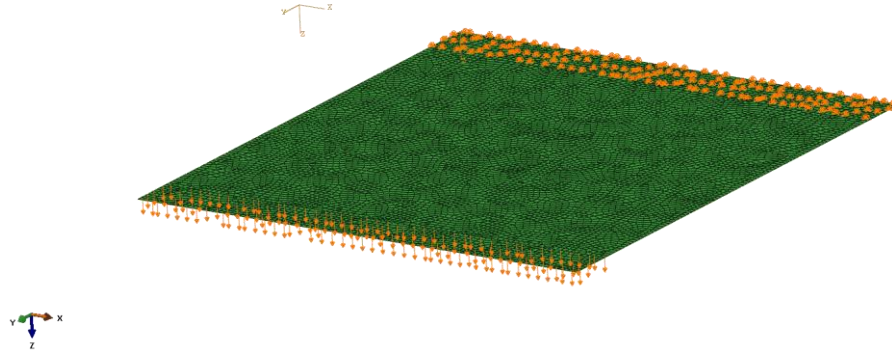


Figure 3.22. The layered shell model of the model group 4 with loading in z-direction parallel to y-axis

To sum up, the finite element method was used for modeling of the sandwich panels. The detailed models represent the sandwich panels in their original shapes while the layered shell models are the 2D representation of them. There are 5 different model groups and only the first model group used for the optimization. The other 4 groups were used for the verification purposes. The transition from 3D to 2D was done by determining the equivalent core properties. The models with analytical equivalent core G sets are called the analytical layered shell models. On the other hand, there are optimum layered shell models whose G sets were found by optimizing the model number 1. The layered shell modeling approach was preferred as an input for the genetic algorithm since it is easy to create and computationally less expensive compared to the detailed model. The reaction forces were collected from all the models. The performance of the optimization was evaluated based on the error rate which is a comparison of the reaction forces obtained from the analytical and optimum layered shell models with the reaction forces obtained from their related detailed models. The optimum layered shell models giving smaller error rates compared to the error rates of analytical layered shell models were found to be successful. The details of the optimization process and the results are explained in the following chapters.

CHAPTER 4

OPTIMIZATION USING GENETIC ALGORITHM

4.1. Genetic Algorithm Terms and Parameters

The evolutionary computation has its bases in the biological evolution process. Thus, most of its terms were inherited from the evolution. Some of the commonly used ones are defined below:

Gene: A single parameter of a solution point converted into the binary coding.

Genome: The entire collection of genes of an organism.

Allele: Any value assigned to a gene.

Chromosome: An array of genes. It is an input for the cost function.

Fitness: A value assigned to a chromosome by the fitness function. It is the relative merit of that chromosome and opposite of the cost.

Fitness function: A function which mathematically assigns a value (a relative merit) to a set of variables (chromosome). It is the opposite of the cost function.

Individual: A chromosome and its related cost function.

Population: The total of individuals.

Generation: One iteration of the algorithm.

Offspring: An individual created by any of the operations of the algorithm.

Parent: An individual that contributes to at least one offspring.

Like many other optimization tools, the genetic algorithms start with the definition of variables to be optimized. In the context of GA, this is called a chromosome. The

number of variables determines the dimension of the problem. For instance, if a problem has N_{vars} variables, then the chromosome is written as follows:

$$chromosome = [p_1, p_2, p_3, \dots, p_{N_{vars}}]$$

For instance, a problem trying find the location where maximum stress (positive) occurs in a plate needs the inputs of longitude (x) and latitude (y), therefore; N_{vars} is 2 and the problem is 2-dimensional.

$$chromosome = [p_x, p_y]$$

All the chromosomes in GA have their related cost values which are found by evaluating the cost function. A cost function may become very complicated and even turn into a well-developed program which can call different subfunctions or other software. For determination of the location of the peak stress problem, the cost function is defined as the negative of the stress read at a certain location and formed as an objective function of a minimization problem:

$$cost = f(chromosome) = f(p_1, p_2, p_3, \dots, p_{N_{vars}})$$

$$f(x, y) = -\sigma(x, y)$$

Determination of the variables is another important point in GA. The more variables are defined, the harder to reach a convergent solution. The variables shall be selected as the ones which can create meaningful data at the end of the optimization. For instance, if one is working for the optimization of the take-off weight of a rotorcraft, the color of the blades has no effect on it. Another critical point is the determination of the maximum and minimum bounds of variables. Most variables have logical physical boundaries. For instance, it is not logical to define the span of a rotorcraft from 0 to 200 meters. Thus, determination of variables and their boundaries is one of the most critical steps along with the correct definition of the cost function.

The last point to be highlighted about the GA is the epistasis. Epistasis is another term the GA borrowed from biology and it means gene interaction. In other words, it

determines whether a variable is dependent or independent. For instance, the number of blades, weight of the engine and the maximum take-off weight of a rotorcraft are dependent variables. When there is no epistasis, the problem is well bounded and not complicated, the minimum seeking algorithms gives the best and fastest solution. However, if the epistasis is medium to high then random search algorithms such as GA performs the best. Therefore, epistasis between the variables shall be correctly determined and defined before running an optimization.

The genetic algorithm is a stochastic global search method and the individuals are encoded as strings using binary alphabet in different bites. For instance, a problem with 2 variables can be encoded in binary format using 10 bits for x_1 and 15 bits for x_2 shown in Figure 4.1.

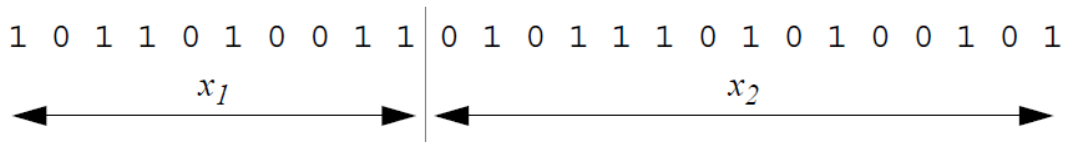


Figure 4.1. Problem with 2 Variables Mapped on the Chromosome Using 10 Bits for x_1 and 15 Bits for x_2

The stochastic search is conducted with the encoded variable. Nevertheless, a chromosome in encoded format does not present a meaningful representation, therefore; they are decoded into phenotypic domain and assigned with a value showing their performance within a population. This process is called fitness evaluation and the value assigned to a chromosome is the fitness value. In the real world, this would be the ability of a habitant of a population to survive in its environment. This evaluation is based on the fitness function defined by the user.

4.1.1. Fitness Scaling

A fitness function is the objective function of the optimization. In the GA context, it is the function creating the raw values for the selection of parent that will create the next generation and determining the way that the GA will proceed. The raw values are

converted into relative scores within a range by the scaling function operator of the GA. In MATLAB, there are 4 scaling functions defined in the library. They are *Rank*, *Proportional*, *Top* and *Shift Linear* functions. *Rank* function simply ranks the fittest individual to 1, the next fittest to 2, and so on. *Proportional* function scales the individuals proportional to their raw fitness scores. It performs low when the raw scores are scattered and cannot fit in a certain range. Figure 4.2 shows the raw fitness value of population of 20 individuals. Rank function reorders the raw values as shown in Figure 4.3 and makes it suitable for the selection process.

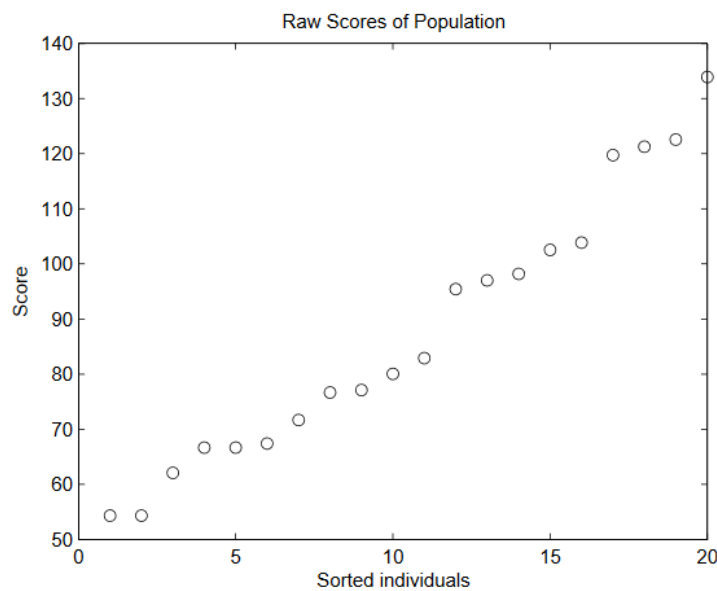


Figure 4.2. Raw scores of a population of 20 individuals. The scores are ranked in increasing order. Score of an individual determines its probability to form an offspring for the next generation. Raw scores are usually not preferred for selecting the parents, instead they are used as inputs to scaling functions [39].

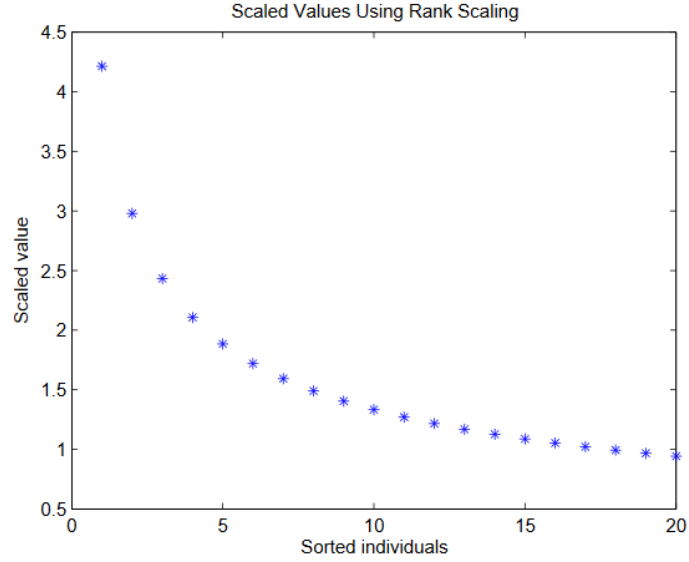


Figure 4.3. Scaled raw values using Rank scaling function. Fitness scaling removes the effects of the spread of the raw scores. Since the GA minimizes the fitness function, lower raw scores have higher scaled values. The higher the scaled value of an individual, the better its chance to form an offspring [38].

Top function evaluates the individuals with the highest fitness value as equal. It requires the number of individuals that will be considered as the best and gives them equal opportunity to reproduce while giving no opportunity to the rest of the population. *Shift Linear* function determines the average score and assigns a constant value to the fittest individual which is a certain multiple of the average value. The value assigned to the fittest individual is called *maximum survival rate*. The term *expectation* defines an individual's probability to form an offspring for the next generation. *Expectation value* of an individual is its scaled fitness value. Figure 4.4 and Figure 4.5 shows the difference between Rank and Top scaling options. *Top* scaling guaranties the best individuals to form an off-spring while it lowers the chance of the other individuals. As a result of this, populations formed with *Top* scaling is less diverse.

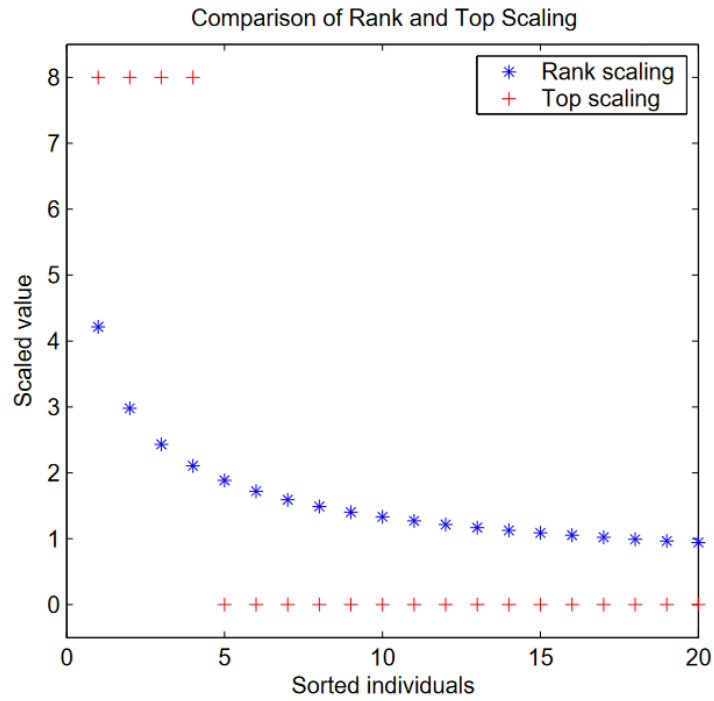


Figure 4.4. Comparison of rank and top scaling options. Top scaling function assigns high scaled values to the best individuals while lower scores are given to the others. The generations formed by top scaling function is less diverse compared to the ones formed by rank scaling. Top scaled populations are likely to converge faster; however, top scaling is likely to prevent the GA to search for other points in the space [39].

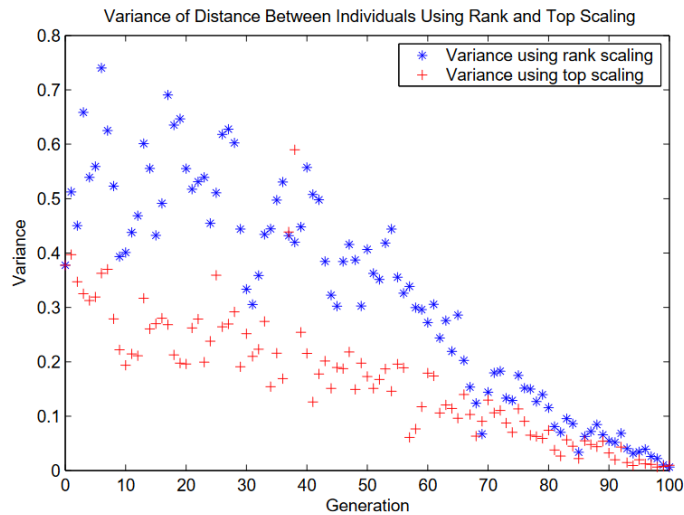


Figure 4.5. Distance between individuals (shows diversity in a population) is less when the generations are formed by top scaling. Rank scaling enables user to search for a broader space [38].

4.1.2. Selection

The selection function of the GA chooses parents that will form the next generation based on their scaled values. There are 5 selection functions in MATLAB library for this operation. They are *stochastic uniform*, *roulette*, *remainder*, *uniform*, and *tournament* functions.

Stochastic uniform function creates a line which is divided into sections whose lengths are proportional to the *expectation* of the parents. The GA moves along that line in equal step sizes and assigns a parent to each step as it moves along the length allocated to a parent. The first step is a random number less than the step size.

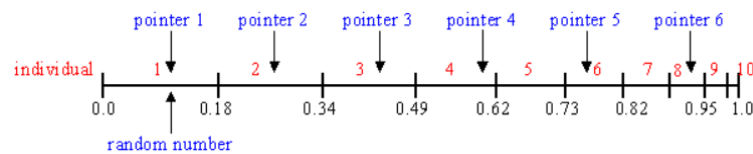


Figure 4.6. Stochastic uniform selection assigns individual to lines whose lengths are proportional to their expectation values. Then the GA moves along that line in step sizes of equal lengths and selects the parent. Step size is determined by dividing the total of expectation values into the number of desired children.

Roulette function creates a roulette divided into areas representing the expectations. The GA uses a random number to select parents. Although the individuals with better expectations have higher chance to be a parent, roulette wheel selection does not guarantee their appearance in the mating pool will be more prevalent than the weakest individual.

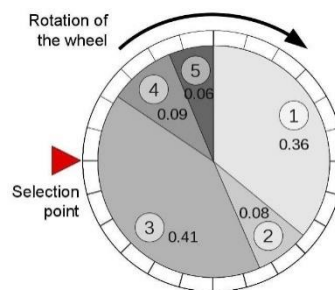


Figure 4.7. Individuals are given proportions according to their expectations. The GA determines a random number to choose a parent. The larger the area of an individual, the higher chance it has to form an offspring.

Remainder selects parents in deterministic approach and performs two steps. Firstly, it takes the integer parts of the scaled values of the individuals and select them as parents accordingly. For instance, if the expectation value of an individual is 4.2, it will be selected as a parent for 4 times. Secondly, stochastic uniform selection is applied according to fractional parts of expectation values. That is, *remainder* function places individuals on a line proportional to fractional parts and moves along the lines in equal step lengths and selects the parents.

Uniform function randomly selects parents from a uniform distribution according to their expectations and the number of parents. *Uniform* function is usually used for testing the GA since it results in an undirected search.

Tournament function randomly selects a number of individuals defined by user and call it *tournament size*, then chooses the best individuals from the group as a parent. In case of non-linear constraints, MATLAB can automatically set tournament size to 2 individuals.

4.1.3. Reproduction

There are three ways of creating individuals of the next generations in the GA shown in Figure 4.8. The selection operation is followed by reproduction phase. The reproduction operation determines the way children are created for the next generation. There are 2 options. The first one is *Elite Count* option. It determines the number of individuals that will pass to the next generation. The second one is *Crossover fraction*. It sets the fraction of the next generation that will be produced by crossover. It can set to be a value between 0 and 1. The remaining part of the population is created by mutation.

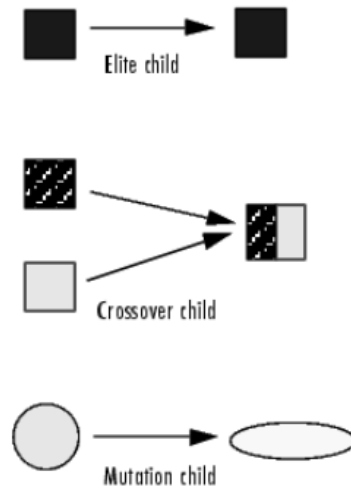


Figure 4.8. Three ways of forming a child in GA. Elite children are the ones formed from the best performing parents. Crossover children are mixture of two different parents. Elite and crossover children direct the population towards the best solution. However, the responsibilities of mutation children are different. Main responsibility of mutation. They is are toto ensure the diversity of the population. In other words, mutation enlarges the search space of the algorithm by making random changes in the selected parents.

4.1.4. Mutation

The mutation functions are the integral parts of the genetic algorithms. They ensure genetic diversity and enlarge the search space of the GA in each generation by making random small changes in the individuals. There are 4 mutation options in MATLAB. They are *Constraint Dependent*, *Gaussian*, *Uniform* and *Adaptive Feasible*.

Constraint Dependent option either uses a *Gaussian* mutation function if there are no constraints or *Adaptive Feasible* otherwise. *Constraint Dependent* option focuses on mutating feasible parents that can create feasible children, where the feasibility is defined with respect to bounds and constraints.

Gaussian is a mutation function which adds random numbers to each vector entry of an individual. The number is chosen from a Gaussian distribution centered at zero and the standard deviation is controlled by the user with *scale* and *shrink* parameters. The scale parameter specifies the standard deviation at the first generation. The shrink parameter determines how the standard deviation will shrink as the generations proceed. The shrink parameter can be set to a value between 0 and 1. If it is 1, the

standard deviation shrinks linearly to 0 through the generations. If it is 0, the standard deviation shrinks linearly to 0 thru the last generation.

Uniform mutation function has 2 steps. First, the function selects a fraction of vector entities of a chromosome for mutation and assigns each of the entities the same probability of being mutated. Second, the function replaces each selected entity with a random number within the range of that entity.

Adaptive Feasible mutation function randomly generates directions and adapts them according to the direction of the last successful or unsuccessful generation. It ensures satisfying the constraints and bounds by determining an appropriate step size in each direction.

4.1.5. Crossover

The crossover is the core operation that produces new chromosomes. The crossover operation creates new individuals from selected parents. There are 6 options in MATLAB for crossover. They are scattered, single point, two point, intermediate, heuristic and arithmetic options. *Scattered* function scheme is shown in Figure 4.9. It creates random binary vector which selects genes from parents.

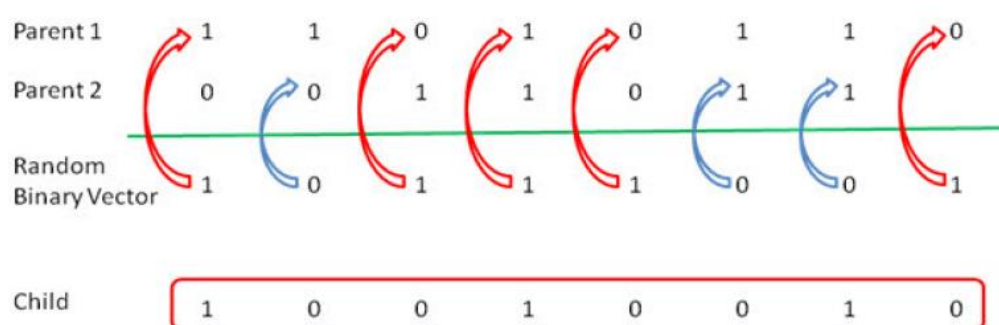


Figure 4.9. Scattered crossover. Genes are selected from the parents according to a random crossover vector [22].

If the entry in the random vector is 1, the genes are selected from the first parent; otherwise the second parent is used. For instance:

$$Parent_1 = [1 \ 2 \ 3 \ 4 \ 5 \ 6]$$

$$Parent_2 = [x \ y \ z \ p \ q \ r]$$

$$Random \ Crossover \ Vector = [0 \ 0 \ 1 \ 0 \ 1 \ 1]$$

$$Child = [x \ y \ 3 \ p \ 5 \ 6]$$

The second option is *single point* function illustrated in Figure 4.10. It determines a number n between 1 and number of variables. Then, the genes from the first parent are selected until the column number is less or equal to n , the remaining rows are selected from the second parent.

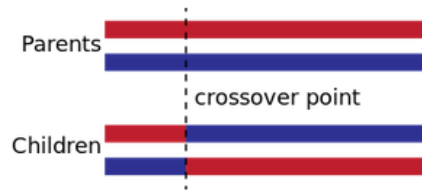


Figure 4.10. Single point crossover. Until a column number less than number of variables, the genes are selected from a parent and the remaining are taken from the other parent.

Considering the same parents stated above, a child can be represented as follows for random cross over point equal to 4, the child would be:

$$Child = [1 \ 2 \ 3 \ 4 \ q \ r]$$

The third option is *two point* option shown in Figure 4.11. It determines 2 random integers, m and n , between 1 and number of variables. The genes of the children are selected from the first parent for the column number less than or equal to m and the second parent is used for the column numbers $m+1$ to n . If n is less than number columns, the remain genes are taken from the first parent.

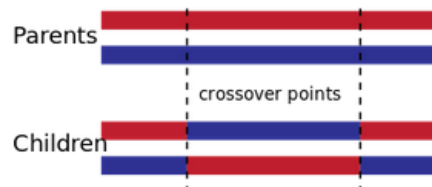


Figure 4.11. Two-point crossover

For instance, for m is equal to 3 and n is 5 the child would be:

$$Child = [1\ 2\ 3\ p\ q\ 6]$$

The forth option is *intermediate* function. It determines a ratio and use random weighted average method to form new children. If the ratio is between 0 and 1, the GA places 2 parents to the opposite vertices of a hypercube and the children are created within it. If the ratio is greater than 1, the children can be created outside of the hypercube. The formulation of a child is defined as follows:

$$Child = parent_1 + rand \cdot ratio \cdot (parent_2 - parent_1)$$

The fifth option is *heuristic* function. It draws a line containing 2 parents and creates children on it. The smaller the distance from the higher performing parent (better fitness value), the better performance of a child and it gets worse when this distance is larger. The distance is defined by the ratio. *Heuristic* crossover is less random compared to *intermediate* crossover. Thus, it can shrink the search space of the algorithm faster.

The last option is *arithmetic* function. It creates a line between parents and takes arithmetic mean of them. The children are uniformly distributed on the line.

4.1.6. Hybrid Function

MATLAB optimization tool box for the genetic algorithms also offers hybrid optimization which can verify the solution using other minimization functions. It runs after the genetic algorithm terminates. Some of the hybrid functions work with unconstrained problems only such as *fminsearch* or *fminunc* while some of them are for constraint problems such as *fmincon*. Hybrid optimization does not run with integer constraints.

4.1.7. Stopping Criteria

The convergence and rate of convergence are also the critical issues when using GA. There are several criteria called *stopping criteria* which can be imposed to stop the algorithm and check the convergence of the solution. There are several ways to stop the GA:

Generations: Maximum number of generations can be set to stop the algorithm. By default, MATLAB sets it to 2 times of number of the variables.

Time limit: The algorithm can be forced to stop after reaching a pre-defined time limit in seconds.

Fitness limit: The desired best fitness value that can be used to stop the algorithm. Once any of the individuals in the current iteration obtains the fitness limit value the algorithm terminates.

Function tolerance: It is the difference between the mean fitness values of the consequent generations. It is set to $1 \cdot 10^{-6}$ by MATLAB by default. The less the mean of the fitness values between generations, the more likely optimum solution is reached.

Stall generations: Once the algorithm converges to a solution, it starts to create optimum generations whose individuals start to become less diverse. The generations whose relative mean fitness values are less than or equal to the function tolerance are called stall generation. A maximum number of stall generations can be set to stop the algorithm.

4.2. Problem Setup and Flowchart

The increased attention on the GA has turned it into a commercially available tool offered by many software such as MATLAB. It is included in the MATLAB optimization tool as built-in function with useful options. A typical binary GA has the flowchart given in Figure 4.12 .

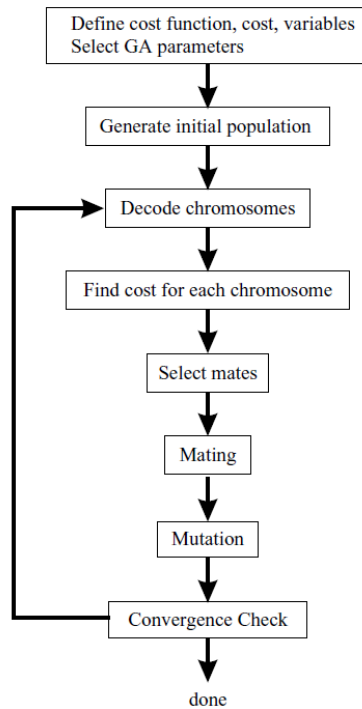


Figure 4.12. Binary Genetic Algorithm Flowchart [40]

4.2.1. Definition of the Problem

The basis of the problem in this study stems from errors encountered when modeling sandwich panels using different finite element modeling approaches explained in 1.1. As discussed before a sandwich panel can be modelled using the detailed model or layered shell model. Detailed modelling approach includes detailed modelling the honeycomb core in its original shape and therefore it is impractical and costly. The layered shell modelling includes modelling a sandwich panel using 2D shell elements where the core is taken into account through equivalent properties. However, it requires transforming the 3D material properties of the core to 2D properties. Such a transformation can be done using the analytically driven core equivalent formulas presented in Chapter 3.3 and it is indeed the source of the error to be overcome in this study.

Two groups of finite element models are created to simulate the problem. These are the detailed and layered shell models. The detailed model group is used as a reference

model and the layered shell model groups are optimized until their response becomes similar to the reference model. The overall objective of the optimization is to obtain accurate shell models and the output is the optimized core material properties. The comparison is based on the minimization of the difference of the reaction forces obtained from the detailed and layered shell models.

Genetic algorithm offered in the optimization toolbox of MATLAB is employed. The tool requires the number of the variables, fitness function and selection of operational parameters from the user. The number of the variables are determined by comparing the effects of each material parameter of the core under certain loading conditions. The fitness function is a MATLAB function that the GA calls for evaluating the performance of the individuals. Indeed, it is the objective function of the optimization problem in which other tools and functions are called. The selection of operational parameters is done by trial-error method. A correct selection of the parameters plays an important role on the convergence and performance of the algorithm. The details are provided in the following sections.

4.2.2. Selection of Variables

The outputs of the optimization process are the optimum core material properties. Thus, 2D orthotropic material properties are the candidate design variables of the problem. The effect of each parameter on the reaction force depends on the loading type. The in-plane properties are more critical if the loading is in-plane such as in-plane tension or compression; the out-of-plane properties become more important for out-of-plane loadings like three-point bending. Therefore, load and boundary conditions are the integral parts when determining the design variables.

The main philosophy behind using sandwich beams is using face sheets for in-plane loads and the core for out-of-plane loads. Reacting against out-of-plane loads is also the nature of the core since it is very weak in in-plane directions but very strong in the out-plane direction. The differences of modulus values in those directions are

immoderate that the in-plane properties of the cores are neglected most of the time [38]. The inputs of 2D orthotropic material are $E_1, E_2, \nu_{12}, G_{12}, G_{13}$ and G_{23} .

Since the finite element method is used for structural analysis, the material stability has to be satisfied to avoid numerical problems. The material stability is checked using the following formula [7]:

$$\frac{E_1}{E_2} > \nu_{12}^2$$

The in-plane properties of the equivalent core are very small numbers and satisfy the stability criteria. Since, the loading type in this study is in the out-of-plane direction, the effects of the in-plane constants on the out-of-plane reaction force are neglected. However, the effect of G_{12} is studied to be sure. In Table 4.1, it is shown that the effect of G_{12} on the out-of-plane reaction force is also negligible.

Table 4.1. *Effect of G_{12} on the reaction force*

G_{12} [MPa]	Reaction Force [N]
0.9	1450.90
100	1451.10
1000	1451.90

The impact of the out-of-plane shear modulus values are expected to be greater than the impact of the other parameters on the reaction force. The analytical formulas presented in Chapter 3.3 suggest the analytical shear modulus of 352.33 MPa for G_{13} (taken from the upper limit formula of Grediac [21]) and of 211.40 MPa for G_{23} , see Grediac [21]. While studying the impact of a parameter on the reaction force other material inputs were kept constant. The impact of the out-of-plane shear modulus on the reaction force are shown in Table 4.2 and Table 4.3.

Table 4.2. *Impact of G_{13} on the reaction force while the other parameters were kept constant*

G_{13} [MPa]	Reaction Force [N]
175	1037.19
350	1450.66
700	1963.70

Table 4.3. *Impact of G_{23} on the reaction force while the other parameters were kept constant*

G_{23} [MPa]	Reaction Force [N]
105	1143.84
211	1450.90
420	1849.60

Therefore, the optimization problem has 2 design variables which are G_{13} and G_{23} . The core and face sheet material used in this study is AL5052 whose material properties are given in Table 4.4. The material strength check is done for the detailed model of the model group 1 and the results are shown in Appendix B. Hexcel is one of the main industrial honeycomb providers [38]. The Hexcel Catalog was taken as the reference for honeycomb core selection. The cell size is 9.53 mm (3/8 inch) and the cell wall thickness is 0.1016 mm (0.004 inch). The ramp angle is 30 degree and the face sheet thickness changes from 0.36 mm to 3.20 mm.

Table 4.4. *Material Properties of AL5052 H38 Sheet [41]*

AL5052 – H38 -Sheet	
Young's Modulus [MPa]	70300
Poisson's Ratio [-]	0.33
Density [g/cc]	2.66

The mechanical properties for the selected honeycomb core are given in Hexcel Catalog and shown in Table 4.5.

Table 4.5. *Honeycomb Core Material Specifications* [38]

Cell size – Alloy – Foil Gauge	L Direction		W Direction	
	Strength [MPa]	Modulus [MPa]	Strength [MPa]	Modulus [MPa]
3/8 – 5052 – .004	2.63	593	1.57	254

The range of modulus defined in the specifications [38] for honeycomb core made of AL5052 is between 48 to 1450 MPa. The design variables are bounded by taking smaller lower and larger upper bounds to enlarge the search space with respect to specification values. Thus, the upper and lower bounds on the design variables are defined as follows:

$$10 \text{ MPa} < G_{13} \text{ and } G_{23} < 2000 \text{ MPa}$$

Therefore, the optimization problem considered in this study has 2 variables which are G_{13} and G_{23} . There are no inequalities or non-linear constraints defined. However, the variables are limited in reasonable range whose lower limit 10 MPa and the upper limit is 2000 MPa. The fitness function is explained the following section.

4.2.3. Fitness Function

The fitness function is the core of the genetic algorithm. It is employed to evaluate the fitness of each of the individuals. In this study, the fitness function takes ABAQUS analysis input file (.inp), two out-of-plane material properties G_{13} and G_{23} and the reference reaction forces as inputs and gives the fitness values of individuals as output. The analysis input file is the input file of the layered shell model created using ABAQUS. Preliminary, it has the equivalent core material properties obtained by analytical formulas discussed before. The fitness function updates the out-of-plane shear modulus values as the genetic algorithm creates new individuals. The reference reaction forces are obtained from the detailed models. At the end, the fitness function compares the reaction forces obtained from the updated ABAQUS input files with the

reference reaction forces and provides fitness values to the algorithm using the following formula whose variables are defined in Table 4.6 and the related explanations are shown in Figure 4.13 and Figure 4.14.

$$Fitness\ Value = \frac{(RF_{Xnodes} - RF_{ref_{Xnodes}})^2}{(RF_{ref_{Xnodes}})^2} + \frac{(RF_{Ynodes} - RF_{ref_{Ynodes}})^2}{(RF_{ref_{Ynodes}})^2}$$

Table 4.6. *Definition of fitness function variables*

Variable	Definition
$RF_{ref_{Xnodes}}$	Reaction force in z-direction obtained from the constrained nodes along x-direction of the detailed model
$RF_{ref_{Ynodes}}$	Reaction force in z-direction obtained from the constrained nodes along y-direction of the detailed model
RF_{Xnodes}	Reaction force in z-direction obtained from the constrained nodes along x-direction of the layered shell model
RF_{Ynodes}	Reaction force in z-direction obtained from the constrained nodes along y-direction of the layered shell model

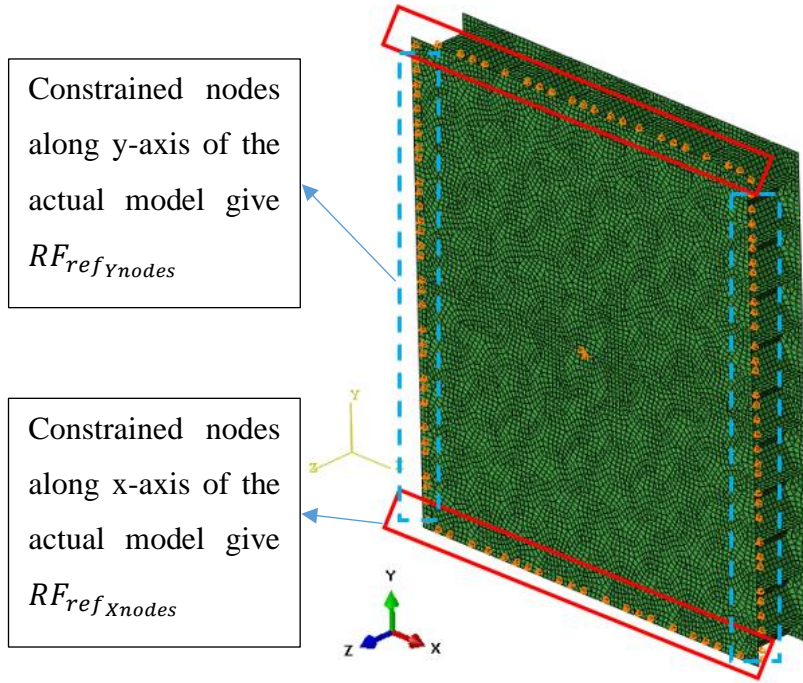


Figure 4.13. Reference reaction forces are obtained from detailed model. Reaction forces obtained from the constrained nodes along x and y direction are evaluated separately.

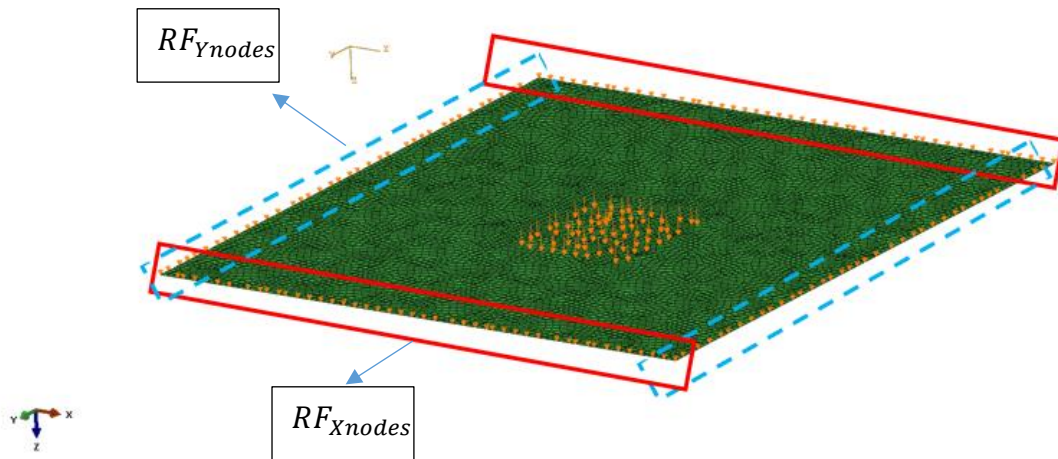


Figure 4.14. The reaction force obtained from the nodes along x-direction of the layered shell model is RF_{Xnodes} and the reaction force obtained from the nodes along y-direction is the RF_{Ynodes} . The reaction forces obtained from the layered shell model tried to be adjusted to reference reaction forces obtained from the detailed model. This is done by changing equivalent G_{13} and G_{23} modulus values of the layered shell model using genetic algorithm optimization method.

The algorithm minimizes the fitness value by pushing both terms close to zero as much as possible. In other words, the algorithm considers the individuals whose reaction forces are close to the reference reaction forces as the best individuals in a population. Note that, the fitness evaluation formula considers the reaction forces of nodes located on edges parallel to x and y-axes separately.

The fitness function algorithm flowchart is shown in Figure 4.15. It takes ABAQUS input file and reference reaction force values from the user, G_{13} and G_{23} from the GA operations. The fitness function reads ABAQUS input file and replaces the material input values with the new shear modulus values. Then, it creates a new directory and copies the modified input file into it. The analysis is run by calling ABAQUS and the output file with reaction forces in the constrained nodes in x and y directions are obtained separately. The output file (.fil) is not in a directly readable format by MATLAB. Therefore, Abaqus2Matlab tool is employed for the conversion. It is developed by the scientists Papazafeiropoulos and Muniz-Calvente [8] and officially recognized by MATLAB as an add-in. After Abaqus2Matlab tool creates the nodal reaction forces matrices, the entities are summed to obtain the total reaction force in z-direction from the nodes along x and y directions. Then, the reaction force obtained is compared with the reference reaction force, which results in the fitness value of the individual comprised of G_{13} and G_{23} submitted as candidate optimum point by the GA. The fitness value is the output of the fitness function and it is used in the GA operations. Having provided the fitness value to the GA, the fitness function goes back to its main directory and erases the analysis directory to save space.

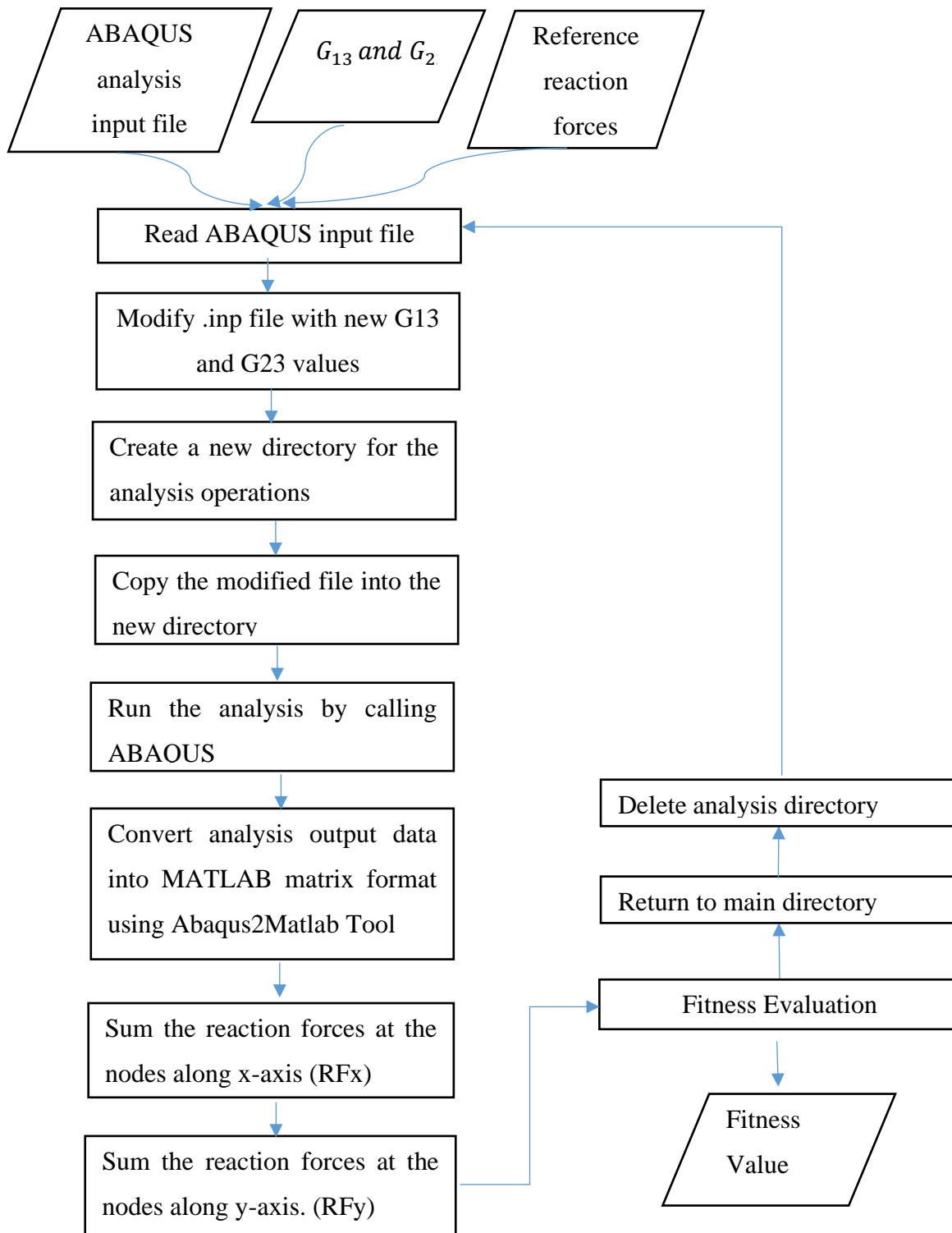


Figure 4.15. Fitness Function Flowchart

4.2.4. Selection of Parameters

4.2.4.1. Population Size

Population size indicates the number of individuals in a generation. Since, each individual is a possible solution point, it is important have enough number of individuals in a population to obtain a convergent solution. The user guide of MATLAB Optimization Toolbox for Genetic Algorithm [39] suggests using 50 individuals for the problems with 5 or less variables and 200 individuals for more than 5 variables. In this study, there are 2 variables which are G_{13} and G_{23} and the convergence of the problem was tested using 50, 100 and 200 individuals. Figure 4.16, Figure 4.18 and Figure 4.20 show the best and mean fitness values at each generation. The best fitness value is the fitness value of an individual at an iteration. The mean fitness value is the arithmetic average of the fitness values in population at an iteration. The smaller the mean fitness value the more efficient a generation is. As the mean fitness value goes to zero, the optimization converges. Figure 4.17, Figure 4.19 and Figure 4.21 show the fitness of the individuals at the last iteration for the selected number of individuals. The last iteration is the results producing iteration; thus, the fitness values of the individuals are close to zero. In Figure 4.21, there is a larger diversity between the individuals compared to the Figure 4.17, Figure 4.19. This is a sign of the mutation property of the genetic algorithm. The mutation can cause random change in the individuals to enlarge the search space. Therefore, there is an individual with higher fitness value compared to the others. However, the mean fitness value of the population is still very close to zero.

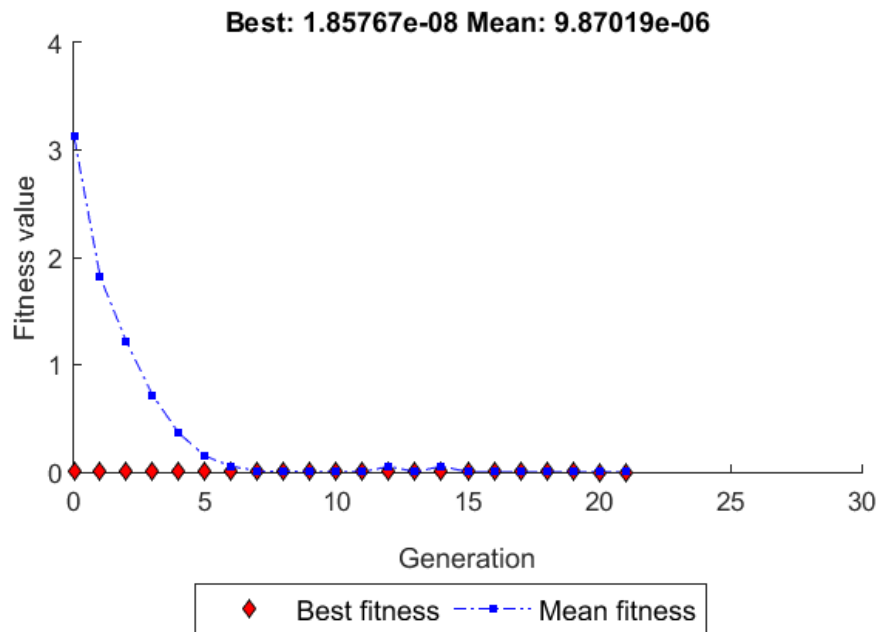


Figure 4.16. Best and mean fitness values of population of 50 individuals at each generation. The lower the fitness value, the better the performance of a generation. As the mean fitness value goes to zero, the solution becomes convergent.

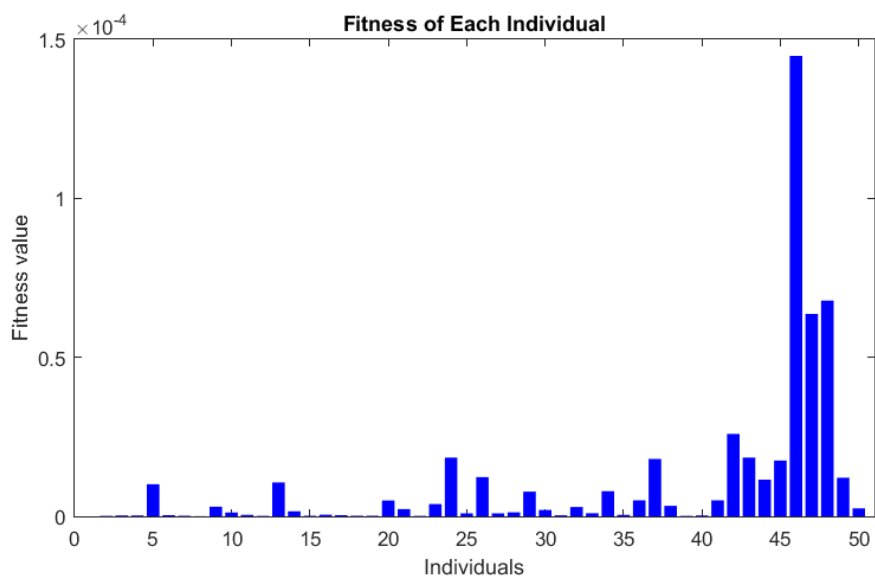


Figure 4.17. Fitness of each individual at the last iteration for population size of 50 while the mean fitness value is close to zero.

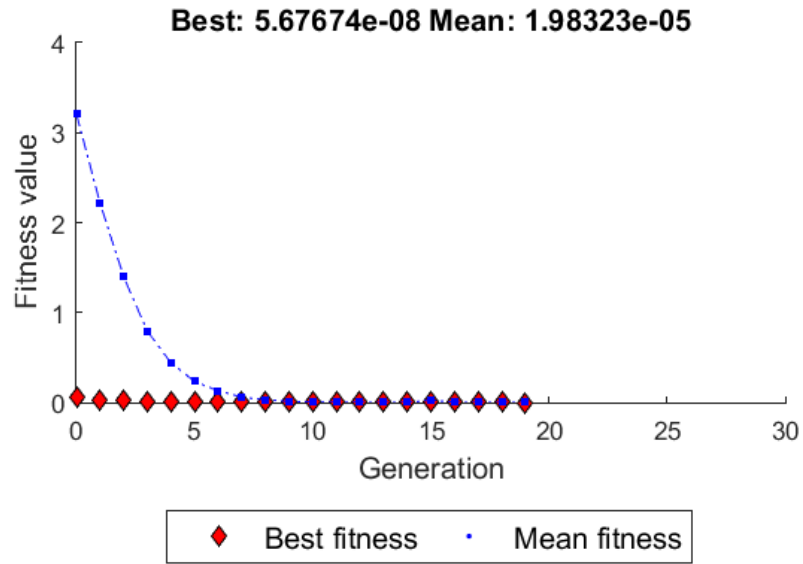


Figure 4.18. Best and mean fitness values of population of 100 individuals at each generation. The lower the fitness value, the better the performance of a generation. As the mean fitness value goes to zero, the solution becomes convergent.

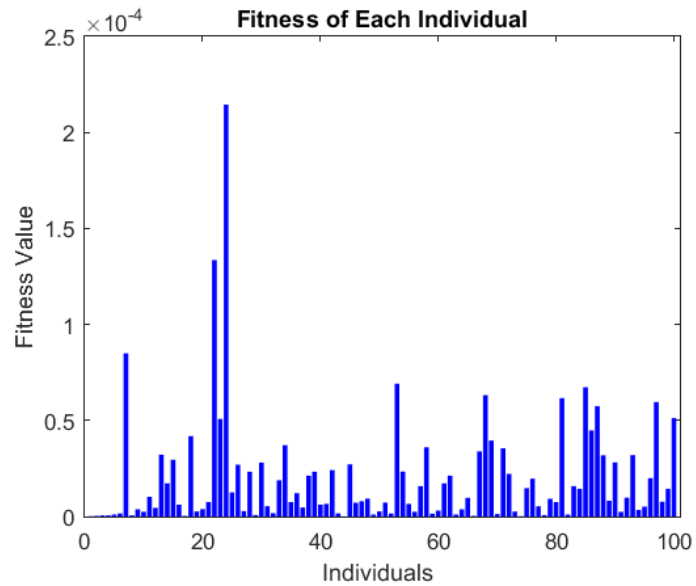


Figure 4.19. Fitness of each individual at the last iteration for population size of 100 while the mean fitness value is close to zero.

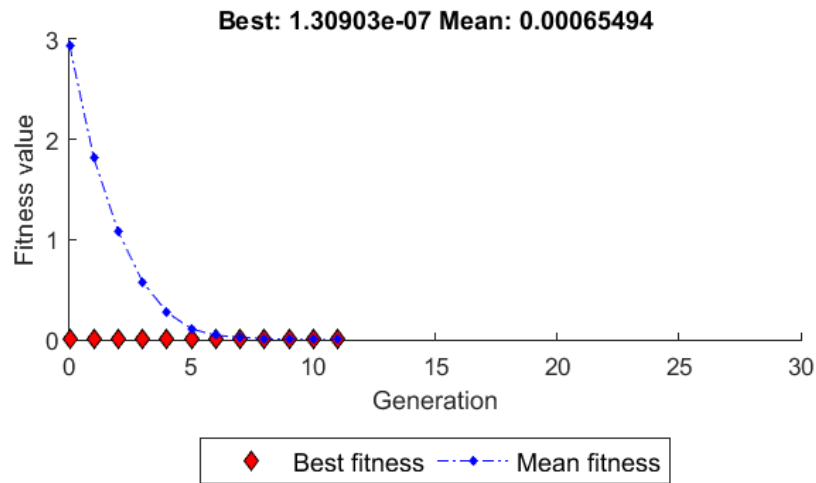


Figure 4.20. Best and mean fitness values of population of 200 individuals at each generation. The lower the fitness value, the better the performance of a generation. As the mean fitness value goes to zero, the solution becomes convergent.

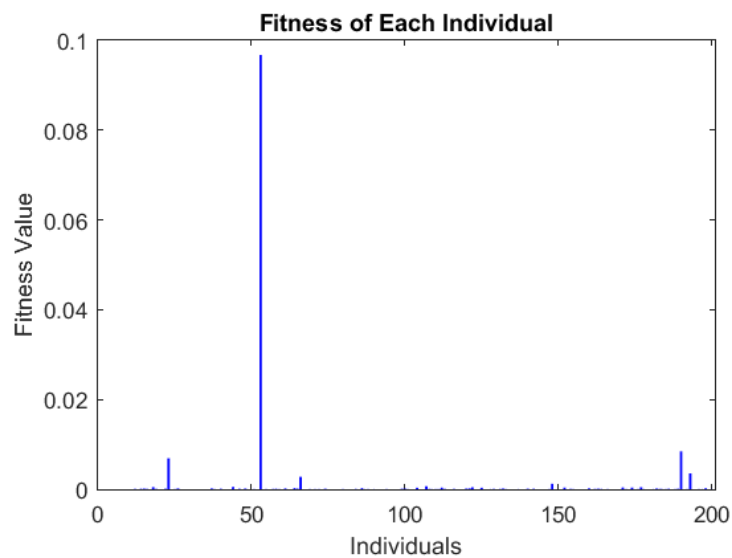


Figure 4.21. Fitness of each individual at the last iteration for population size of 200 while the mean fitness value is close to zero. Although the mean fitness value is close to zero there are 5 individuals whose fitness values are obviously higher than the others.

Table 4.7. Comparison of the results obtained with different population size

Population Size	Optimum G_{13} [MPa]	Optimum G_{23} [MPa]	Number of Generations
50	173.13	184.15	21
100	172.96	184.06	19
200	173.08	183.95	11

The results presented in Table 4.7 agrees with population size suggested by MATLAB user manual. However, it was experienced that the optimization runs with 50 individuals stopped progressing unexpectedly for a few times. Therefore, 100 individuals were selected as the population size.

4.2.4.2. Operational Options

MATLAB genetic algorithm tool offers more than one option for the genetic algorithm operations. A suitable combination of the options is specific to nature of problem and can be found by trial-error method. The details of the options are provided in Chapter 4.1 and a summary is given in Table 4.8.

Table 4.8. Genetic Algorithm Options

Fitness Scaling	Selection	Mutation	Cross-over
Rank	Stochastic Uniform	Constraint Dependent	Constraint Dependent
Proportional	Reminder	Gaussian	Scattered
Top	Uniform	Uniform	Single Point
Shift Linear	Roulette	Adaptive Feasible	Two point
	Tournament		Intermediate
			Heuristic
			Arithmetic

The study conducted by Çınar et al. [22] in 2015 involves optimization of the modal behavior of the composites sandwich panels and suggests using *rank* for scaling,

remainder for selection, *adaptive feasible* for mutation and *intermediate* for crossover functions. Considering the similarities between the geometries and processes, these options were used as reference options and summarized in Table 4.9. The results produced by the algorithm using these options are the reference values and shown in Table 4.10. Based on the reference values a comparison study was conducted.

Table 4.9. *Reference GA options*

Scaling	Selection	Mutation	Crossover
Rank	Remainder	Adaptive feasible	Intermediate

Table 4.10. *Reference Optimized Results*

Ref. Optimum G_{13} [MPa]	Ref. Optimum G_{23} [MPa]	Ref. RF13 [N]	Ref. RF23 [N]	Number of Generations
172.96	184.06	280.59	444.75	19

Table 4.11. *Effect of fitness scaling options*

Fitness Scaling	Opt. G_{13} [MPa]	Opt. G_{23} [MPa]	RF13 [N]	RF23 [N]	Diff. G_{13} (%)	Diff. G_{23} (%)	Diff. RF13 (%)	Diff. RF23 (%)
Rank	172.96	184.06	280.59	444.75	Ref	Ref	Ref	Ref
Shift	185.56	181.16	278.49	464.91	7.28	1.58	0.75	4.53
Linear								
Top	173.06	184.13	280.59	444.91	0.06	0.04	0.00	0.04

Table 4.12. *Effect of selection options*

Selection	Opt. G_{13} [MPa]	Opt. G_{23} [MPa]	RF13 [N]	RF23 [N]	Diff. G_{13} (%)	Diff. G_{23} (%)	Diff. RF13 (%)	Diff. RF23 (%)
Remainder	172.96	184.06	280.59	444.75	Ref	Ref	Ref	Ref
Stoc. Uni.	173.07	184.10	280.59	444.91	0.06	0.02	0.00	0.04
Roulette	div.	div.	div.	div.	-	-	-	-
Tournament	173.06	184.14	280.59	444.91	0.06	0.04	0.00	0.04

Table 4.13. *Effect of crossover options*

Fitness Scaling	Opt. G_{13} [MPa]	Opt. G_{23} [MPa]	RF13 [N]	RF23 [N]	Diff. G_{13} (%)	Diff. G_{23} (%)	Diff. RF1 3 (%)	Diff. RF23 (%)
Inter.	172.96	184.06	280.59	444.75	Ref	Ref	Ref	Ref
Scattered	171.72	185.75	282.07	443.02	0.72	0.92	0.53	0.39

There are no trials done for the mutation function because there are bounds in design variables and adaptive feasible mutation option had to be selected [39]. The results presented in Table 4.11 and Table 4.12 suggest using top as fitness scaling and tournament as selection function as an alternative to reference selection of options given in Table 4.10. However, using these options led to unexpected divergent results for a few times. MATLAB genetic algorithm options are specific to problem most of the time. Therefore, the best way to determine the correct combination of the options is to do trial-error runs. In this study, 6 different face sheet thicknesses were investigated in one run and the most important thing was the stability of the algorithm. In other words, the optimization had to run without any stagnation. Therefore, the combination of rank, remainder, adaptive feasible and intermediate functions were selected.

MATLAB genetic algorithm tool also enables users to run another optimization function after the GA terminates as a way of verification of the solution point. In this study, *fmincon* function was enabled as hybrid function since it is suggested by the user guide for the problems with boundaries [39]. The hybrid optimization is useful to make sure that the final solution is the global minimum.

There are several ways to stop GA. Like biological evaluation, the GA continues forever until all the individuals in a population becomes the best solutions. As it can be seen from Figure 4.16, Figure 4.18 and Figure 4.20 the mean fitness value of a population converges to zero after a few generations; in other words, the fitness function lands on a stall region and the fitness values of the individuals start to converge to zero. At this point, the user can stop the algorithm by defining function tolerance and stall generation limit. . In this study, the function tolerance is 1×10^{-6} and the stall generation was tested and the results are presented in Table 4.14. In this study, the problem is bounded and there are not non-linear constraints, which result in comparatively fast convergence rate. To be on the safe side, the optimization of the model group 1 presented in Figure 3.7 is done with 10 stall generations. The stall generation limit is not the only way to stop the GA. Maximum generation limit, time limit or a certain fitness value limit can be used to stop the algorithm but in this study the stall generation limit is enforced.

Table 4.14. *Stall generations test*

Stall Generation	Opt. G_{13} [MPa]	Opt. G_{23} [MPa]	RF13 [N]	RF23 [N]
3	173.84	184.11	281.03	444.91
10	172.96	184.06	280.59	444.75
50	172.94	184.05	280.59	444.75

4.2.5. Algorithm of the Optimization Process

The overall approach of the optimization of the out-of-plane core properties of a sandwich panel includes several steps. Firstly, the finite element models are created. There are mainly 2 model groups and 6 face sheet thicknesses. The model groups include detailed and layered shell models which were explained in Chapter 3.4 in detail. The reference forces are extracted from the detailed models. Each detailed model has its layered shell model. While creating the layered shell models core equivalent properties explained in Chapter 3.3 is employed. These models are named as the analytical layered shell model from which the analytical reaction forces are extracted. Secondly, the fitness function is created. The fitness function is the core of the GA and it includes the formula which mathematically describes the objective of the problem and several external tools such as ABAQUS [7] and Abaqus2Matlab [8]. Thirdly, the GA is set with convergent parameters and required inputs. The GA gives the optimum shear modulus values. Lastly, the optimum shear modulus values (G_{13}, G_{23}) are plugged into ABAQUS input files and optimum layered shell models are obtained. These models are analyzed for different geometries and load cases for verification. To sum up, the finite element models are created and reaction forces are computed; a suitable fitness function is created; the GA is run and optimum G values are obtained; the optimum layered shell modes are created and finally the optimum G values are validated. The flowchart of the optimization process is given Figure 4.22 and that of the verification process is given in Figure 4.23.

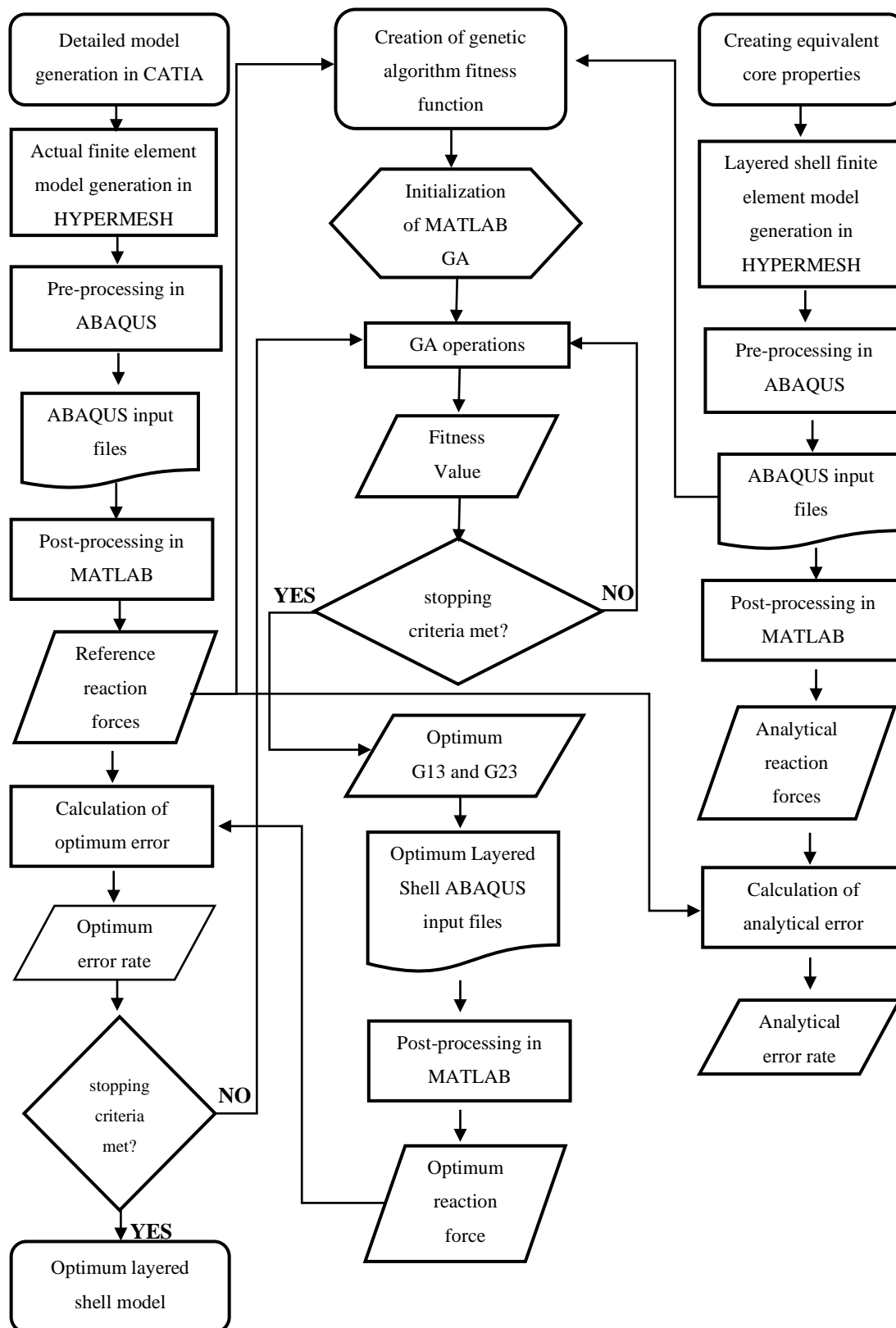


Figure 4.22. Optimization Process Flowchart

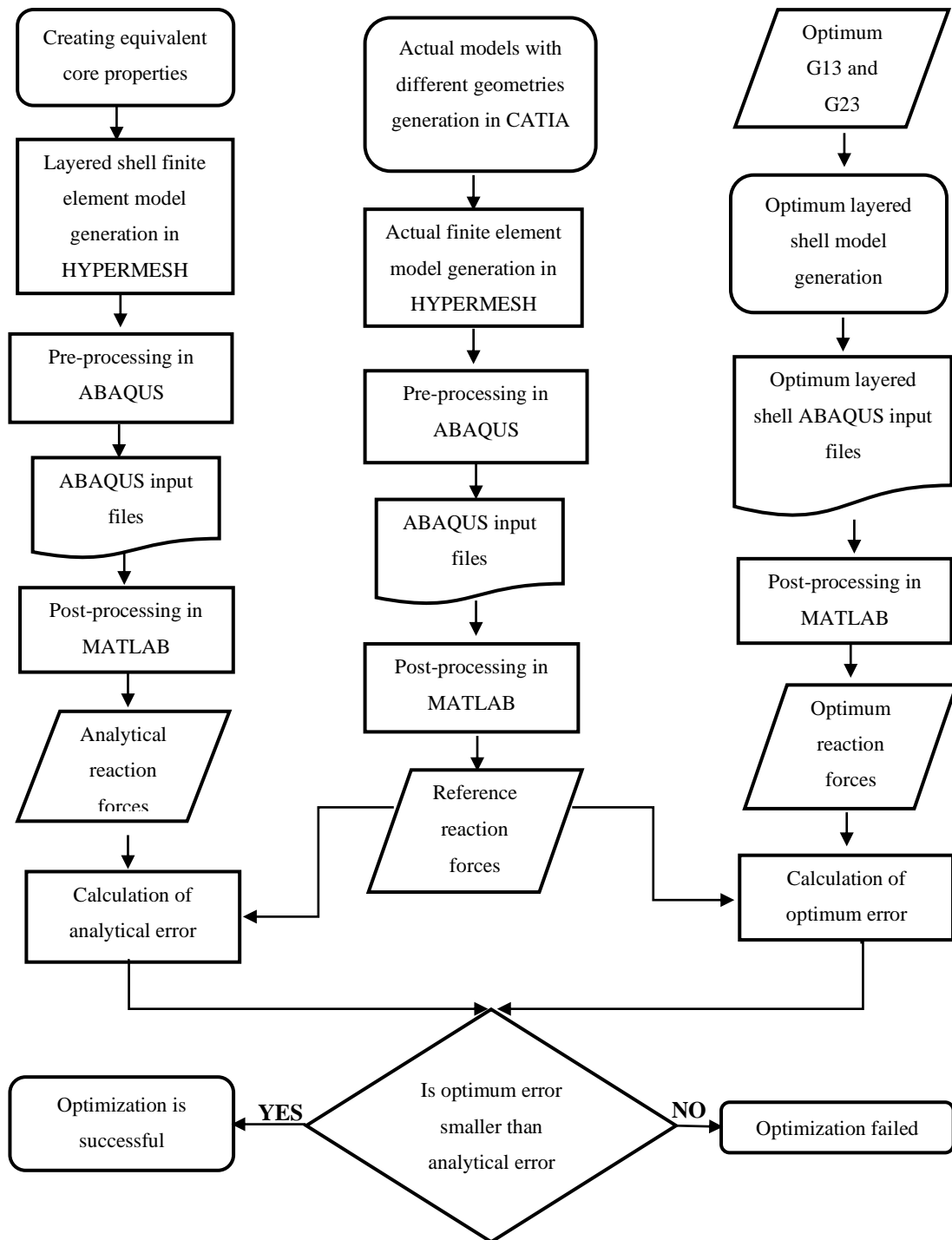


Figure 4.23. Verification process flowchart. Optimized G_{13} and G_{23} values are tested on sandwich panels with different geometries and loads and boundary conditions

CHAPTER 5

RESULTS

5.1. Results of the Optimization

The model group 1 is the optimized group. Other model groups are used to verify the optimum results obtained from it. The details of the detailed finite element of the model group 1 is shown in Figure 3.7, Figure 3.8 and Figure 3.9 and the related layered shell finite element model is shown in Figure 3.17. The results are presented from Figure 5.1 to Figure 5.6 for all face sheet thicknesses.

The detailed models have honeycomb cores modelled in their original hexagonal geometries whereas analytical or optimized models are two-dimensional layered shell model with equivalent core properties. Detailed reaction forces (RF-detailed) are obtained from the detailed models and used as reference reaction forces. Analytical reaction forces (RF-analytical) are obtained by plugging in the equivalent transverse shear moduli to the layer which represents the core. Figure 5.1 shows the difference between RF-detailed and RF-analytical. Figure 5.2 shows the percentage of error between them (Error-initial). Table 5.1 shows the related data. This rate of error is considered as the initial error since it is the error before optimization. The difference between those reaction forces is minimized by optimization. The reaction forces after optimization are shown in Figure 5.3. According to the figure, the reaction force after optimization (RF13-opt or RF23-opt) coincide with the reference reaction forces (RF-detailed). The related data is shown in Table 5.2. Thus, the error rate reduces to almost zero.

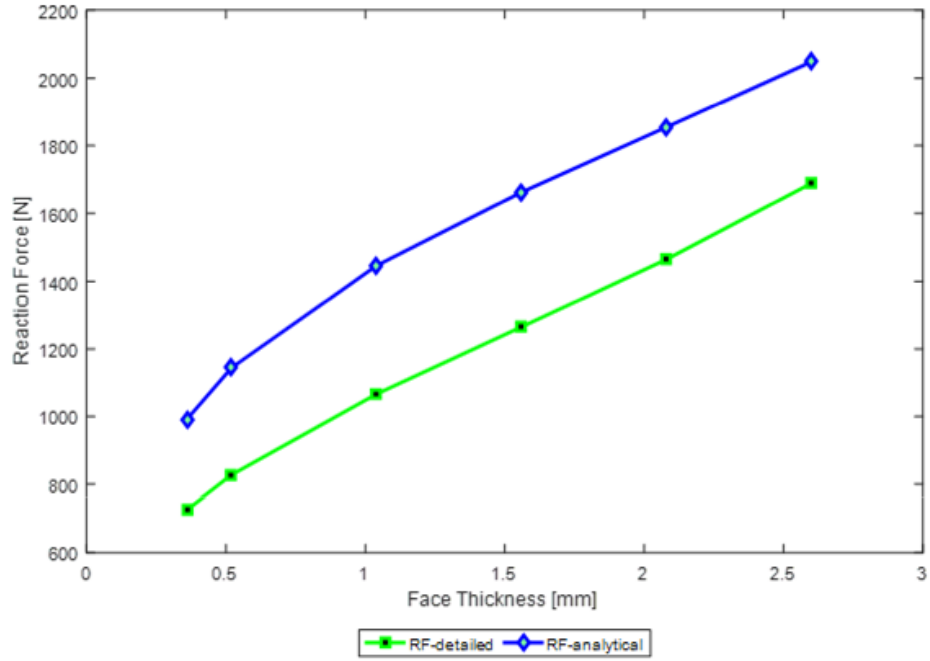


Figure 5.1. Total of the reaction forces in z-direction obtained from the detailed model (RF-detailed) compared with the reaction force obtained from the layered shell whose shear modulus obtained from analytical formulas in the literature (RF-analytical). The analytical core equivalent formulas are empirically driven and gives high error rates with respect to reference reaction forces. The aim of the optimization is to deal with this error gap by optimizing equivalent G_{13} and G_{23} shear modulus values.

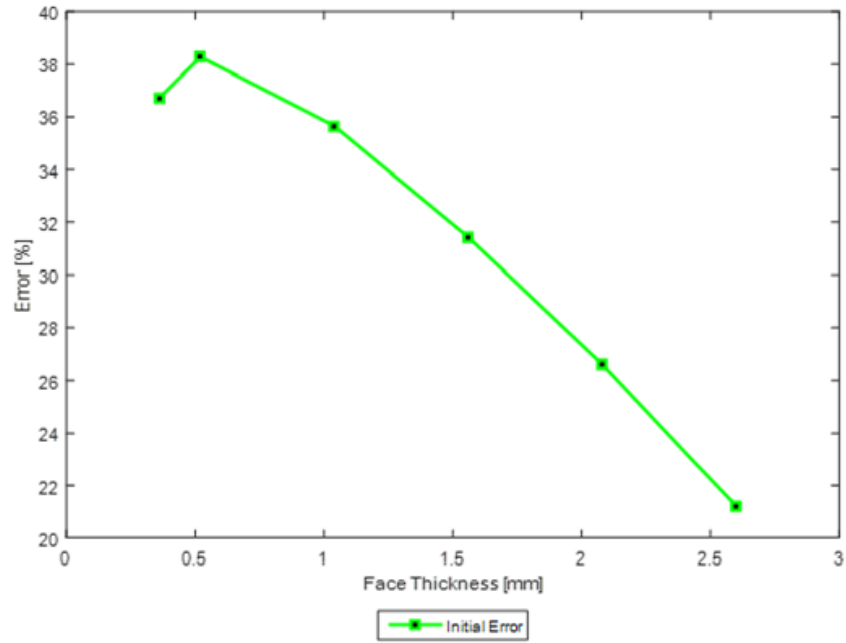


Figure 5.2. The rate of initial error. It is the percentage difference between the total reaction forces of the detailed and analytical layered shell models. The error is as high as 95 percent in the beginning and reduces to 86 percent as the face sheet thickness increases. The error after optimization is not presented since it reduces to zero percent.

Table 5.1. Detailed and analytical reaction forces of model group 1. Initial error is the percentage difference between the total detailed and analytical reaction forces

Face Thickness [mm]	Detailed RF_{13} [MPa]	Detailed RF_{23} [MPa]	Analytical RF_{13} [MPa]	Analytical RF_{23} [MPa]	Initial Error [%]
0.36	280.59	444.85	322.46	669.25	36.70
0.52	316.21	511.23	359.58	784.57	38.27
1.04	385.45	680.93	426.61	1024.38	36.06
1.56	439.35	825.96	472.86	1194.27	31.75
2.08	498.42	966.73	515.49	1343.29	26.86
2.60	571.01	1118.50	558.15	1485.67	20.97

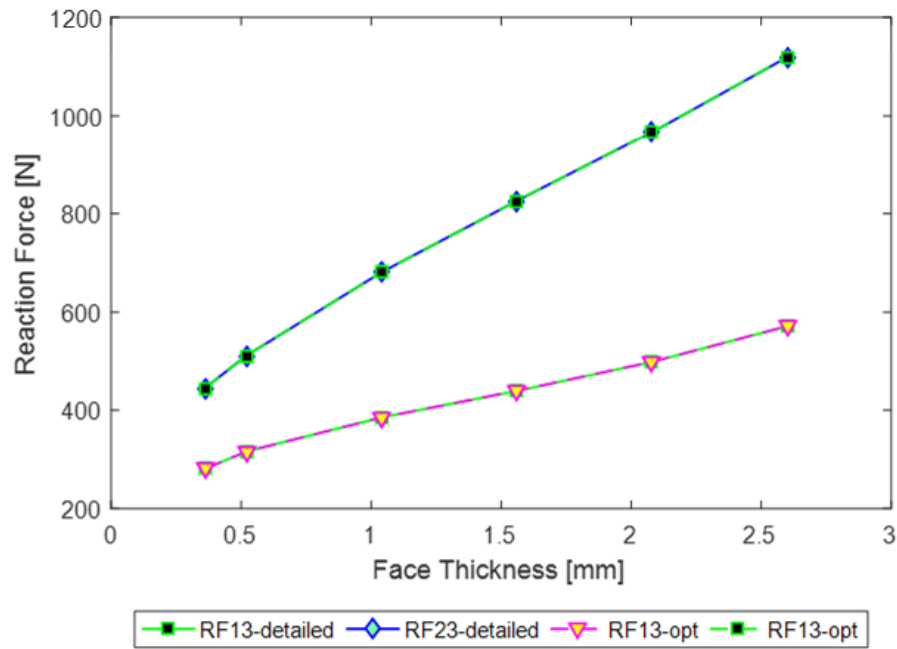


Figure 5.3. Detailed reaction forces vs. optimized reaction forces obtained from the constrained nodes along x-axis (RF13) and along y-axis (RF23). The optimum reaction forces and the reference reaction forces are coincident. Thus, the GA is able to perfectly match the reaction forces in each of the planes.

Table 5.2. The detailed and optimum reaction forces. Error after optimization is the percentage difference between the total detailed and optimum reaction forces. The error reduces almost to zero percent after optimization.

Face Thickness [mm]	Detailed RF_{13} [MPa]	Detailed RF_{23} [MPa]	Optimum RF_{13} [MPa]	Optimum RF_{23} [MPa]	Error After Optimization [%]
0.36	280.59	444.85	280.59	444.74	0.02
0.52	316.21	511.23	316.23	511.54	0.01
1.04	385.45	680.93	385.36	680.78	0.02
1.56	439.35	825.96	439.58	825.92	0.02
2.08	498.42	966.73	498.46	966.74	0.01
2.60	571.01	1118.50	571.08	1118.60	0.01

Figure 5.4 compares the analytical and optimized transverse shear moduli of the honeycomb core. According to equivalent core formulas presented in Chapter 3.3, the analytical formulas are independent of the face sheet thicknesses. Thus, the lines representing the analytical moduli are vertical. However, the optimized transverse moduli lines suggest that the out-of-plane properties are affected by the stiffness of the face sheets.

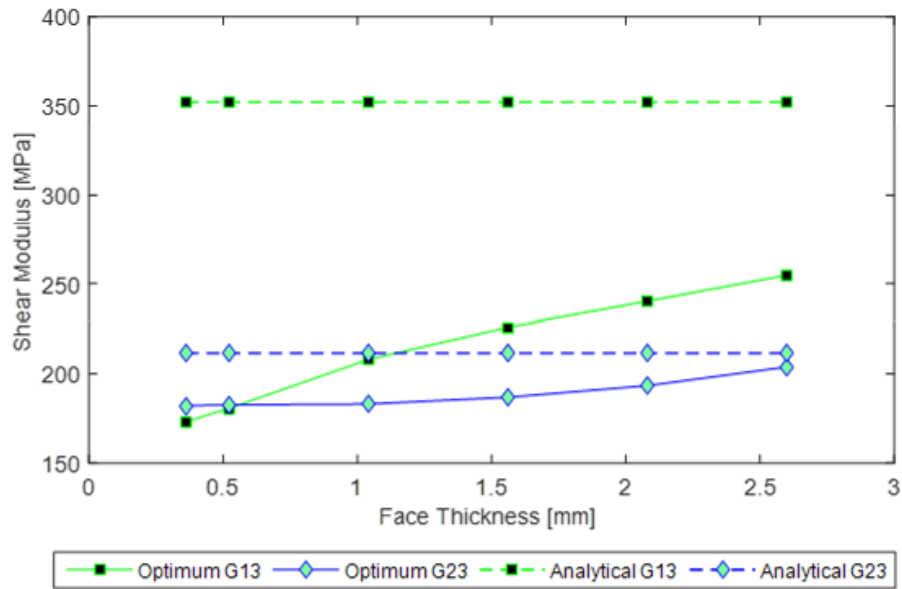


Figure 5.4. Analytical shear modulus vs. Optimum shear modulus. The dashed lines are analytical values and they are independent of the face sheet thicknesses. The solid lines are optimized shear modulus. The convergence of optimum G_{23} to analytical G_{23} is considered as a coincidence.

The figures show that there is a large discrepancy between the detailed and analytical model, initially. However, the GA can successfully match the reference reaction forces with the layered shell model by adjusting the out-of-plane shear modulus of the core. The optimized shear modulus values are presented in Table 5.3. These values are used as shear modulus inputs for the verification whose flowchart is as shown in Figure 4.23.

Table 5.3. Analytical and optimized shear modulus values with respect to face sheet thicknesses. The analytical values are independent of the face sheet thickness.

Face Thickness [mm]	Analytical G_{13} [MPa]	Analytical G_{23} [MPa]	Optimized G_{13} [MPa]	Optimized G_{23} [MPa]
0.36	352.33	211.40	172.96	184.06
0.52	352.33	211.40	180.49	182.40
1.04	352.33	211.40	207.87	182.97
1.56	352.33	211.400	225.75	186.73
2.08	352.33	211.40	240.16	193.26
2.60	352.33	211.40	254.78	203.73

Figure 5.5 and Figure 5.6 are the output figures of the optimization process. Figure 5.5 shows the best and mean fitness values at each generation for the model whose face sheet thickness is 0.36 mm. The mean fitness value converges to zero in about 20 generation satisfying the stall generation stopping criteria. Figure 5.6 shows the fitness of each individuals in the last generation. Detailed values of the individuals at the last generation and the information between the average distance between the individuals are provided in Appendix 0. The fitness value of the individuals at the last iteration are all around zero; therefore, the optimization is considered to be convergent. Similar figures are obtained for the other face sheet thickness and optimum transverse modulus of the core are extracted. The performance of the optimized modulus values is tested using models with different geometries and load-boundary conditions. The results of the verification process are presented in the following chapter.

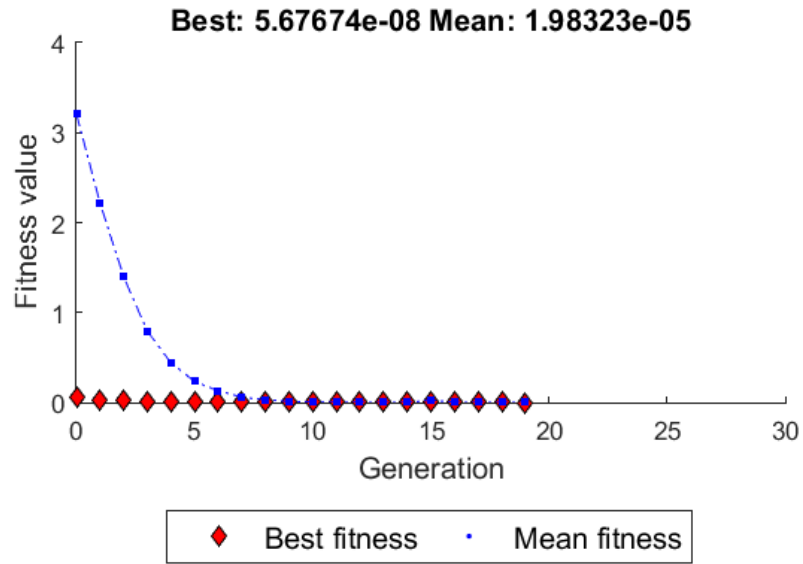


Figure 5.5. Best and mean fitness values of the optimization for face sheet thickness of 0.36 mm. The algorithm converges to zero fitness value in 10 generations.

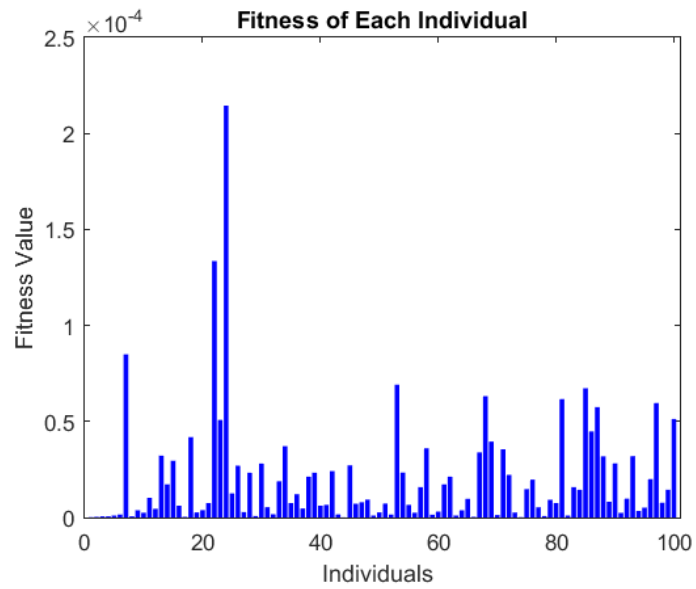


Figure 5.6. Fitness value of each individual at the last generation. Fitness values of the most individuals were reduced to zero.

5.2. Results of the Verification Models

The verification models are model groups 2, 3 and 4 whose detailed models and layered shell models are shown from Figure 3.10 to Figure 3.15 and layered shell models details are shown from Figure 3.18 to Figure 3.22. The following figures visually show the results of the verification process.

5.2.1. Results of Verification of the Model Group 2

Compared to optimized model (model group 1), model group 2 has a ramp region. It is a quarter model with symmetrical boundary conditions. It is constrained in z-direction in the monolithic edge region and uniform displacement of 0.1 mm is applied in the center. The details of the finite element models are shown in Figure 3.10, Figure 3.11 and Figure 3.18. The reaction forces for various face thicknesses of detailed and layered shell models are shown in Figure 5.7 to Figure 5.9.

Figure 5.7 shows the difference between the reaction forces. RF-detailed is obtained from the detailed model, RF- analytical is obtained by using analytically driven equivalent transverse modulus values and the RF-optimum is obtained by using the optimized transverse modulus values of the model group 1. RF-optimum values are closer RF-detailed values than RF-analytical values.

Similar process is applied when the ribbon direction was changed from x-axis to y-axis. The reaction force results are presented in Figure 5.8. This time, the difference between the results are smaller but the optimized modulus values created closer results to detailed ones.

Figure 5.9 and Table 5.4 make a comparison between the initial error rates and the optimized error rates in both ribbon directions for all face sheet thicknesses. According to the figure, a considerable improvement is obtained by using optimized transverse modulus values of the equivalent honeycomb core.

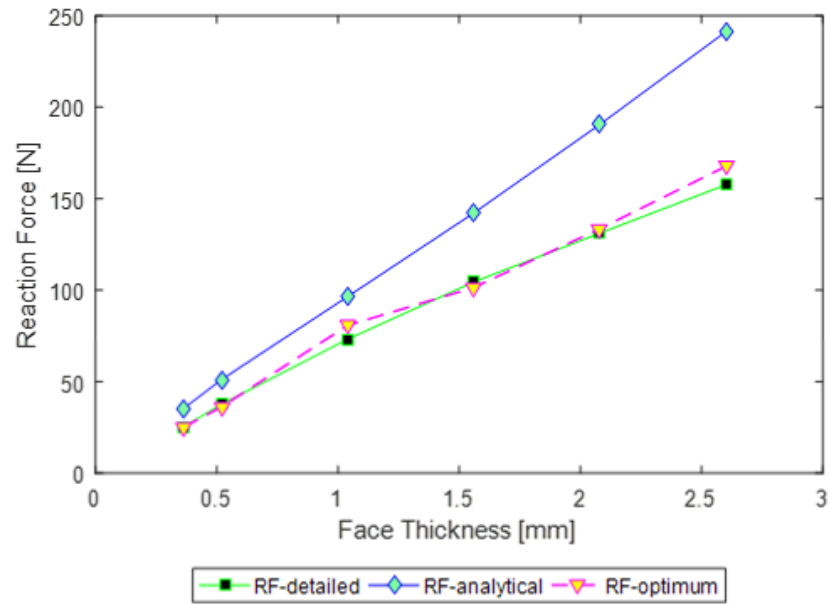


Figure 5.7 Detailed, analytical and optimum reaction force comparison of the model group 2. Ribbon direction is in the x-axis direction. The optimum reaction force is obtained by plugging in the optimum shear modulus of the optimized model (model group 1) into model group 2. This model group has a central loading and ramp region. RF-optimum results are better than RF-analytical results.

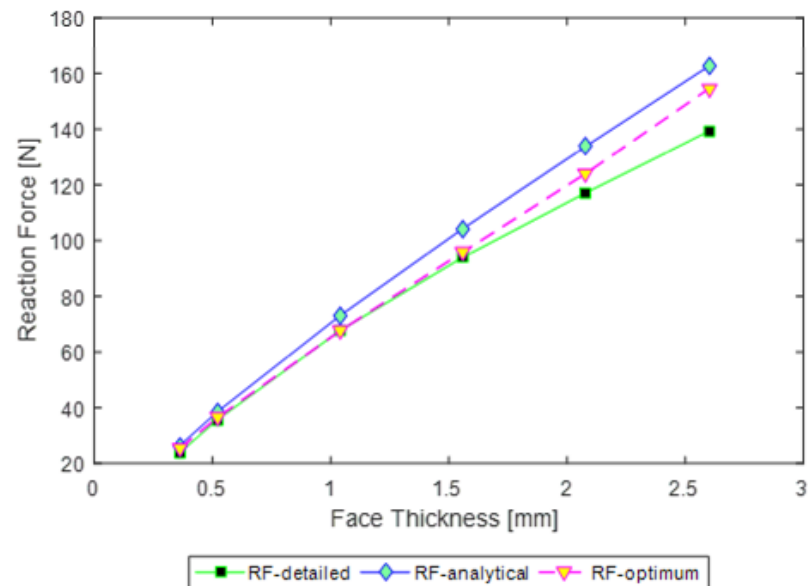


Figure 5.8. Detailed, analytical and optimum reaction force comparison of the model group 2. Ribbon direction is in the y-axis direction. RF-optimum results are better than RF-analytical.

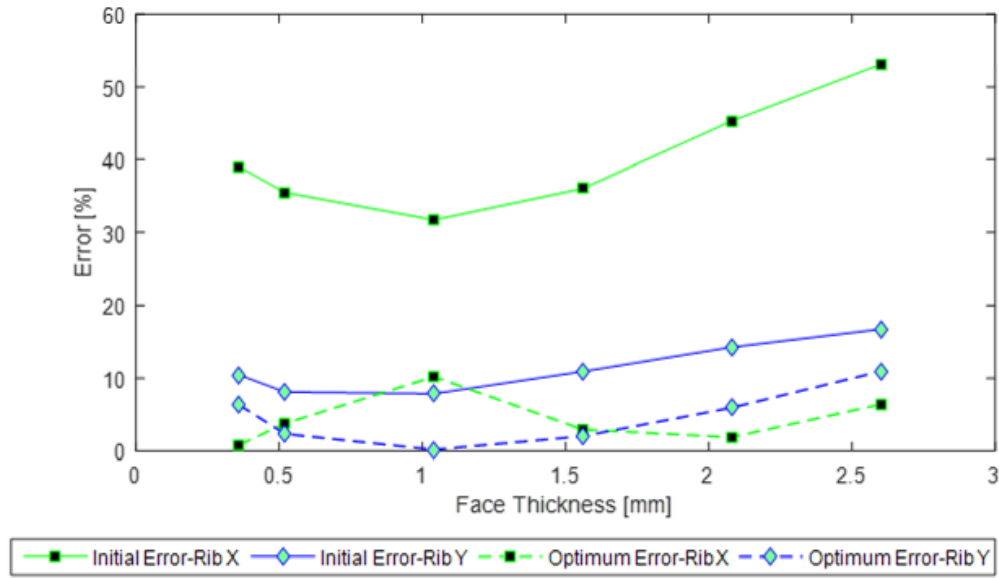


Figure 5.9. Comparison of rate of errors stemming from the differences of the reaction forces of the detailed models and analytical models (initial error) with the optimum models. The error rates of the optimum models are lower than the rate of analytical models for all the face sheet thicknesses.

Table 5.4. The rate of initial and optimum errors for model group 2. Initial error is the percentage difference between the detailed reaction forces and the analytical reaction forces. Optimum error is the percentage difference between the detailed reaction forces and the reaction force obtained by using optimized material parameters of the model group 1.

Face Thickness [mm]	Initial Error-Rib X [%]	Initial Error-Rib Y [%]	Optimum Error-Rib X [%]	Optimum Error-Rib Y [%]
0.36	38.99	10.48	0.80	6.33
0.52	35.49	8.13	3.78	2.33
1.04	31.74	7.89	10.24	0.17
1.56	36.04	10.96	2.93	2.02
2.08	45.29	14.29	1.87	5.96
2.60	53.11	16.76	6.42	10.98

5.2.2. Results of Verification of the Model Group 3

Like model group 2, model group 3 is a quarter model with ramp region but it simulates three-point bending test. It is constrained in z-direction in the monolithic edge region and uniform displacement of 0.1 mm is applied. The details of the finite element models are shown in Figure 3.12, Figure 3.13 and Figure 3.20.

Figure 5.10 and Figure 5.11 compares the reaction forces obtained from detailed, analytical and optimum models with different ribbon directions. In each of the cases, the optimized modulus values provide better results than the analytical ones.

Figure 5.12 and Table 5.6 compare the rates of the errors between the models. According to the figure, the optimized transvers modulus values of the model group can provide improvement for a sandwich beam under three-point bending conditions as well.

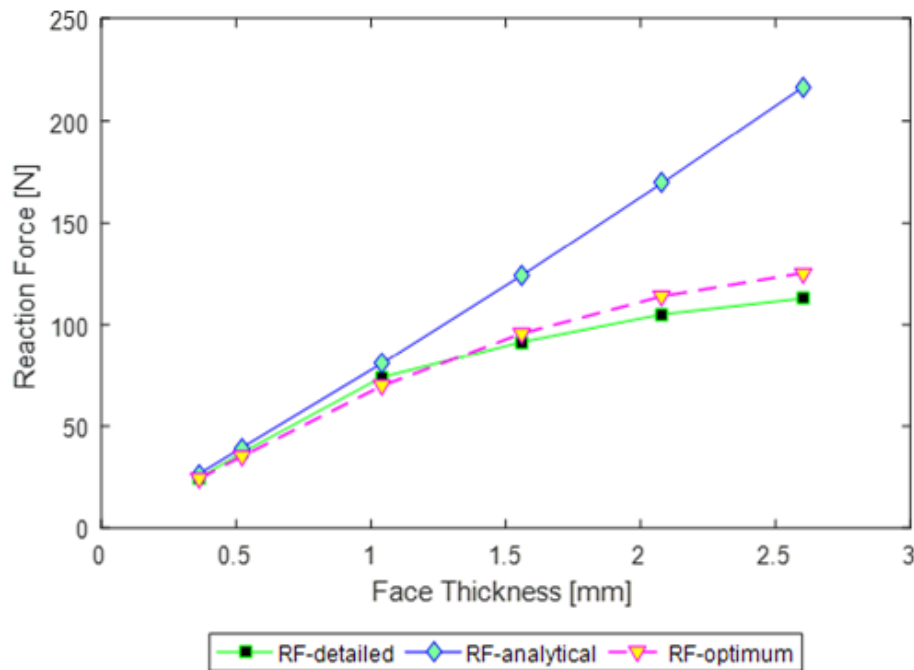


Figure 5.10. Detailed, analytical and optimum reaction force comparison of the model group 3. Ribbon direction is in the x-axis direction. The optimum reaction force was obtained by plugging in the optimum shear modulus of the optimized model (model group 1) into model group 3. This model group is under three-point bending. RF-optimum results are significantly better than RF-analytical results.

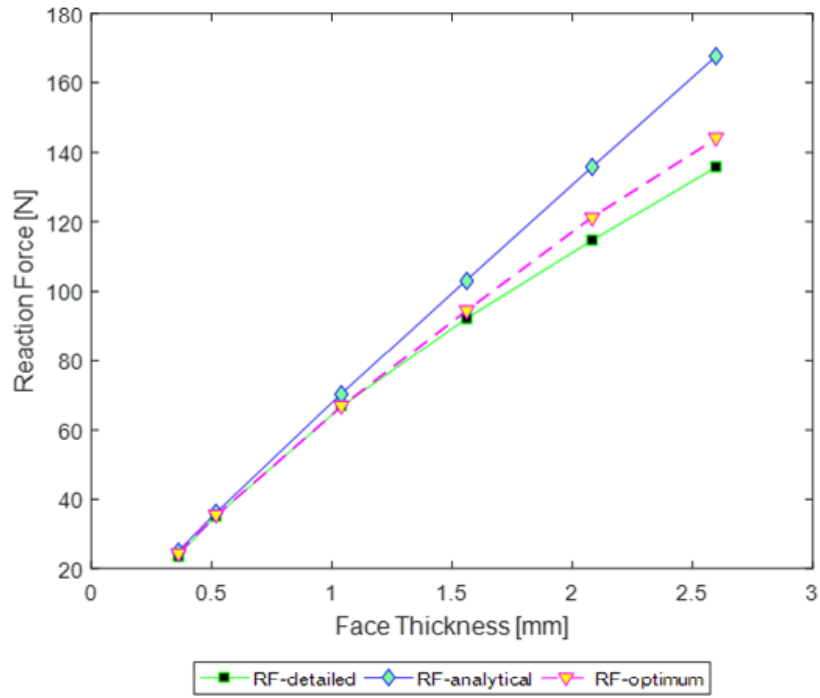


Figure 5.11. Detailed, analytical and optimum reaction force comparison of the model group 3. Ribbon direction shifted to the y-axis direction. RF-optimum results are better than RF-analytical.

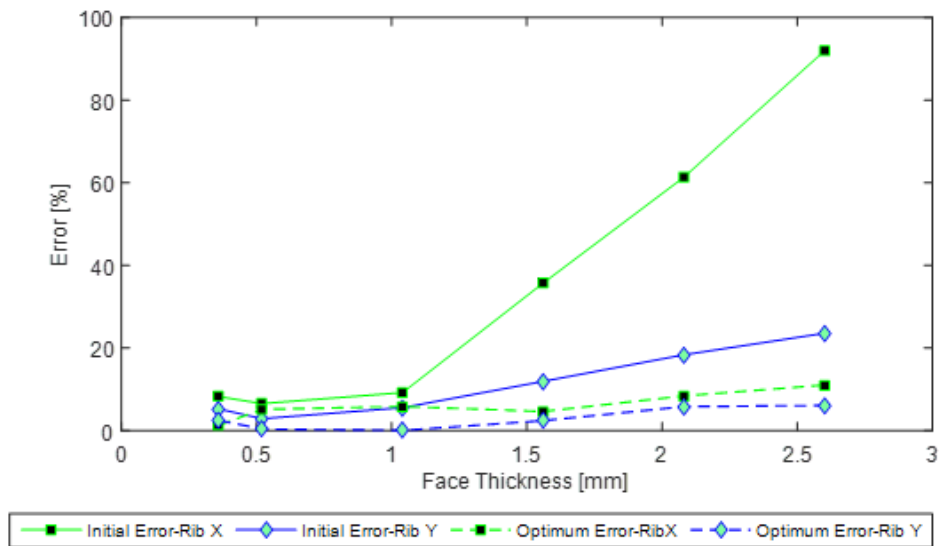


Figure 5.12. Comparison of rate of errors of the analytical models (initial error) with the optimum errors. Optimum errors are less for all face sheet thicknesses.

Table 5.5. The rate of initial and optimum errors for model group 3. Initial error is the percentage difference between the detailed reaction forces and the analytical reaction forces. Optimum error is the percentage difference between the detailed reaction forces and the reaction force obtained by using optimized material parameters of the model group 1.

Face Thickness [mm]	Initial Error- Rib X [%]	Initial Error- Rib Y [%]	Optimum Error-Rib X [%]	Optimum Error- Rib Y [%]
0.36	8.22	5.22	1.27	2.46
0.52	6.50	2.87	5.13	0.36
1.04	9.18	5.53	5.82	0.02
1.56	35.71	11.90	4.60	2.38
2.08	61.30	18.32	8.37	5.78
2.60	91.87	23.54	11.01	6.08

5.2.3. Results of Verification of the Model Group 4

Model group 4 is similar to optimized model (model group 1) but the loading and boundary conditions are changed. The model group 4 corresponds to a cantilever structure. The detailed models are shown in Figure 3.14 and Figure 3.15. The layered shell models are shown in Figure 3.21 and Figure 3.22.

Figure 5.13 and Figure 5.14 show the reaction forces obtained from detailed, analytical and optimized models. Figure 5.15 and Table 5.6 compare the related error rates. The results show that the performance of the layered shell models increases with the optimized transverse shear modulus values even if load and boundary conditions are different from the optimized model.

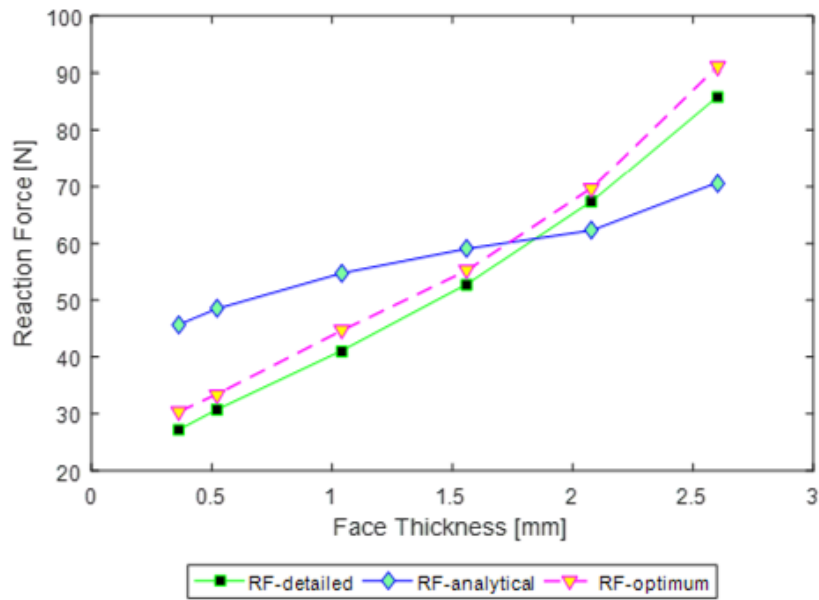


Figure 5.13. Detailed, analytical and optimum reaction force comparison of the model group 4. Ribbon direction is in the x-axis direction. This model represents a cantilever structure. RF-optimum results are very close to the reference values while RF-analytical results can both over- and under-predict the reference values.

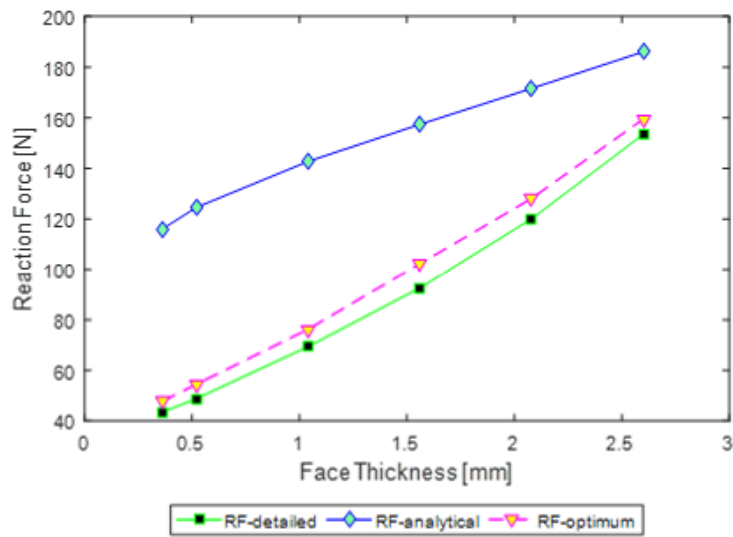


Figure 5.14. Detailed, analytical and optimum reaction force comparison of the model group 4. Load and boundary conditions were replaced in the y-direction. RF-optimum results are significantly better than RF-analytical.

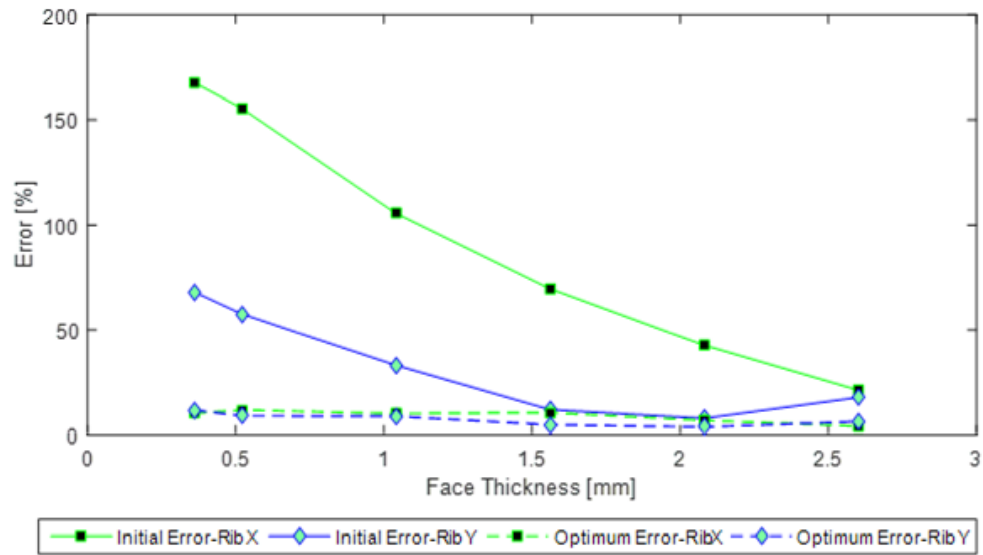


Figure 5.15. Comparison of rate of errors of the analytical models (initial error) with the optimum errors. Optimum errors are less for all face sheet thicknesses.

Table 5.6. The rate of initial and optimum errors for model group 4. Initial error is the percentage difference between the detailed reaction forces and the analytical reaction forces. Optimum error is the percentage difference between the detailed reaction forces and the reaction force obtained by using optimized material parameters of the model group 1.

Face Thickness [mm]	Initial Error-Rib X [%]	Initial Error-Rib Y [%]	Optimum Error-Rib X [%]	Optimum Error-Rib Y [%]
0.36	167.79	68.12	10.05	11.63
0.52	155.47	57.73	11.65	8.79
1.04	105.65	33.17	9.94	8.62
1.56	69.73	11.81	10.38	4.57
2.08	42.81	7.64	6.67	3.51
2.60	21.19	17.63	3.92	6.12

CHAPTER 6

DISCUSSION AND FUTURE WORK

The sandwich structures are commonly employed design solutions with a large area of application. They consist of two face sheets filled with a porous low-density core material and an adhesive material. In other words, sandwich structures are an efficient mixture of different materials. In an idealized sandwich structure, the face sheets are designed to carry the in-plane loads whereas the core carries the transverse loads. Therefore, core materials like honeycomb cores have weak in-plane but strong shear strength properties.

The sandwich structures are preferred over traditional structures because of the strength and weight saving advantages they offer. For instance, a typical sandwich beam can save up to 95% from weight compared to a solid metal with the same strength properties [1]. These advantages increase the interest on the sandwich applications; thus, they have become an important research subject for the structural area where numeric methods widely preferred. One of the most popular numeric methods is the finite element method. It has become an important issue create accurate finite element methods for the structural analysis purposes. In other words, the accurate finite element modeling of the sandwich structures has become a critical step in their development process. There are mainly three finite element modeling approaches employed for the finite element analysis of sandwich structures. The first

one is the detailed modeling approach. In this approach the core is modelled in its original shape. For instance, an detailed finite element model of a honeycomb core involves a hexagonal core whose cell are meshed with shell elements and connected to the mesh representing the face sheets. This modeling approach, is the least preferred one because it is difficult to model, computationally expensive and not practical especially with the complex geometries. The second modeling approach is the solid modeling approach where complex core geometry is replaced with equivalent solid element with 3D orthotropic material properties. This approach is more practical than the detailed modeling approach but solid elements are also computationally expensive. The last approach is the layered shell modeling approach. In this approach, face sheets and the core are modeled as 2D layers which are stacked on each other. The 3D core is reduced to 2D model with 2D orthotropic material properties. The layered shell approach is the easiest, most practical and preferred approach and it is computationally the cheapest one. The solid and layered shell modeling approaches involves the representation of the core with an equivalent solid or shell form. Therefore, the behavior of the detailed core is converted into a solid or shell. This transformation is called the crating an equivalent core. One of the methods employed for creating an equivalent core is the analytical approach where analytically derived formulas [7,11,14] existing in the literature are used. In this study, detailed and layered shell finite element models of the sandwich structures with honeycomb core and different face sheet thicknesses are developed. The analytical formulas are used for the layered shell models and the reaction forces obtained from them are compared with the

reaction forces obtained from the detailed models. It is observed that there is a large difference between the detailed and layered shell models with equivalent core properties. To overcome this difference, an optimization tool employing the genetic algorithm is developed. The optimization tool takes the reaction forces of the detailed models as reference values and makes the reaction forces obtained from the layered model approximate to the reference values by optimizing the equivalent core transverse shear moduli. At the end of the optimization, the tool outputs optimum G_{13} and G_{23} values of the equivalent core for different values of the face sheet thicknesses. In this way, the effect of the stiffness of the face sheets on the equivalent core properties are investigated. It is found that the equivalent core properties change with the face sheet thickness and stiffness of the face sheets are effective on the behavior of the equivalent core. In order to show this, there are four model groups created. The first model group was used for the optimization, the others were employed for the verification of the optimization. The verification models have different geometric properties, loads and boundary conditions than the optimized model.

The performance of the optimization is evaluated based on the improvement obtained by using optimized core properties instead of analytical ones when they are plugged into layered shell models whose loads and boundary conditions and geometric properties are different than the model from which optimum core properties are obtained. For instance, for model group 2, it was found that the reaction forces obtained from the optimized layered shell model whose core properties are the ones obtained by optimizing model group 1 are closer to the reference reaction forces than

the reaction forces obtained from the analytical layered shell model. Since, the optimized core properties result in better approximations to the reference reaction forces when the geometry and load boundary conditions are changed, the optimization is considered to be successful. For instance, the average analytical error for the model group 3 is around 35% whereas it is 6% with the optimized properties. It was also found the stiffness of the face sheet is effective on the behavior of the sandwich panel. Although the analytically derived equivalent formulas do not take the effect of the face sheets thicknesses into consideration, the analytical error rate increases as the thickness of the face sheets increase. The optimized transverse core modulus also shows an increasing trend with the face sheet thickness.

Therefore, the genetic algorithm optimization process is found to improve the performance and accuracy of the layered shell sandwich modeling approach. In addition, it was found that the stiffness of the face sheets are effective on the equivalent core properties.

This study can be improved by creating more data for the optimized transverse core moduli using different materials and physical cell properties such as cell wall thickness, cell size and angle. The variety of the detailed models from which the reference reaction forces are obtained can also be increased by applying different loads and boundary conditions to them. Similarly, the number and variety of the verification models can be increased to evaluate the performance of the optimization. Finally, the data obtained from the different models can be statistically evaluated and physically

tested to obtain global optimum core shear moduli trends for sandwich structures with different face sheet thicknesses.

REFERENCES

- [1] T. Bitzer, *Honeycomb Technology*. 1997.
- [2] O. T. Thomsen, “Sandwich materials for wind turbine blades - Present and future,” *J. Sandw. Struct. Mater.*, 2009.
- [3] J. Y. R. Liew and K. M. A. Sohel, “Lightweight steel-concrete-steel sandwich system with J-hook connectors,” *Eng. Struct.*, 2009.
- [4] E. Torenbeek and H. Wittenberg, “History of Aviation,” in *Flight Physics*, 2009.
- [5] J. R. Vinson, “Sandwich Structures: Past, Present, and Future,” in *Sandwich Structures 7: Advancing with Sandwich Structures and Materials*, 2005.
- [6] A. S. Herrmann, P. C. Zahren, and I. Zuardy, “Sandwich Structures Technology in Commercial Aviation,” in *Sandwich Structures 7: Advancing with Sandwich Structures and Materials*, 2005.
- [7] H. D. Hibbit, B. I. Karlsson, and E. P. Sorensen, “ABAQUS user manual, version 6.12,” *Simulia*. 2012.
- [8] G. Papazafeiropoulos, M. Muñoz-Calvente, and E. Martínez-Pañeda, “Abaqus2Matlab: A suitable tool for finite element post-processing,” *Adv. Eng. Softw.*, 2017.
- [9] SAE International, *COMPOSITE MATERIALS HANDBOOK: Volume 1. Polymer Matrix Composites: Guidelines for Characterization of Structural Materials*. 2014.
- [10] Composite Materials Handbook-17 (CMH-17), *Composite Materials Handbook, Volume 6 - Structural Sandwich Composites (CMH-17)*. 2013.
- [11] I. G. Masters and K. E. Evans, “Models for the elastic deformation of honeycombs,” *Compos. Struct.*, vol. 35, no. 4, pp. 403–422, 1996.
- [12] G. Shi and P. Tong, “Equivalent transverse shear stiffness of honeycomb cores,” *Int. J. Solids Struct.*, vol. 32, no. 10, pp. 1383–1393, 1995.
- [13] S. Kelsey, R. A. Gellatly, and B. W. Clark, “The Shear Modulus of Foil Honeycomb Cores,” *Aircr. Eng. Aerosp. Technol.*, 2008.
- [14] G. Shi and P. Tong, “Equivalent transverse shear stiffness of honeycomb cores,” *Int. J. Solids Struct.*, 1995.
- [15] M. F. A. L. J. Gibson, *Cellular Solids: Structure and Properties*, 2d ed. 1997.

- [16] J. Zhang and M. F. Ashby, "The out-of-plane properties of honeycombs," *Int. J. Mech. Sci.*, 1992.
- [17] F. Albracht, H. Altenbach, and E. Nast, "On the prediction of effective elastic moduli of honeycomb-type sandwich plates," in *Computer Aided Design in Composite Material Technology - International Conference*, 1996.
- [18] W. S. Burton and A. K. Noor, "Assessment of continuum models for sandwich panel honeycomb cores," *Comput. Methods Appl. Mech. Eng.*, 1997.
- [19] M. Pietrzyk *et al.*, "Conventional Modeling," *Comput. Mater. Eng.*, pp. 69–151, Jan. 2015.
- [20] I. Aydinçak and A. Kayran, "An approach for the evaluation of effective elastic properties of honeycomb cores by finite element analysis of sandwich panels," *J. Sandw. Struct. Mater.*, vol. 11, no. 5, pp. 385–408, 2009.
- [21] M. Grediac, "A finite element study of the transverse shear in honeycomb cores," *Int. J. Solids Struct.*, 1993.
- [22] O. Çınar, M. Erdal, and A. Kayran, "Accurate equivalent models of sandwich laminates with honeycomb core and composite face sheets via optimization involving modal behavior," *J. Sandw. Struct. Mater.*, 2017.
- [23] D. B. Fogel, "Advances in genetic programming: Kenneth E. Kinneer, Jr., (ed.), MIT Press, Cambridge, MA, 1994, 518 pp., \$45.00," *Biosystems*, 1995.
- [24] D. E. Goldberg, *Genetic Algorithms in Search, Optimization, and Machine Learning*. 1989.
- [25] N. A. Barricelli, "Esempi numerici di processi di evoluzione," *Methodos*, 1954.
- [26] B. J. Copeland and D. Proudfoot, "Alan Turing's forgotten ideas in computer science," *Sci. Am.*, 1999.
- [27] M. Mitchell, S. Forrest, and J. H. Holland, "The Royal Road for Genetic Algorithms: Fitness Landscapes and GA Performance," *Proc. FIRST Eur. Conf. Artif. LIFE*, 1991.
- [28] M. Mitchell, "An Introduction to Genetic Algorithms (Complex Adaptive Systems)," *MIT Press*, 1998.
- [29] D. Simon, *Evolutionary Optimization Algorithms*. 2013.
- [30] C. M. Fonseca and P. J. Fleming, "An Overview of Evolutionary Algorithms in Multiobjective Optimization," *Evol. Comput.*, 2008.
- [31] M. Abouhamzeh and M. Sadighi, "Buckling optimisation of sandwich cylindrical panels," *Curved Layer. Struct.*, vol. 3, no. 1, pp. 137–145, 2016.
- [32] T. Wang, S. Li, and S. R. Nutt, "Optimal design of acoustical sandwich panels

- with a genetic algorithm,” *Appl. Acoust.*, 2009.
- [33] A. Boudjemai, R. Amri, A. Mankour, H. Salem, M. H. Bouanane, and D. Boutchicha, “Modal analysis and testing of hexagonal honeycomb plates used for satellite structural design,” *Mater. Des.*, 2012.
 - [34] A. Boudjemai, M. H. Bouanane, L. Merad, and A. M. Si Mohammed, “Small satellite structural optimisation using genetic algorithm approach,” in *Proceedings of the 3rd International Conference on Recent Advances in Space Technologies, RAST 2007*, 2007.
 - [35] P. Qiao, W. Fan, J. F. Davalos, and G. Zou, “Optimization of transverse shear moduli for composite honeycomb cores,” *Compos. Struct.*, vol. 85, no. 3, pp. 265–274, 2008.
 - [36] T. IMAMURA and Y. YAMAGUCHI, “Composite Materials for Aircraft Structures,” *J. Japan Soc. Aeronaut. Sp. Sci.*, 2011.
 - [37] L. J. Gibson, M. F. Ashby, and M. P. Wolcott, “Mechanics of honeycombs,” in *Cellular solids: structure and properties*, 1990.
 - [38] HEXCEL, “Attributes and Properties guide to standard Hexcel honeycomb materials , properties,” 2015.
 - [39] Mathworks, “Optimization Toolbox User’s Guide R2017a,” 2017.
 - [40] R. L. Haupt and S. E. Haupt, *Practical Genetic Algorithms Second Edition*. 2004.
 - [41] “MMPDS-02: Metallic Materials Properties Development and Standardization,” *Anti-Corrosion Methods Mater.*, 2007.

APPENDICES

A. The Individuals of the Last Iteration

The values of the individuals of the last iteration of the model group 1 for face sheet thickness 0.36 mm are given in Table A.1.

Table A.1. *Individuals In the last iteration*

Ind. No.	G_{13} [MPa]	G_{23} [MPa]	Ind. No.	G_{13} [MPa]	G_{23} [MPa]
1	173.15	184.05	23	175.03	184.00
2	172.89	184.09	24	176.91	184.53
3	173.24	183.88	25	173.90	184.40
4	172.87	184.02	26	174.53	183.77
5	173.33	183.94	27	173.41	183.70
6	173.34	183.82	28	174.43	183.78
7	175.60	183.79	29	173.31	184.12
8	173.06	184.25	30	174.33	183.01
9	172.73	183.80	31	173.72	183.98
10	173.49	183.99	32	173.42	183.88
11	173.30	184.92	33	174.20	184.22
12	173.54	183.63	34	174.69	184.11
13	174.20	184.90	35	173.60	184.49
14	173.70	184.87	36	172.21	183.90
15	174.22	184.82	37	173.53	184.37
16	173.66	184.21	38	174.27	184.09
17	173.21	184.04	39	174.45	183.77
18	174.80	184.10	40	173.70	184.22
19	173.53	183.91	41	173.58	183.51
20	173.64	183.87	42	174.38	183.55
21	173.80	184.12	43	173.25	184.34
22	176.17	183.96	44	172.96	184.06

Table A.1. continued

Ind. No.	G_{13} [MPa]	G_{23} [MPa]	Ind. No.	G_{13} [MPa]	G_{23} [MPa]
45	174.47	183.60	76	174.35	183.63
46	173.76	183.95	77	173.65	183.90
47	173.56	183.39	78	173.31	184.01
48	173.89	184.01	79	173.87	183.83
49	173.32	183.88	80	173.80	184.07
50	173.49	184.11	81	174.96	184.62
51	173.82	183.75	82	173.33	183.94
52	173.45	184.14	83	173.75	183.09
53	175.28	184.08	84	174.15	184.05
54	174.41	183.66	85	175.00	184.78
55	173.62	183.50	86	174.89	183.89
56	173.54	184.05	87	175.10	184.07
57	174.11	184.21	88	174.55	184.05
58	174.32	184.90	89	173.26	184.82
59	173.28	183.84	90	173.89	185.09
60	173.50	184.17	91	173.30	184.43
61	174.02	183.23	92	172.87	185.02
62	174.34	184.09	93	173.76	185.32
63	173.26	183.86	94	172.56	183.96
64	173.63	184.04	95	172.57	183.82
65	173.91	184.10	96	171.87	184.02
66	172.92	184.15	97	175.24	183.44
67	174.61	184.21	98	172.32	184.28
68	175.24	184.11	99	174.15	184.05
69	174.81	183.84	100	174.77	182.72
70	172.82	184.01			
71	174.72	183.88			
72	174.34	184.23			
73	173.44	184.26			
74	173.07	184.05			
75	174.05	183.58			

The difference between the individuals in the last iteration very low. As the genetic algorithm advances through the generations, the gap between the individuals shrinks since it selects the best individuals from the population under consideration to form the next generation. In Figure A.1, it can be seen that the average distance between the individuals is the highest in the first iteration and it shrinks to zero through the last generation as the algorithm converges to an optimum point.

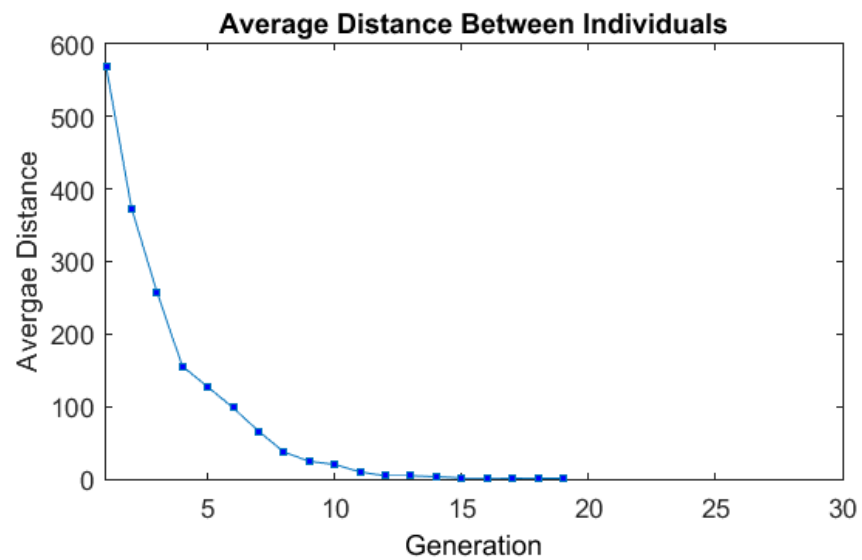


Figure A.1. Average distance between the individuals.

B. Von Mises Stress Results of the Detailed Model

The detailed FE model of the model group 1 is checked against the yield and ultimate strength criteria. The face sheet thickness of the model is 0.36 mm. Materials of the face sheets and the core are AL5052. The tensile yield strength of AL5052 is 193 MPa and ultimate tensile strength is 228 MPa [41]. The Von Mises stress is stress plot is shown in Figure B.2 where the maximum value is MPa and occurs on cell walls near the right edge of the lower face sheet. The maximum von Mises stress level is around 26 MPa which is significantly smaller than 193 MPa. Therefore, no plastic deformation is expected in the structure.

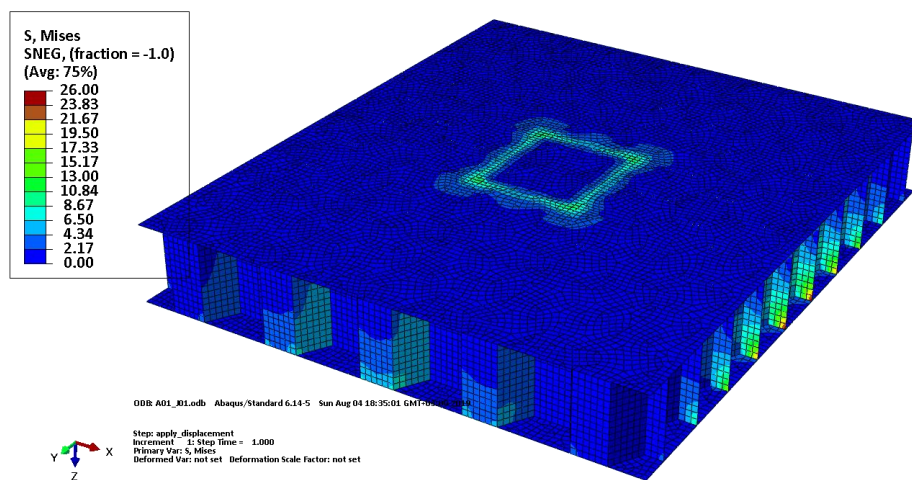


Figure B.2. Von Mises stress results of the detailed FE model of the model group 1 with face sheet thickness equal to 0.36 mm.